ELECTROSPINNING OF SUPER TOUGH NYLON 6,6 FIBERS AND THEIR USE IN LAYERED COMPOSITES

SÜPER TOK NAYLON 6,6 FİBERLERİN ELEKTROEĞRİLMESİ VE KATMANLI KOMPOZİTLERDE KULLANIMI

ALİCAN KARA

PROF. DR. BORA MAVİŞ
Supervisor

Submitted to

Graduate School of Science and Engineering of Hacettepe University

as a Partial Fulfillment to the Requirements

for the Award of Degree of Master of Science in Mechanical Engineering

2023

ABSTRACT

ELECTROSPINNING OF SUPER TOUGH NYLON 6,6 FIBERS AND THEIR USE IN LAYERED COMPOSITES

Alican KARA

Master of Science, Department of Mechanical Engineering

Thesis Supervisor: Assoc. Prof. Dr. Bora MAVİŞ

Jan 2023, 97 pages

Despite their obvious advantages in applications that require a high strength-to-weight ratio, delamination problems in layered composite structures continue to be a major drawback. Interleaving the layers with films or fibers of thermoplastics has been among the viable strategies to increase the interlaminar toughness. Although a wide variety of polymers have been assessed for this purpose, polyamides (such as PA 6, PA 6,6) and polycaprolactone (PCL) come forward with their high intrinsic toughness. It is also possible to combine fibers of polymers physically or embed fibers of one into the film matrix of the other. More recently, blending the polymers at the fiber level has been suggested for the sequential activation of multiple toughening mechanisms. PA 6/PCL, PCL/rubber, and PA 6,6 /rubber blends were the three blends that have been electrospun and were interleaved in the veil (i.e. tulle) form. Super tough (ST) PA's are commercially available blends of either different PA's or PA with impact modifiers like ethylene propylene diene monomer (EPDM) rubber and their intrinsic toughness values can be up to 50% higher compared to those of PA's and PCL. Electrospinning of such ST-PA's and the interleaving of their veils forms have not been studied.

In this study, ST-PA 6,6 (can also be named as ST-Nylon 6,6 or ST-N 6,6) was dissolved in various solvents in various mass ratios and the mixture suitable for electrospinning was determined after consecutive scanning electron microscope (SEM) analysis. Fixing all parameters, but the electrospinning time three different areal densities (3.5 g/m^2, 7 g/m^2, 10 g/m^2) was spun and transferred on an epoxy-impregnated carbon fiber prepreg which was laid up with unmodified layers from bottom and top. Lay-up processes were completed in accordance with standards by a double-sided bagging-vacuuming process in a cleanroom of a fully certified facility, and the final stack was cured in an industrial scale fully controlled autoclave. After the curing process, the double cantilever beam (DCB) test was carried out in accordance with the AITM 1-0053 standard.

With 3.5 g/m^2 veil, Mode I toughness, G_{IC}, in the initiation increased by 21% and for the propagation it increased by 15% compared to the unmodified composite. When interleaving was 7 g/m^2, G_{IC} initiation increased by 50% and enhancement in the propagation remained low at 18%. Increasing the veil areal density to 10 g/m^2, decreased the improvements in the initiation to 35% and the enhancement in the propagation decreased to 10%.

Results indicate that there is an optimum areal veil concentration for maximizing the improvements against delamination. If a better solvent can be designed for ST-PA6 and even for its potential blends with PCL, for a better adhesion between epoxy and fiber surfaces, this may lead to higher interlayer fracture toughness improvements in both initiation and propagation.

Keywords: carbon fiber reinforced polymer matrix composites (CFRP), electrospinning, electrospraying, polymer blends, super tough nylon 6,6, interlaminar fracture toughness

ÖZET

SÜPER TOK NAYLON 6,6 FİBERLERİN ELEKTROEĞRİLMESİ VE KATMANLI KOMPOZİTLERDE KULLANIMI

Alican KARA

Yüksek Lisans, Makina Mühendisliği

Tez Danışmanı: Doç. Dr. Bora MAVİŞ

Ocak 2023, 97 sayfa

Yüksek dayanım/ağırlık oranı gerektiren uygulamalarda bariz avantajlarına rağmen, katmanlı kompozit yapılarda delaminasyon sorunları önemli bir dezavantaj olmaya devam etmektedir. Katmanları termoplastiklerin filmleri veya lifleri ile serpiştirmek, katmanlar arası tokluğu artırmak için geçerli stratejiler arasında yer almıştır. Bu amaçla çok çeşitli polimerler denenmesine rağmen, poliamidler (PA 6, PA 6,6 gibi) ve polikaprolakton (PCL) yüksek içsel tokluklarıyla öne çıkmaktadır. Polimer fiberlerini fiziksel olarak birleştirmek veya birinin fiberlerini diğerinin film matrisine gömmek de mümkündür. Daha yakın zamanlarda, çoklu sertleştirme mekanizmalarının sıralı aktivasyonu için polimerlerin fiber seviyesinde harmanlanması önerilmiştir. PA 6/PCL, PCL/kauçuk ve PA 6,6/kauçuk harmanları, elektro eğirme işleminden geçirilmiş ve peçe (yani tül) formunda serpiştirilmiş üç harmandı. Süper tok (ST) PA'lar, farklı PA'ların veya etilen propilen dien monomer (EPDM) kauçuğu gibi darbe iyileştiricilerle PA'nın ticari olarak temin edilebilen karışımlarıdır ve içsel tokluk değerleri, PA'lar ve PCL'ye kıyasla %50'ye kadar daha yüksek olabilir. Bu tür ST-PA'ların elektrospinlenmesi ve tül formlarının serpiştirilmesi çalışılmamıştır.

Bu çalışmada ST-PA 6,6 (ST-Nylon 6,6 veya ST-N 6,6 olarak da adlandırılabilir) çeşitli çözücülerde çeşitli kütle oranlarında çözündürülmüş ve ardından taramalı elektron mikroskobu (SEM) analizinden sonra elektroeğirmeye uygun karışım belirlenmiştir. Elektroeğirme süresi hariç tüm parametreler sabitlendi, üç farklı alan

yoğunluğu (3.5 g/m^2, 7 g/m^2, 10 g/m^2) spinlendi ve alttan ve üstten değiştirilmemiş katmanlarla döşenen bir epoksi emdirilmiş karbon fiber prepreg üzerine aktarıldı. Serim işlemleri tam sertifikalı bir tesisin temiz odasında çift taraflı torbalama-vakumlama işlemi ile standartlara uygun olarak tamamlanmış ve nihai istif endüstriyel ölçekte tam kontrollü otoklavda kürlenmiştir. Kürleme işleminin ardından AITM 1-0053 standardına uygun olarak çift konsol kiriş (DCB) testi yapılmıştır.

3.5 g/m^2 peçe ile mod I tokluğu, G_{IC}, modifiye edilmemiş kompozite göre başlangıçta %21, ilerlemede ise %15 arttırılmıştır. Arayüze serpiştirme 7 g/m^2 olduğunda, G_{IC} başlangıcı %50 arttı ve ilerlemedeki artış %18 ile düşük kaldı. Örtü yoğunluğunun 10 g/m^2'ye çıkarılması, başlangıçtaki iyileştirmeleri %35'e ve ilerlemedeki iyileştirmeyi %10'a düşürdü.

Sonuçlar, delaminasyona karşı iyileştirmeleri maksimize etmek için optimum bir alansal tül konsantrasyonu olduğunu göstermektedir. ST-PA 6,6 için ve hatta PCL ile olası karışımları için daha iyi bir solvent tasarlanabilirse, epoksi ve fiber yüzeyler arasında daha iyi bir yapışma için bu, hem başlatma hem de ilerlemede daha yüksek ara katman kırılma tokluğu iyileştirmelerine yol açabilir.

Anahtar Kelimeler: karbon fiber takviyeli polimer matrisli kompozit (KFTP), elektroeğirme, elektropüskürtme, polimer karışımları, süper tok naylon 6,6, katmanlararası kırılma tokluğu

ACKNOWLEDGEMENTS

I would like to thank my advisor Prof. Dr. Bora Maviş for his continuous support during my experiments & thesis. With his different approach to every subject and his deep knowledge on all relevant subjects, he led me not only in my thesis work but also in looking at life positively.

I would also like to thank Assoc. Dr. Erhan Bat for his invaluable contributions to solvent selection.

I find no harm in saying this; Thanks to Mustafa Utku Yıldırım & Kamil Urgun's deep contributions and being my lab mentor, I was able to execute such a large number of experiments and tests.

Special thanks to UNAM-National Nanotechnology Research Center at Bilkent University for using their facilities.

I also acknowledge use of the services and facilities of Turkish Aerospace. I am grateful to take a chance to finish my thesis while working in Turkish Aerospace thanks to my former & current superiors. Special thanks to Demirel Sıcakdemir and his clean room crew who helped me in every single lay-up operation. Another appreciation to Mode I test master Celal Murat Gündeş who thought me DCB.

And my dear family… You have supported me unconditionally in all situations, in all impossibilities. I owe my entire education to you. In this process, every time I said "impossible", you became a "you can do it" voice to me. I hope I can be someone worthy of you all your life. No words of thanks can express my love and respect for you!

And finally my beloved wife Gizem Kara, I feel so lucky to be with you that this page is not enough for me to describe it. After work, while I was experimenting in the laboratory until the night, you became my lab friend, sometimes you became my editor, sometimes you became my hope. All my effort for you and our baby Kartal Deniz to be born, and always will be...

Alican Kara

January 2023, Ankara

TABLE OF CONTENTS

ABSTRACT i

ÖZET iii

ACKNOWLEDGEMENTS v

TABLE OF CONTENTS vi

TABLE OF FIGURES viii

LIST OF TABLES x

SYMBOLS AND ABBREVIATIONS xi

1. INTRODUCTION 1

2. LITERATURE SURVEY 6

2.1. Composite Materials 6

2.2. Damage Modes of Composite Materials 7

2.3. Methods to Increase Delamination Resistance/Fracture Toughness 10

2.4. Electrospinning 13

3. EXPERIMENTAL STUDIES 16

3.1. Electrospinning Solution Preparation 16

3.2. Electrospinning 19

3.3. Prepreg 23

3.4. Lay-up of CFRPs 24

3.5. Mechanical Test for Mode I Fracture Toughness 29

3.6. Material Characterization 31

4. RESULTS AND DISCUSSION 33

4.1. Solvent Studies 33

4.2. Electrospinning 38

4.2.1. Setup Improvements 38

4.2.2. Distance, Voltage & Flowrate 40

4.3. Mode I Fracture Toughness Tests of Laminates 41
4.3.1. Reference (Base) Laminates..... 41
4.3.2. ST-PA 6,6 Interleaved Composites 43
5. CONCLUSIONS 46
6. REFERENCES 47
7. APPENDIXES.....52
A. TABLES OF LITERATURE BASED ON ITS TEST RESULTS 52
B. SOLVENT EXPERIMENTS DETAILED FLOW CHART 61
C. DCB RESULTS ON TABLE 67
D. SEM RESULTS OF EXPERIMENTS 73
8. PERSONAL BACKGROUND.....97

TABLE OF FIGURES

Figure 1.1 Composite structure with nanofiber added between layers 1
Figure 1.2 Electrospinning 2
Figure 1.3 Interleaved veil 2
Figure 2.1 Composite material lay-up 6
Figure 2.2 Damage mechanisms 7
Figure 2.3 Failure modes 8
Figure 2.4 DCB (Double Cantilever Beam) test sample 9
Figure 2.5 Resistance curve 9
Figure 2.6 a) 3D Orthogonal & Knitted fiber b) Edge design changes c) Edge reinforcement 10
Figure 3.1 Solution experiments flow chart 17
Figure 3.2 Composition diagram of general solvent experiments 18
Figure 3.3 Composition diagram of selected solvent experiments 19
Figure 3.4 Drawing of ES cabin used in experiments 20
Figure 3.5 ES cabin used in experiments 21
Figure 3.6 ES cabin used in experiments 21
Figure 3.7 Weight sample for 4 different locations 22
Figure 3.8 Prepreg 24
Figure 3.9 Lay-up sequences 25
Figure 3.10 Pre-compaction 25
Figure 3.11 UD bonding to micro-nanofiber veil 26
Figure 3.12 UD bonding with the help of double sided bagging 27
Figure 3.13 Separation of fiber adhered UD from titanium collector 27
Figure 3.14 Final compaction 28
Figure 3.15 Autoclave cure cycle of prepreg 28
Figure 3.16 Demolded samples (Base & Fiber configurations) 29
Figure 3.17 Piano hinges with DCB coupon 30
Figure 3.18 DCB test & Smartzoom machine 31
Figure 3.19 DCB test inputs 31
Figure 3.20 SEM sample 32

Figure 3.21 Example of SEM data with different scale values 32
Figure 4.1 FTIR results of ST-PA 6,6 and PA 6,6..... 33
Figure 4.2 DSC results of ST-PA 6,6 Pellet, Film & Fiber 34
Figure 4.3 SEM image with a)5.00 kx b)1.00 kx of D59 35
Figure 4.4 SEM micrographs with a)5.00 kx b)2.00 kx c)1.00 kx of D57 35
Figure 4.5 SEM micrographs with a)5.00 kx b)2.00 kx c)1.00 kx of D58 36
Figure 4.6 SEM micrograph with 5.00 kx of D56 36
Figure 4.7 SEM micrograph with 2.00 kx of D56 37
Figure 4.8 SEM micrograph with 1.00 kx of D56 37
Figure 4.9 Veil removal process with aluminum collector 39
Figure 4.10 Veil removal process with titanium collector 39
Figure 4.11 Result of veil removal process with titanium collector 40
Figure 4.12 DCB graph for experiment A (Reference of B-3.5 g/m^2)..... 42
Figure 4.13 DCB graph for experiment C (Reference of D-7 g/m^2) 42
Figure 4.14 DCB graph for experiment E (Reference of D-10 g/m^2) 42
Figure 4.15 DCB graph for experiment B (3.5 g/m^2)..... 43
Figure 4.16 DCB graph for experiment D (7 g/m^2) 43
Figure 4.17 DCB graph for experiment F (10 g/m^2)..... 44
Figure 4.18 % Improvements due to fiber densities 44
Figure 4.19 % Improvements due to fiber densities (Comparison)..... 45

LIST OF TABLES

Table 1.1 CES result comparison 3
Table 3.1 Manufacturer designation table 24
Table 3.2 Header for DCB test 30
Table 4.1 Reference panel (base) results 41

SYMBOLS AND ABBREVIATIONS

CFRP	Carbon Fiber Reinforced Polymer Matrix Composites
DCB	Double Cantilever Beam
G_{IC}	Mod I Interlaminar Fracture Toughness
K_{IC}	Fracture Toughness
E	Elastic Modulus
PA 6,6	Nylon 6,6
SEM	Scanning Electron Microscope
FTIR	Fourier-Transform Infrared Spectroscopy
DSC	Differential Scanning Calorimetry
PCL	Polycaprolactone
ASTM	American Society for Testing and Materials
FA	Formic Acid
TFA	Trifluoroacetic Acid
TFE	Trifluoroethanol
TCM	Trichloromethane or Chloroform
IPA	Isopropyl Alcohol
THF	Tetrahydrofuran
XYL	Xylene
TAI	Turkish Aerospace Industry
ST	Super Tough
°C	Centigrade Degree

1. INTRODUCTION

In aerospace industry, interest in composite parts is increasing day by day. Because composite parts have high strength to weight ratio, high impact strength, good corrosion resistance and design flexibility. For that reason, number of composite components is increasing substantially every year.

Firms and researchers are also working to improve the material properties of composite materials every day. For example, in almost all aircraft projects, at Turkish Aerospace Industry (TAI), the problem of delamination between layers is observed during the demolding process after the production of the canopy skeleton of the aircrafts. For this reason, it is important to create a structure that will produce a solution to this and all similar delamination situations by conducting scientific research on the issue of increasing interlayer fracture toughness.

There are various methods for solving delamination, such as using 3D orthogonal & knitted fiber, edge design change, edge reinforcement, and resin toughening. With the electrospinning method used in this work the aim is to achieve this without a change in the geometry and by keeping the weight penalty and thickness increase as minimum as possible. Composite structure with fiber addition is shown on Figure 1.1. In this way, a multiscale lightweight structural intervention will provide the much needed resistance in the direction of separation [1].

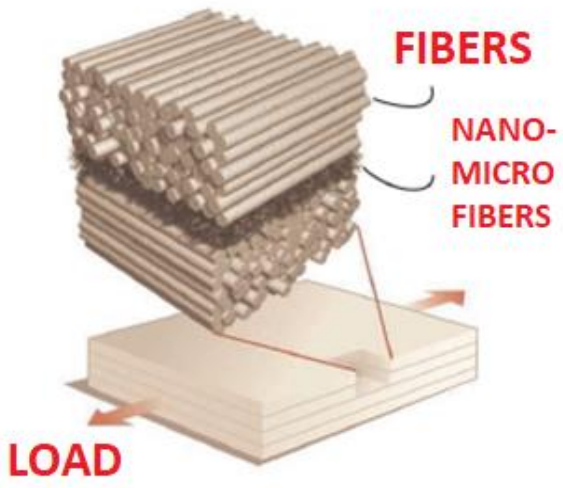

Figure 1.1 Composite structure with nanofiber added between layers [2]

Basically, electrospinning is a method of fiber production which uses electrical voltage difference to spin a polymer that was dissolved before as shown on Figure 1.2 [3]. Before electrospinning, the polymer to be used must be dissolved with a suitable solvent. Afterwards, the dissolved polymer passes through the syringe and is spun in electrical field created by applying a voltage difference between the tip of the syringe and a conductive collector. Randomly oriented nanofibers that are collected on collector create micro-nanofiber veil as shown on Figure 1.3.

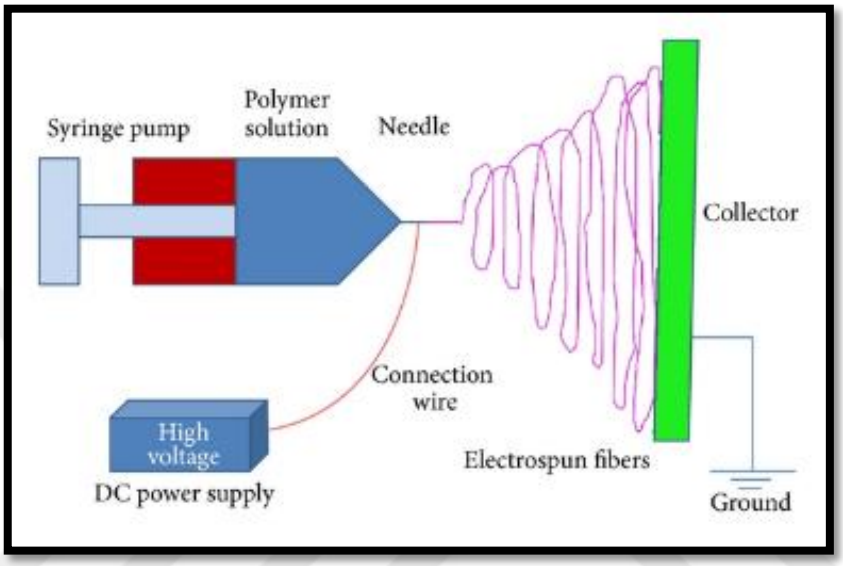

Figure 1.2 Electrospinning [3]

Figure 1.3 Interleaved veil [1]

Another issue that is as important as the process is the selection of the material that will be used in the electrospinning process. An approach can be to select the interface material using a materials selection software and database like CES. The matrix material of the CFRP is epoxy and the interface to be toughened can be considered as pure epoxy. Therefore, comparisons can be made with epoxy [4]. The intrinsic toughness can be estimated by the following equation 1;

$$G_0 = \frac{K_{IC}^{\ 2}}{E}\left(\frac{kJ}{m^2}\right) \quad \text{Equation 1}$$

where K_{IC} is fracture toughness in MPa·m$^{1/2}$ and E is the Young's Modulus in GPa. Comparison of several thermoplastics with epoxy reveals that commercially available PA 6, PA 6,6, ST-PA 6,6 are rather on top of the list (Table 1.1) and significantly tougher than epoxy alone. Among them, toughened PA's or ST-PA's (examplified by the ST-PA 6,6) have the potential to increase the resistance against delamination more than the regular PA's.

Table 1.1 CES result comparison

Name	Performance Index
PA (type 46, super-tough)	14.1
PA (type 6, toughened)	11.2
PA (type 4,6,extrusion)	10.4
PA (type 6,6, toughened)	10.1
PA (type 6,6, molding)	8.2
PA (type 6, cast)	7.39
Epoxy (Unfilled)	0.15

The toughness increment in ST-PA's are generally due to the added impact modifiers in the blend. This makes it challenging to dissolve such a polymer and it is necessary to choose the appropriate solvent [5] or solvent mixture [6] Another challenge is to adjust the electrospinning set-up to suit the material. In addition, curing processes should be reevaluated with this new interface to be created.

After all these processes are completed, the improvement in Mode I fracture toughness can be compared with the help of Double Cantilever Beam (DCB) test [1].

Interface toughening with electrospun veils is promising in that it is a low cost, scalable and effective method. It was also shown that multiple toughening mechanisms can be triggered at the same time or sequentially. An example of such triggers was shown with blends of two thermoplastics in one of our group's previous study [7]. There polycaprolactone (PCL) and PA 6 were blended in different proportions in the fiber level. PA 6 peeled off without any resistance and PCL alone formed an interpenetrating network with epoxy. Their co-existence in the fiber activated an effective bridging mechanism after debonding.

ST-PA's are generally commercial blends of a certain PA with an elastomer like ethylene propylene diene monomer (EPDM) rubber. Generally such compositions are trade secrets of companies and the specifications sheets do not indicate the used components. One of the primary goals of this work was to identify a solvent or solvent mixture for the successful electrospinning of a commercially supplied ST-PA, so that it can be interleaved in the veil form in a layered composite after electrospinning. With its relatively high toughness, the supplied ST-PA was hypothesized to give an improvement in resistance against delamination, if the previously observed mechanisms could be triggered in a similar way in this blend too.

The interface epoxy content of a layered composite is a function of the overall fiber/matrix ratio of the prepreg used. With higher matrix contents, the interfaces are already quite strong, but overall in-plane properties would be not as high as they should be. For many applications higher in-plane mechanical properties are desired. Therefore, fiber/matrix ratio in the prepreg level needs to be maximized, which in turn weakens the interfacial properties. It is these CFRP's that may especially benefit from the interleaving interventions. On the other hand, the epoxy amount left for the interface being low, means that there might be an optimum veil concentration at which the intervention would maximize its effect. This is a fact that was studied very rarely in the literature.

In addition, special care is needed in the layup and curing of these fiber rich prepregs. Accurate measurement of the transferred veil quantity was another

weakness in our previous studies. The layup, curing and testing stages of the process could be performed or controlled more accurately and reproducibly using the industrially controlled and certified capabilities of TAI. With these advantages, it was also possible to transfer accurately measured variable quantities of veils to the interface. Therefore, the hypothesis that there would be a distinct behavioral change in the improvement levels of toughness values in high fiber/matrix prepreg based CFRP interfaces could be studied rigorously. In this study, solubility of ST-PA 6,6 pellets, electrospinning of ST-PA 6,6 fibers and their use in layered composites are examined with the help of FTIR/DSC results of pellet, film and fibers, SEM results of fibers and DCB results of fiber reinforced layered composites.

2. LITERATURE SURVEY

2.1. Composite Materials

The physical combinations that are formed to obtain the mechanical or physical properties that cannot be obtained with a single material, generally consisting of the main component called matrix and other components called reinforcement, are called composite material. The main purpose in the formation of composite material is to take the superior feature of each material it contains and to reveal a new characteristic at a more desired level.

In most sectors, composite materials are preferred due to their great strength and stiffness combined with a light weight. The duties of the elements that make up the composite can be summarized as follows; reinforcement provides the desired strength and stiffness, while the matrix plays a very important role in transferring external loads to the reinforcement and forming the component in the desired geometry.

As seen in Figure 2.1, fiber-reinforced composite materials consist of layered structures arranged at different fiber angles. In this structure, the laying angles are selected according to the loading direction of the material. All fibers can be laid in the same direction (unidirectional) or at different angles of ±90˚ or ±45˚.

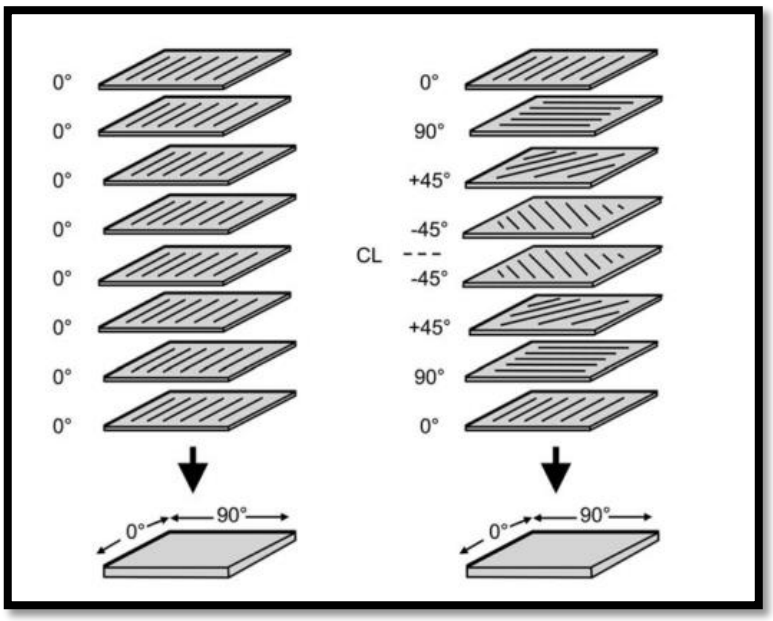

Figure 2.1 Composite material lay-up [8]

2.2. Damage Modes of Composite Materials

The damage mechanisms that can occur in a typical fiber reinforced polymer matrix are shown in Figure 2.2. In an FRP, the load on the matrix is borne by the fibers. The load transmission to the fibers takes place via the matrix. The initial form of destruction occurs when the fiber is unable to cope with the load when it is subjected to in-plane tension. The level of adhesion between the fiber and the matrix is the deciding factor for the third element, which will subsequently determine how the matrix's load is transferred to the fiber. When the matrix is subjected to out-of-plane loads, Mechanisms 2 and 4 take place. Delamination, the fifth mechanism, is the most frequent type of damage in composite matrices and leads to a decrease in the material's fatigue life [1, 9].

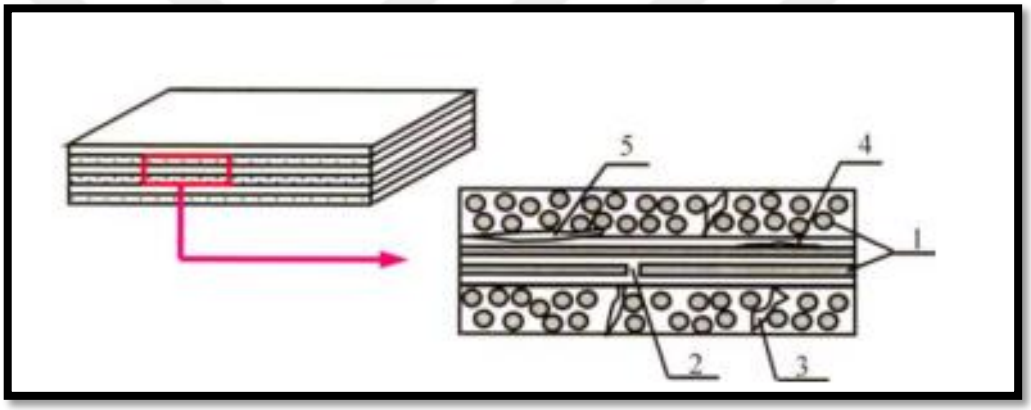

Figure 2.2 Damage mechanisms [10]

1) Reinforcement fibers
2) Fiber break
3) Matrix cracking
4) Fiber-matrix separation
5) Layer separation (delamination)

Damage modes in the delamination mechanism are examined with 3 main modes (Figure 2.3); Mode I (Tensile Mode), Mode II (Shear Mode) and Mode III (Tear Mode). There are also mixed modes where they can be seen together. Delamination may occur in one of these three modes or a mixture of them, depending on the load to which the matrix is exposed. The tensile delamination mode, called Mode I, is the most common type of failure and is also called crack opening mode.

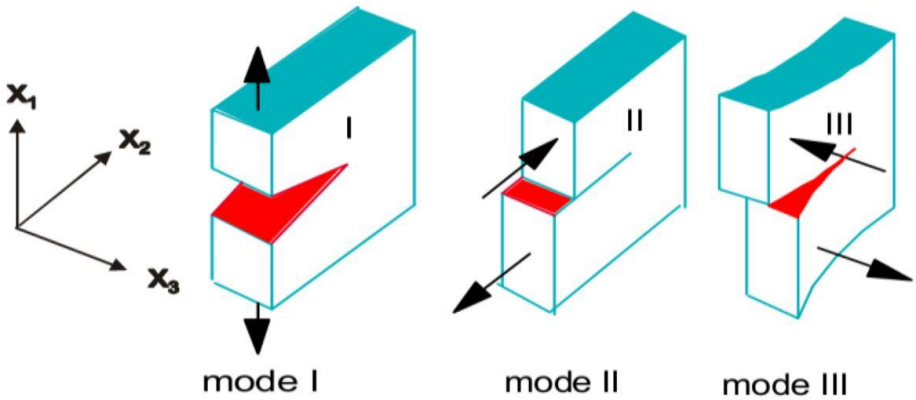

Figure 2.3 Failure modes [11]

The ability of FRP material to prevent the initiation and propagation of cracks in different conditions is called interlayer fracture toughness (G_{IC} for Mode I), and it is an important factor of the material's mechanical strength. There are multiple test methods used to determine this characteristic of the material, created by international standard organizations such as European Structural Integrity Society (ESIS), American Society for Testing and Materials (ASTM), and Japan High Polymer Center (JHPC). During the research, Airbus standard named AITM 1-0053 “Carbon fibre reinforced plastics - Determination of fracture toughness energy of bonded joints - Mode I - G_{IC}” was taken as reference [1, 9, 12].

This standard is used to determine the Mode I interlayer fracture toughness G_{IC} value using a double cantilever beam (DCB) sample of fiber-reinforced composite materials. DCB sample is a composite material that is rectangular and of a consistent thickness, with a non-adhesive insert situated in the center of the layers. Layer separation is provided by piano hinges or loading blocks according to standard document requirements. (Figure 2.4)

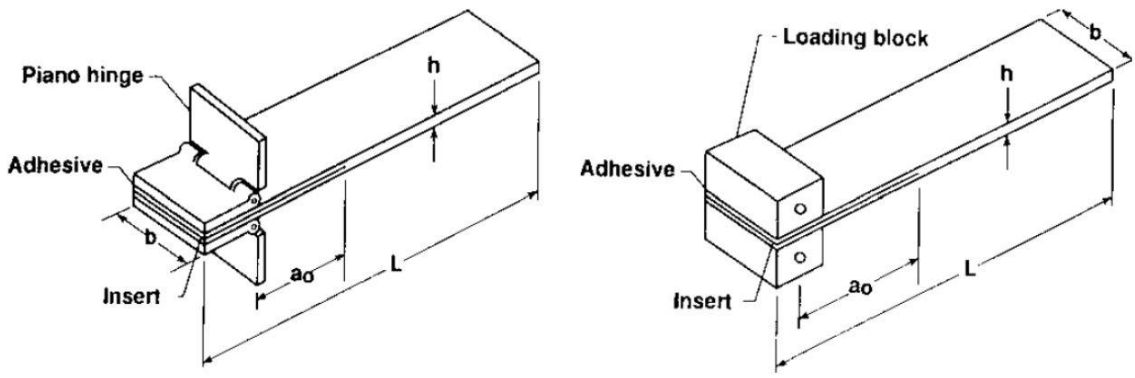

Figure 2.4 DCB (Double Cantilever Beam) test sample [9, 13]

During the experiment, the force and elongation that were put onto the sample are documented. With the help of these values, the Mode I interlayer fracture toughness G_{IC} value can be calculated.

The Resistance Curve displays the G_{IC} value as a function of crack length, beginning with the delamination of the non-stick insert in the middle layer in the DCB test and then gradually increasing (Figure 2.5) [1, 9].

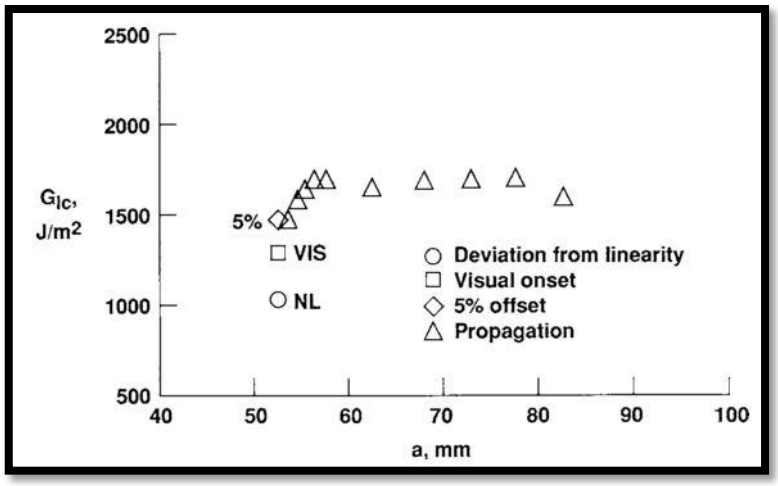

Figure 2.5 Resistance curve [9, 14]

Detailed information and formulas can found in original document [12]

2.3. Methods to Increase Delamination Resistance/Fracture Toughness

The method of increasing the interlayer fracture toughness is one of the possible solutions for delamination, such as the use of 3D orthogonal & knitted fiber, edge design change, edge reinforcement (Figure 2.6), and resin toughening methods [10]. The main differences here are lightness and thinness when we add weight penalty to the equation. Moreover, with this method, a solution proposal is presented without changing the design geometry [15].

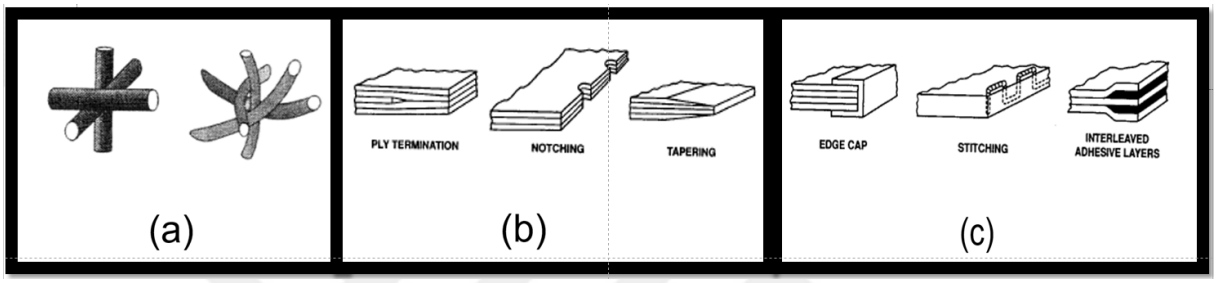

Figure 2.6 a) 3D Orthogonal & Knitted fiber b) Edge design changes c) Edge reinforcement [10]

To toughen the composite matrix, it is widely studied to add elastomeric[16], thermoplastic[17], micro[18]/nano-sized[19] inorganic particles or polymeric nanofibers to the matrix.

In addition to the structural toughening provided by single materials in this manner, it is also observed in papers that discuss toughening of epoxy matrices, hybrid systems, or epoxy-based composites. For instance, Sprenger et al. studied a hybrid mechanism formed with nano-silica particles to eliminate the influence of elastomeric tougheners which lower the elastic modulus of epoxy. While an increase in fracture toughness was observed in the system using only elastomer, a decrease was observed in elastic modulus, while an increase in fracture toughness and modulus was observed in composites using only with nano-silica. In the hybridized system with nano-silica particle elastomer mixture, it was observed that the decrease in elastic modulus was almost prevented and a significant increase in fracture toughness was achieved [20]. In another example, Mirmohseni and Zavareh toughened the epoxy with a hybrid system of thermoplastic poly(acrylonitrile-co-butadiene-co-styrene) (ABS), nano clay and nano titania particles. Thanks to

synergetic system, a simultaneous increase in tensile and impact strength has been observed [21].

Coating the carbon fibers used in carbon fiber reinforced polymer matrix composites (CFTP) with diverse chemicals or constractions (functionalization) is another method used to increase the interlayer mechanical properties. In one example, Sager applied carbon nanotubes to the fibers of carbon fiber reinforced epoxy matrix composites and then studied the consequences this had on the interlayer mechanical features of the composite. The coating of the fibers resulted in a decline in the tensile characteristics of the composite but increased the shear strength between the layers [22].

Alternative method of increasing the fracture toughness of composites is to place toughening particles, films, toughened resins, micro/nanofibers or hybrid systems. These are performed together between the composite layers. Jiang et al. placed polyethylene terephthalate (PET) films between the composite layers and a decrease in Mode I fracture toughness and an increase in Mode II fracture toughness were observed [23]. McGarry et al. placed a tougher silicone resin different from the matrix resin between the composite layers with silicone matrix resin, observed an increase in the toughness of the composite [24].

Hybrid matrices/systems that more than one material is used in interface toughening procedures are also encountered. Between the layers, Sue and White placed polyamide particles with an epoxy layer (epoxy/PA) and epoxy layers (epoxy/PA/CNT) with carbon nanotubes added with PA particles. An increase in the fracture toughness of the composite reinforced with epoxy/PA was observed. In addition, it was observed that the fracture toughness of the epoxy/PA/CNT reinforced composite increased 50% due to epoxy/PA composite [25]. Meireman T. & Daelemans L. used Polyamid 11 (PA11) & Polyether block amide (PEBA) and dissolved them separately but electrospun to the same collector to create combined matrix which improved the structure fracture toughness in both Mode I and Mode II [26]. Emanuele Maccaferri & Matteo Dalle Donne are recently studied electrospinning of PA 6,6 and after NBR impregnation which creates even tougher

mechanism than one single material. Also effect of different type of thicknesses are examined in that work [27].

Although the effects of increasing fracture toughness are observed in all these applications; the amount of material placed between the layers should increase up to a certain level. For these reasons, the weight penalty that comes with add-ons to be high. In the literature, it is researched that this point is being addressed by reducing the size/amount of the materials used in interface toughening strategies to submicron and nanoscale and adding them to the interface [1, 10].

The strategy of adding thermoplastic nano-micro fiber between CFRP layers is shown earlier in Figure 1.1 in the Introduction. Having a high specific surface area allows better bonding with the matrix resin, and being thin and light, they do not significantly affect the layer thickness and weight of the composites to which they are added. An important advantage of lightweight thermoplastic tulle in nano-micro size is that they do not block resin flow during curing, thanks to their high porosity [28].

Interface toughening studies with nano-micro fiber insertion method between layers in the literature can basically be divided into three groups:

1) Studies using single polymer (homopolymer) nanofibers.
2) Multiple polymer nanofibers; studies in which fiber blends are used, in multiple layers or in core shell form.
3) Studies in which hybrid systems obtained by mixing another component into the polymer are used by turning them into nanofibers (i.e. blends).

These studies can be examined with test results in appendix A. Tests, polymers, fiber materials, solution parameters, fiber diameters, areal density of fibers, production-cure methods, ply sequence & orientations are the different information that can be found in this table.

The table given in Appendix B is a version of the table prepared by Palazetti in 2017 [29]. As can be seen from the table, many polymers have been studied, but the common ones are PA and PCL. The reason for this is that, as we mentioned in the Introduction, the intrinsic toughness of these two is relatively high and they are easily accessible commercially. PA 6 and PA 6,6 are frequently used among PA varieties, and solvents such as TFE, TFA, FA are mainly used for the dissolution of these materials [1]. Although standard PAs without any additives can be dissolved with a single solvent, modified PAs and blend PAs cannot achieve complete dissolution with a single type of solvent [7] [30].

Considering the blend work, Biber used FA, Xylene, 2-Propanol solvents to create the n-butyl acrylate-maleic anhydride/E-nBAMAH + PA 6 blend in 2010 [6].

Saghafi used FA:AA solvents with a ratio of 50:50 to create the PA 6,6/PCL blend in 2014. As a result, 30 µm thick veil provided a 56% improvement in Mode II [31].

Kılıçoğlu worked with PA6/PCL blend in 2018 and used TFE as a solvent. The veil with a areal density of 6.4 g/m^2 obtained by spinning as a result of dissolution provided 69% improvement for crack initiation and 59% for crack propagation. In the same study, PA 6 material was continued due to the absence of a transparent solvent for the dissolution of ST-PA 6,6 material [1].

Maccaferri used 55:45 ratio FA:TCM solvents to create the PA 6,6/NBR blend in 2022. As a result, tulle with a areal density of 9-10 g/m^2 provided 180% improvement in Mode I [27].

The common feature of blend systems is the addition of different solvents to ensure complete dissolution. And these systems generally provided tougher structures compared to single polymer tulle. As a ST-PA 6,6 blend, there was no study other than Kılıçoğlu's preliminary trial.

2.4. Electrospinning

Electrospinning is a method of producing polymer-based fibers with diameters ranging from nanometers to micrometers using electrostatic forces. Polymer/polymers must be mixed with solvent or multiple solvents to create a proper solution which lead to electrospinning. In this method, certain voltage is applied between the pre-mixed polymer solution placed in a syringe and the collector. Under this voltage, the charged polymer jet accelerates towards the counter-charged collector. This system can be vertical or horizontal. The polymer solution drop

collected at the tip of the needle, which moves at a certain flow rate with the help of the pump, is in a spherical shape with the effect of surface tension forces. As soon as the applied potential voltage reaches the threshold voltage value, electrostatic forces and surface tension forces are equalized. At this point, the polymer solution drop takes the form of a cone called the Taylor Cone. After this point, the droplet moves towards the collector by whipping and pulling under the electric field. During this movement, the solvent evaporates and the polymer remains, resulting in collection on the collector. Figure 2.7 shows the formation of the Taylor cone and the exit of this cone as a jet.

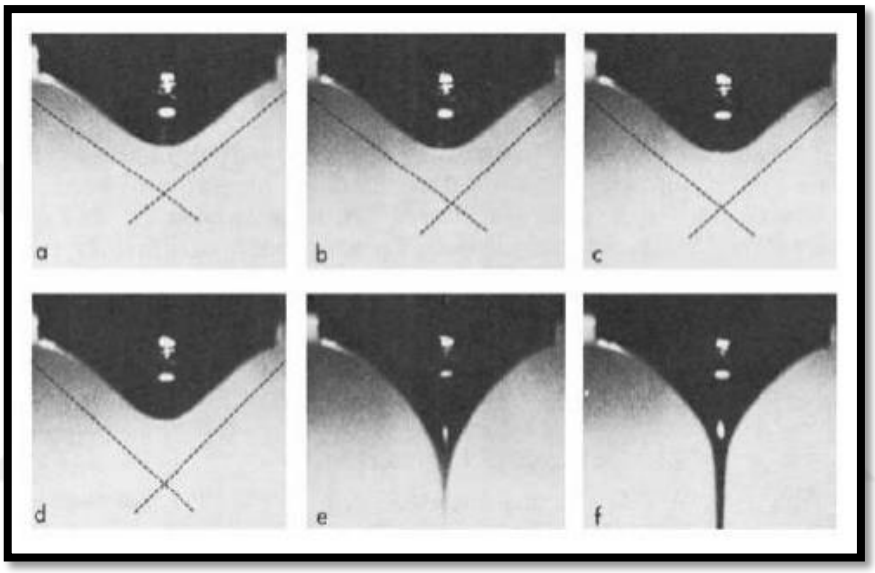

Figure 2.7 Taylor cone formation diagram and droplet jet flow [32]

A simple electrospinning mechanism (Fig. 2.8) basically consists of a high voltage source, polymer feeder (Syringe/pump), needle and collector.

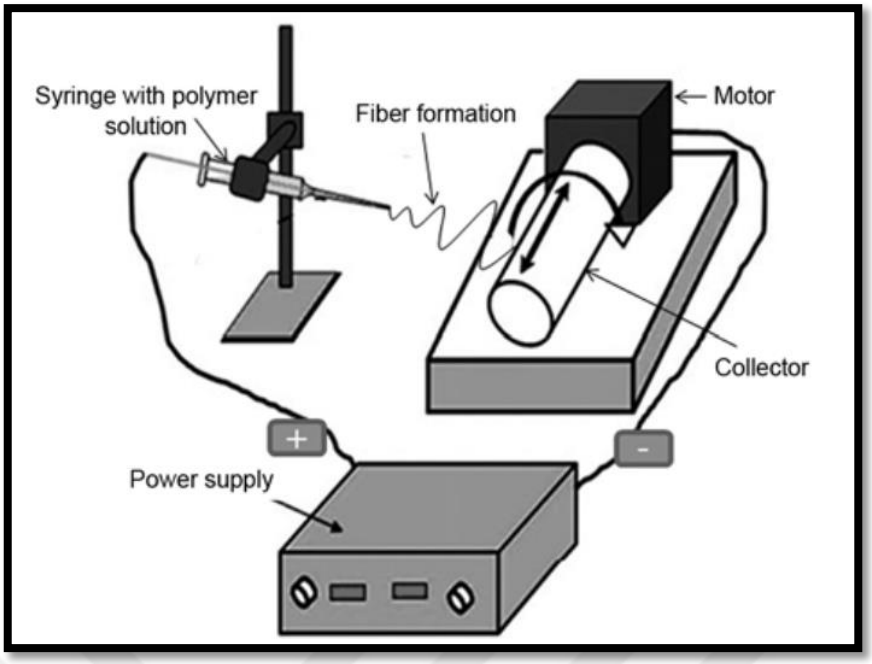

Figure 2.8 Simple electrospinning mechanism

Electrospinning process parameters can be grouped as follows:

Polymer solution parameters:

- polymer molecular weight
- solution electrical conductivity
- solvent dielectric coefficient
- solution viscosity
- solution surface tension

Application parameters:

- voltage
- solution feed flow
- needle-to-collector distance
- collector material/shape and surface quality
- needle tip diameter

Ambient conditions:

- temperature
- air pressure
- humidity

Electrospinning process can be applied any polymer solution under proper conditions & parameters which are noted above.

3. EXPERIMENTAL STUDIES

3.1. Electrospinning Solution Preparation

ST-PA 6,6 used in the studies was purchased from GoodFellow Cambrige Limited and used as it is. Trifluoroethanol (TFE), formic acid (FA), hexafluoroisopropanol (HFIP), trifluoroacetic acid (TFA), trichloromethane (a.k.a. choloroform) (TCM), isopropyl alcohol (IPA), xylene (XYL) were supplied from Merck and used to form various solvents. All solvents were first tested individually by mixing a fixed quantity of the ST-PA 6,6 with a magnetic stirrer overnight. None of them could fully dissolve this blend alone, but with some mixtures (either a single solvent or a solvent mixture) "milky" consistency could be obtained and spinning processes were carried out with these. All solvent experiments carried out and the reasons why these experiments were performed in this specific sequence is given in Figure 3.1.

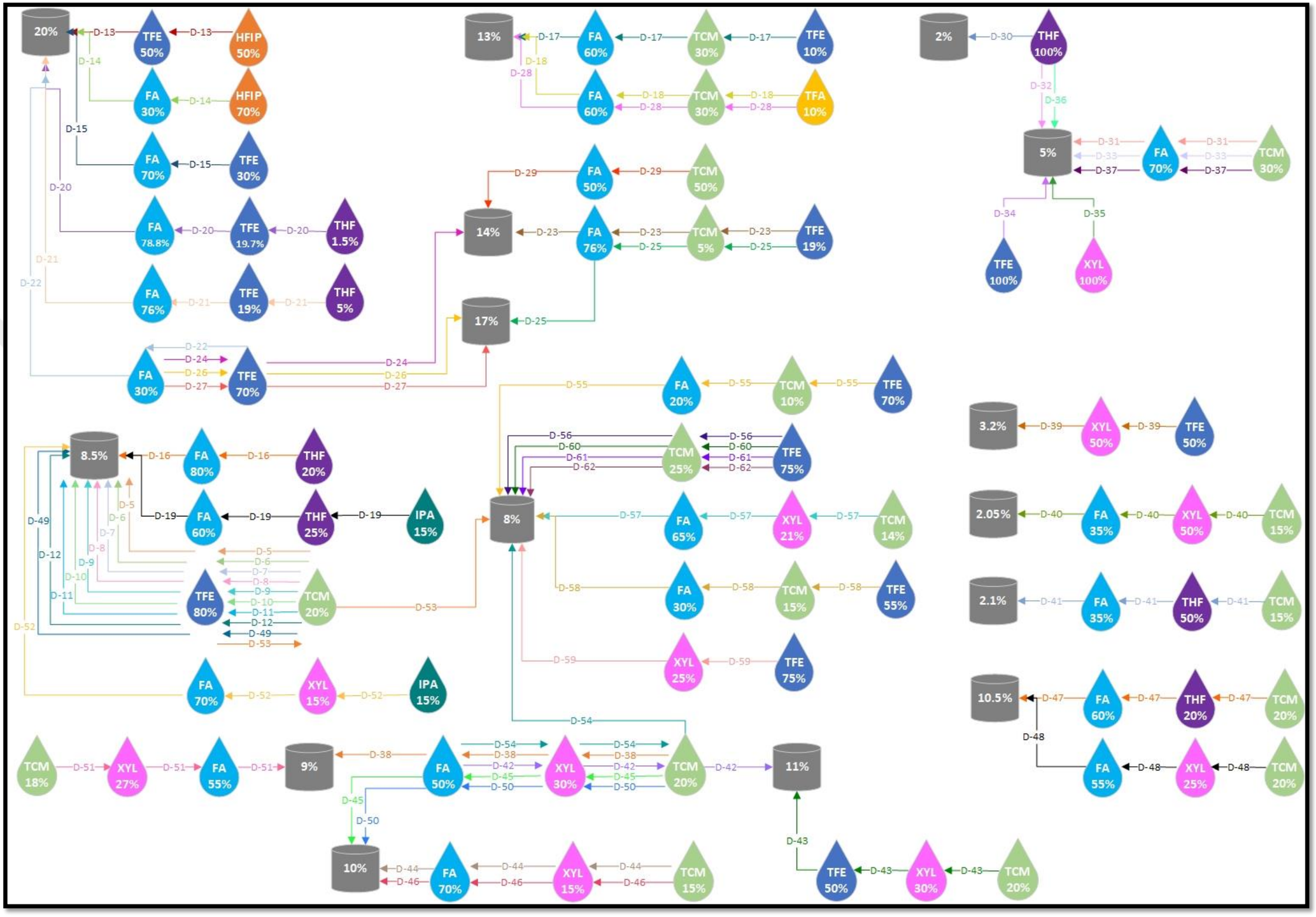

Figure 3.1 Solution experiments flow chart

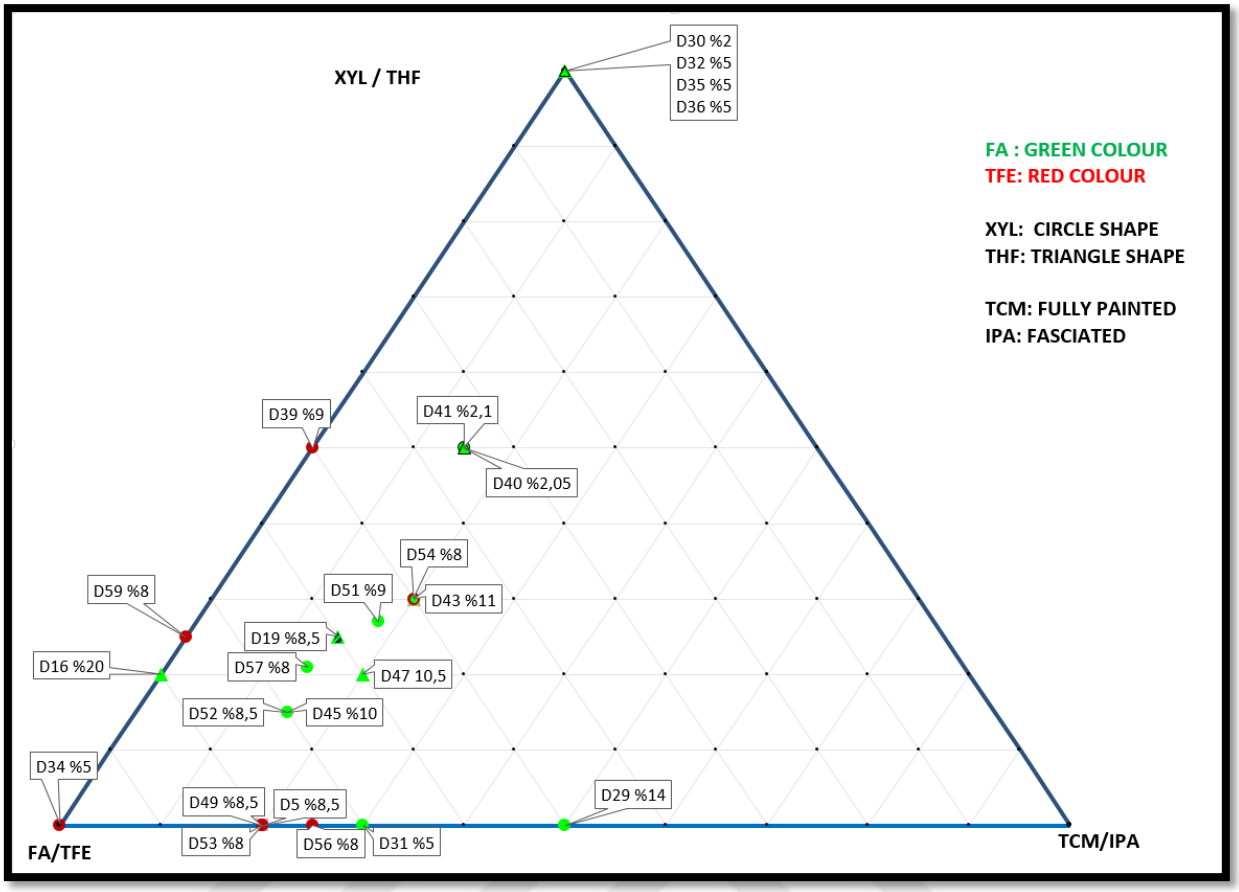

Figure 3.2 Composition diagram of general solvent experiments

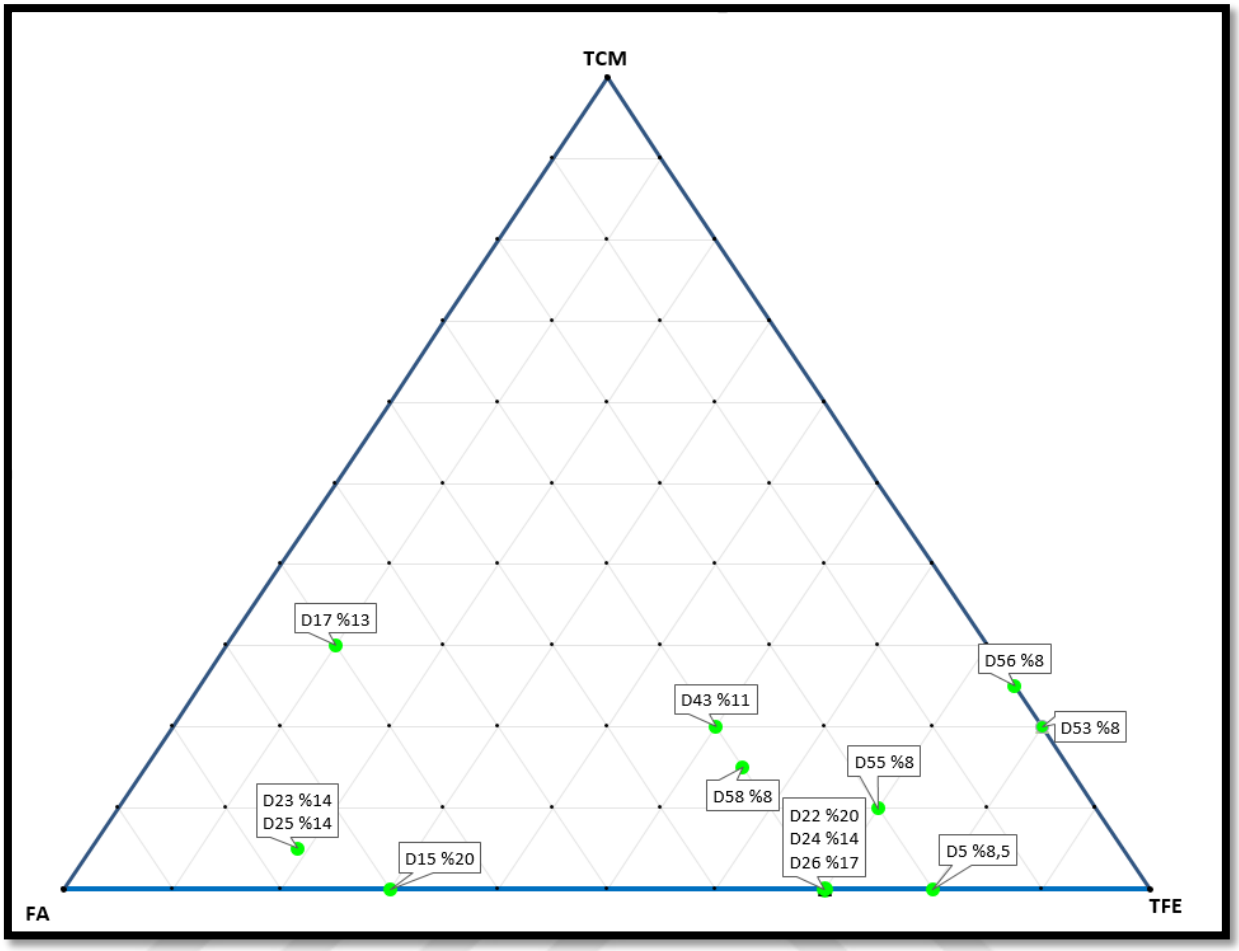

Figure 3.3 Composition diagram of selected solvent experiments

Significant solvent experiments are shown in Figure 3.1, some of these experiments were created with binary and triple combinations of alternative solvents given in Figure 3.2. Figure 3.3 shows its triple combinations specific to FA, TCM and TFE. These combinations are placed in the triangle according to their % values. The detailed description of all experiments, respectively, is given in appendix B. As a result, D56 formula 75:25 TFE:TCM was used because it gave the best and most efficient result.

3.2. Electrospinning

For electrospinning part several materials were used. Moving syringe system has a motor which is powered and controlled by Arduino Uno and a driver. Moving mechanism is basically a rubber which is non-conductive. Also auxiliary electrode holder is made from wood for the same reason. Auxiliary electrode made from thin copper to build electrical field intensity. Pipe, syringe & pump mechanism are non-

conductive plastic. Needle is steel which is bought from pharmacy with syringe. Set up cover box is made from plexiglass to prevent effect of any other electrical field.

Spherical thin titanium sheet metal is made with roll operation. This collector was located over 4 rotating aluminum discs (Figure 3.4). The reason for choosing collector material as titanium is removal of micro-nanofiber veil from collector surface to the prepreg thoroughly. Both copper & aluminum collectors were tested. Best result was obtained with titanium. In addition to this, after every experiments, systematically, collector surface was ground with 500 & 800 grit sandpaper.
Since most of the solvents have harmful content, the controlled environment is split because they will affect respiration. In addition, the mixture should be prepared using personal protective equipment. Here, solvents such as TFE & FA, previously used for PA6, will also be tested for the super tough in different configuration. It is important to achieve as homogeneous dissolution as possible for electrospinning.

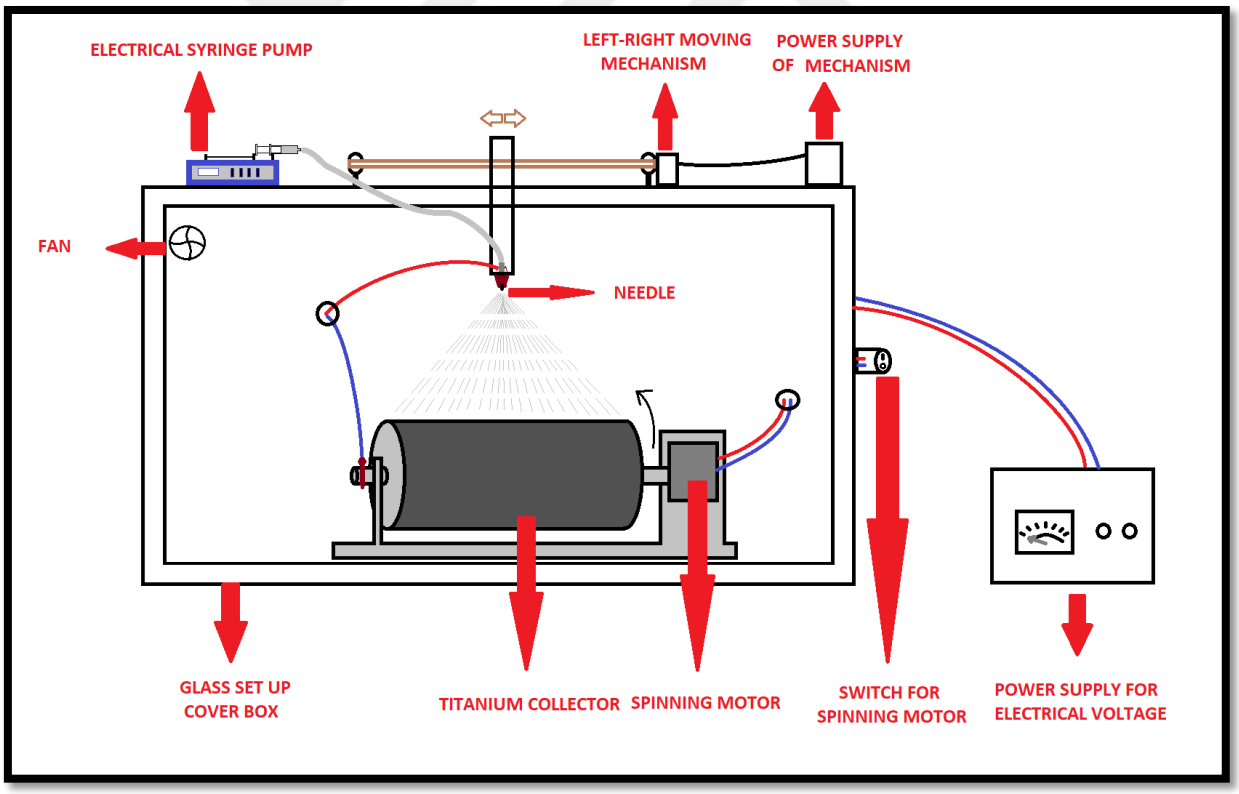

Figure 3.4 Drawing of ES cabin used in experiments

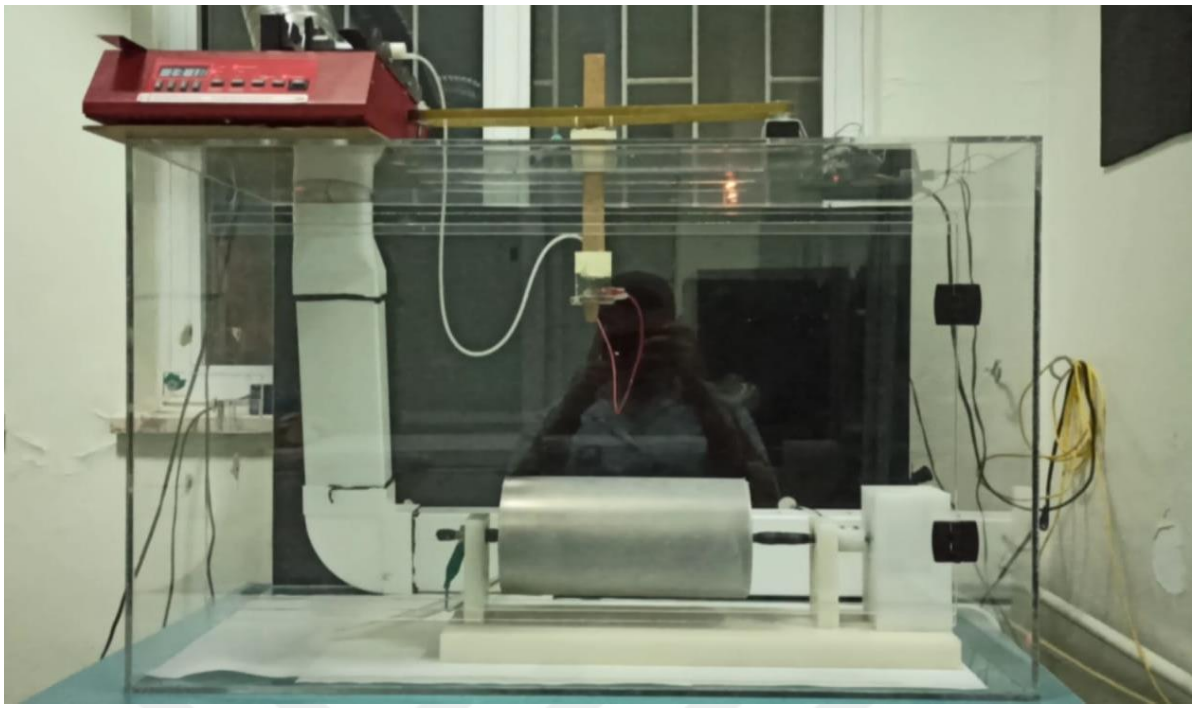

Figure 3.5 ES cabin used in experiments

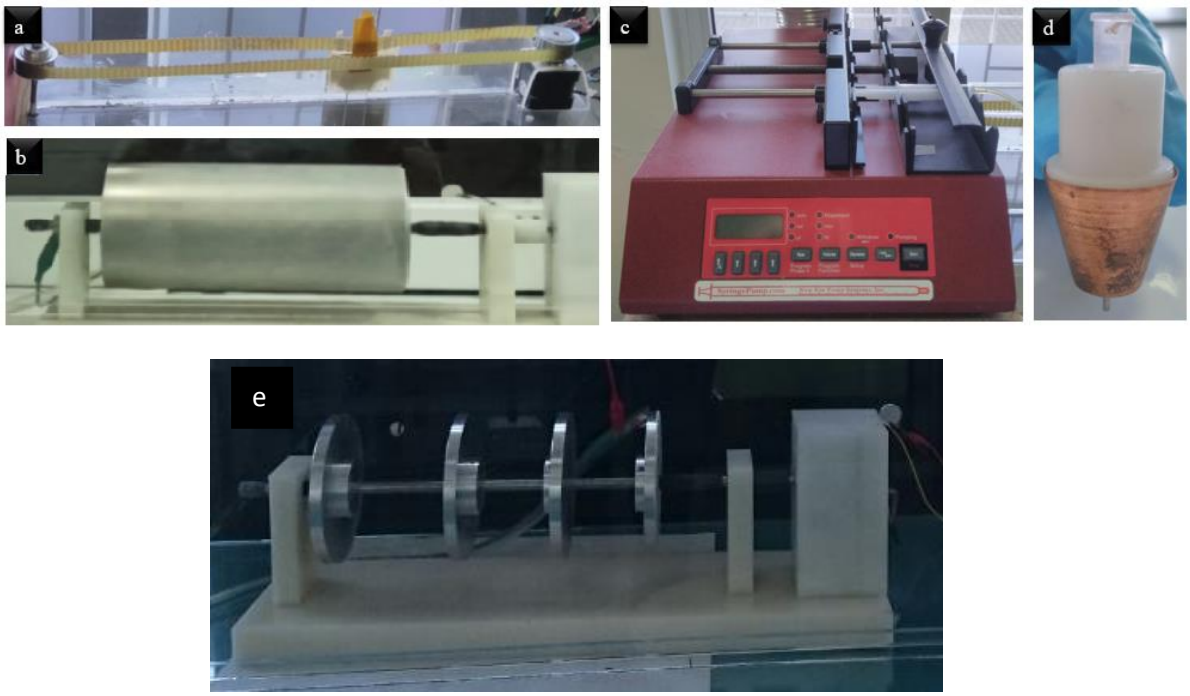

Figure 3.6 ES cabin used in experiments

(a) Moving syringe system, (b) thin titanium plate collector wrapped around 4 rotating aluminum discs, (c) syringe pump, (d) auxiliary electrode, (e) collector base with aluminum discs.

Thanks to the moving syringe system and the collector's rotation system (Figure 3.5 & 3.6), homogeneous spinning and the same areal density in every region of the sample are obtained. To prove that, after interface transfer, remaining veils were removed from 4 different location (Figure 3.7) and measured weights. It showed same results for each of them.

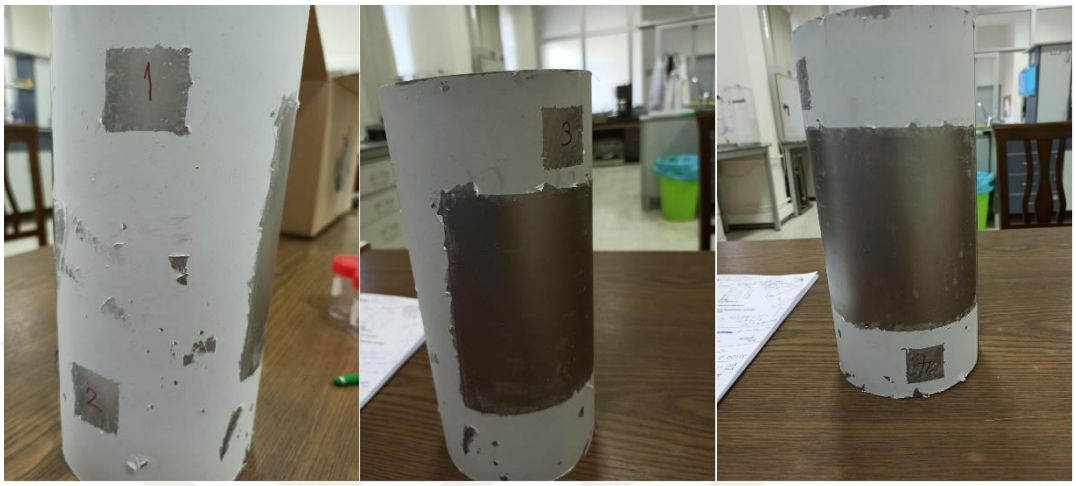

Figure 3.7 Weight sample for 4 different locations

On the other hand calculated weight and densities were so close with measured values. (Equation 2,3,4 &5)

Sample Calculation formula;

$$\text{Calculated Weight (g)} = \text{Spinning time (hr)} \times \text{Solvent Density} \left(\frac{\text{g}}{ml}\right) \times \text{Flow Rate} \left(\frac{ml}{\text{hr}}\right)$$

$$\text{Calculated Weight (g)} = 1\ (\text{hr}) \times 0.1 \left(\frac{\text{g}}{ml}\right) \times 2.8 \left(\frac{ml}{\text{hr}}\right) = 0.28\ (\text{g})$$

Equation 2

$$\text{Calculated Density} \left(\frac{\text{g}}{m^2}\right) = \frac{\text{Calculated Weight (g)}}{\text{Spinned Area } (m^2)}$$

$$\text{Calculated Density} \left(\frac{\text{g}}{m^2}\right) = \frac{0.28\ (\text{g})}{0.07425\ (m^2)} = 3.8 \left(\frac{\text{g}}{m^2}\right)$$

Equation 3

$$\text{Measured Density } \left(\frac{\text{g}}{m^2}\right) = \frac{\text{Measured Weight (g)}}{\text{Measured Area } (m^2)}$$

$$\text{Measured Density } \left(\frac{\text{g}}{m^2}\right) = \frac{0.0014 \text{ (g)}}{0.0004 \ (m^2)} = 3.5 \ \left(\frac{\text{g}}{m^2}\right)$$

Equation 4

$$\text{Loss } (\%) = \frac{3.8 - 3.5}{3.8} \times 100 = 7.9 \ (\%)$$

Equation 5

The spun veil was placed in the transport box in the clean room of the laboratory in such a way that it would not be breathed in or come into contact with, and was stored in that box until it was opened in the clean room of the factory. This process took place between 8-12 hours, because with the passage of time, the spinnned fibers adhered to the collector more and became more difficult to remove.

In addition to all these, calibrating the pipettes used while preparing the mixture, with the help of the parafilm, closing the caps of the glass bottles in which the mixture takes place, keeping the mixture temperature as constant as possible are some of the most important precautions in these processes.

3.3. Prepreg

All prepregs in which micro-nanofibers are added to the interface are named "CARBON FIBER REINFORCED EPOXY PREPREG UNIDIRECTIONAL TAPE 180˚C CURE STANDARD MODULUS FIBER, IPKC2-1/A49/34RC/UD/194/12K", manufactured by Dowaksa Advance Composites used in TUSAS (Figure 3.8). The resin in its content has a curing class at 180 ˚C. Also resin density and fibre density values are 1.298 g/cm^3, 1.799 g/cm^3.

Table 3.1 Manufacturer designation table

IPKC2-1/A49/34RC/UD/194/12K	
C2-1	Resin Designation
A49	Carbon Fibre Type
34RC	Resin Content by Weight
UD	Uni-Directional Tape
194	Fiber Areal Weight (g/m^2)
12K	Number of Fibers in a Fiber Bundle

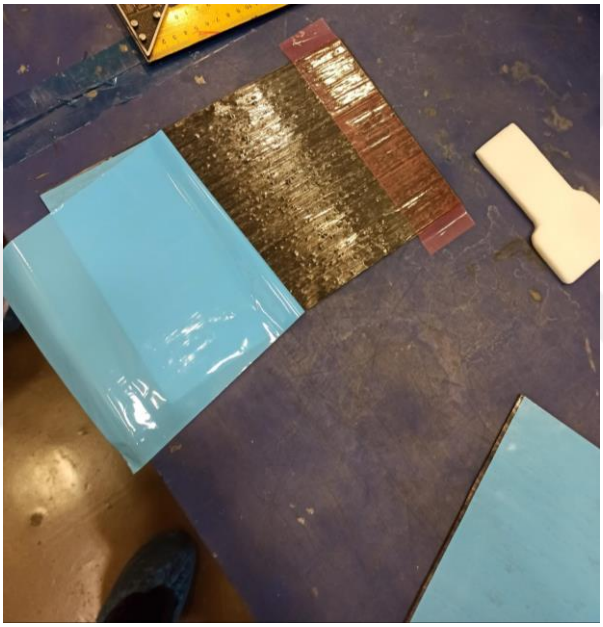

Figure 3.8 Prepreg

3.4. Lay-up of CFRPs

Before lay-up process, the prepregs were taken out of the refrigerator 1 day before they were ready for cutting in the desired dimensions, and the out-date & time from the refrigerator and the remaining life information are noted. The next day, the preregs were cut to the desired size with the help of a ply cutter. The cut prepregs are marked as a package. Afterwards, it was transferred to the clean room for the clean room lay-up process. Meanwhile, a flat metal tool (Figure 3.9) to be used for laying is cleaned with alcohol-based chemicals and taken to the clean room by applying a separator. And again the remaining life is noted. In accordance with the clean room rules, after wearing gloves, bonnets and overshoes, Teflon strip tape and sealant tape are applied to the tool surface.

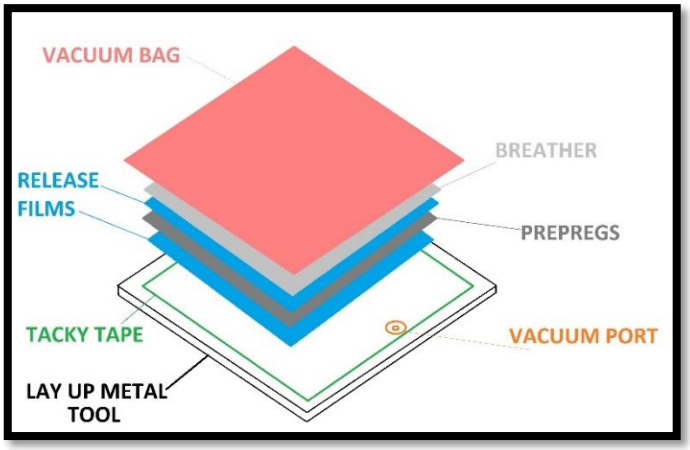

Figure 3.9 Lay-up sequences

The release film is carefully placed inside to prevent the prepregs from sticking directly to the tool. The prepreg prepared by cutting 9 layers on the right and left for the base and fiber configuration is laid by separating from its own protector. A pre-compaction is taken on the first and every 4 layers. See Figure 3.10 for pre-compaction.

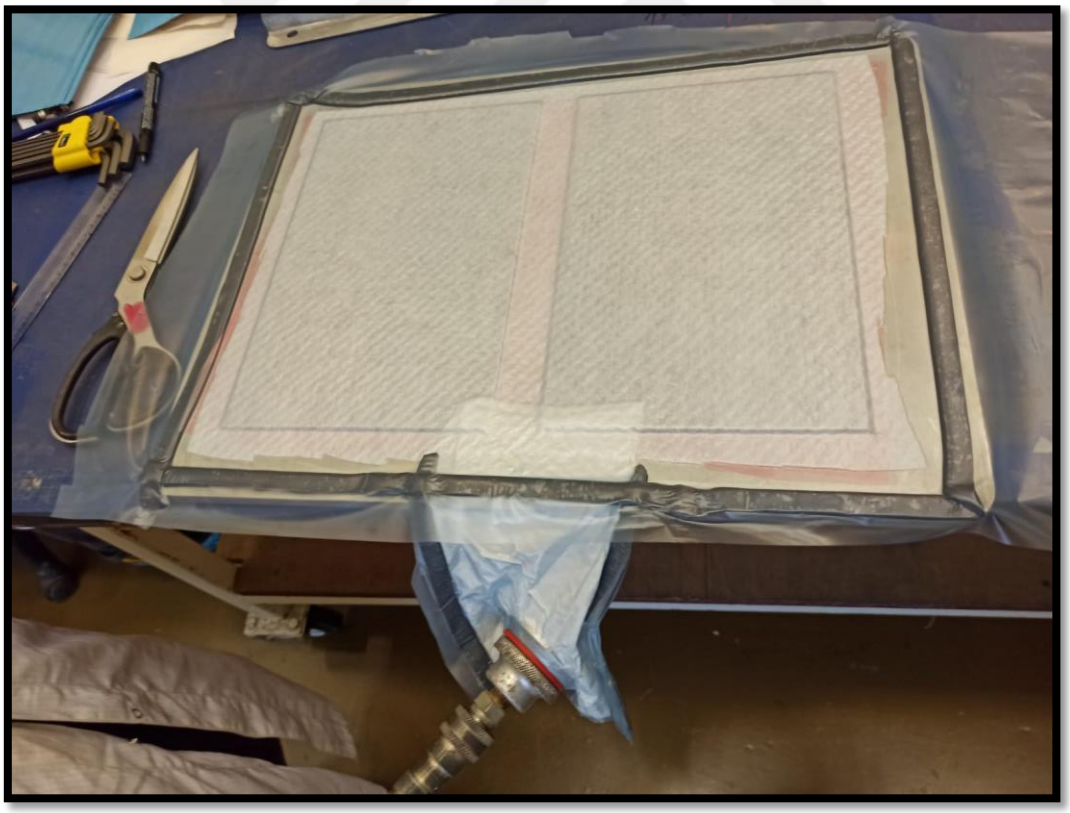

Figure 3.10 Pre-compaction

In the pre-compaction process, 1 more layer of release film and breather is drawn on the prepreg. The vacuum port is placed so that it does not touch the plies. And the bag is well adhered to the sealant. Where the vacuum port is, a small cut on the bag is made with the help of a razor blade knife. From here, the port is connected to the vacuum system. In the meantime, 1 ply UD is tucked up (Figure 3.11) and adhered on the micro-nanofiber tulle on the cylindrical collector.

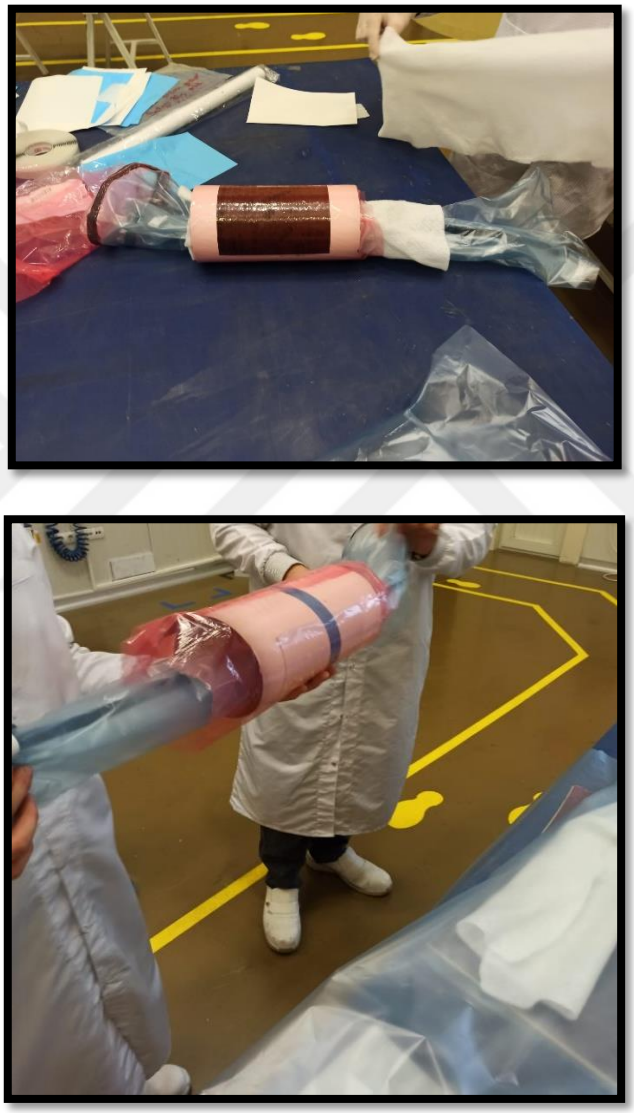

Figure 3.11 UD bonding to micro-nanofiber veil

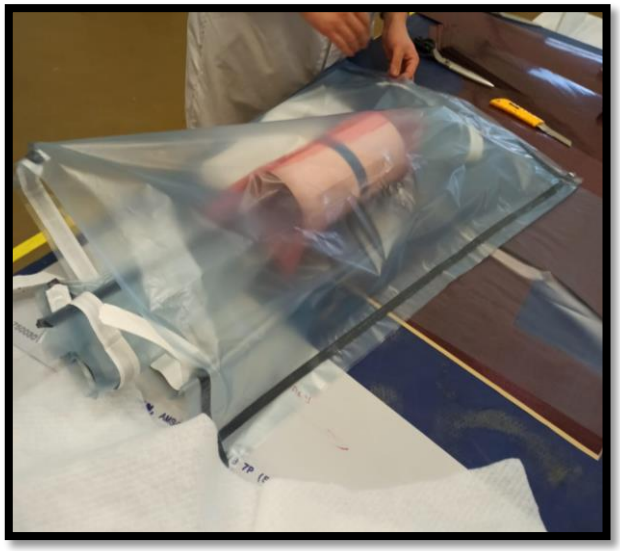

Figure 3.12 UD bonding with the help of double sided bagging

As shown in the figure 3.12, double-sided bagging is done to hold each other inside and outside the cylinder. This process facilitates the transfer of all micro-nanofiber tulle transferred to the surface with the help of vacuum of the bonded ply. After the vacuum process, the veil is slightly scratched from all its edges so that while separating the ply from the cylindrical surface, the other tulle does not come with a sticky ply (Figure 3.13).

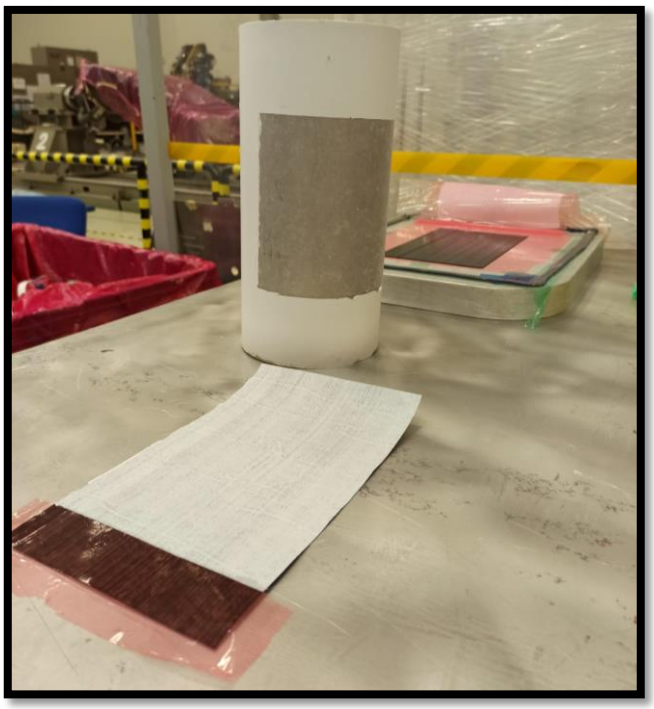

Figure 3.13 Separation of fiber adhered UD from titanium collector

Then, a release film for pre-crack is placed on the laying in base and fiber configurations coming out of the intermediate vacuum on the side, as in the DCB standard. For the fiber configuration, the bonded tenth ply is carefully placed upside down with the fibrer part inside. For the base configuration, 1 UD is placed at the same time. Then it is taken to pre-compaction again. Afterwards, the remaining 8 plys are laid by considering the pre-compaction method. Thereafter, it is taken to the final compaction and sent to the autoclave cycle (Figure 3.14 & 3.15).

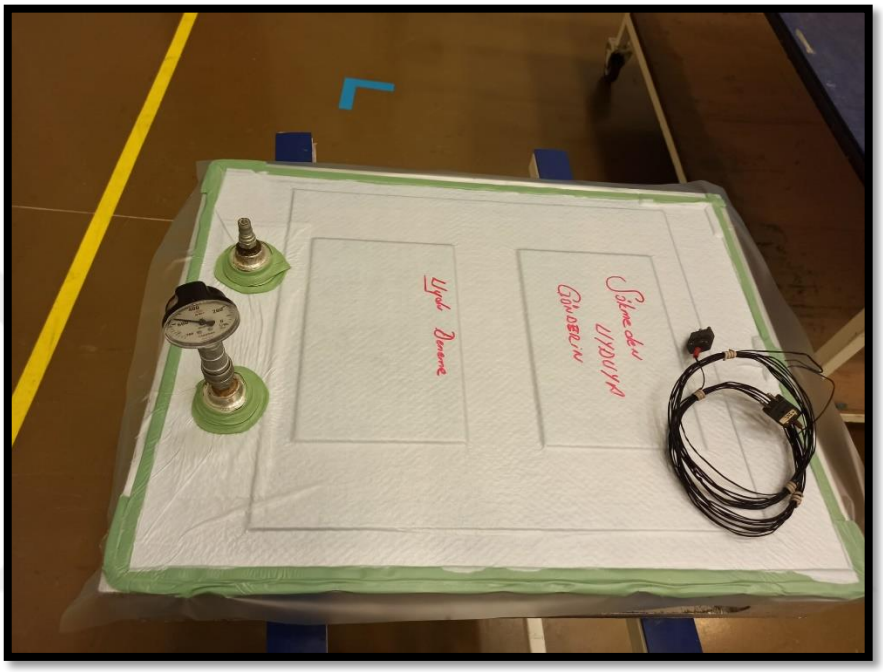

Figure 3.14 Final compaction

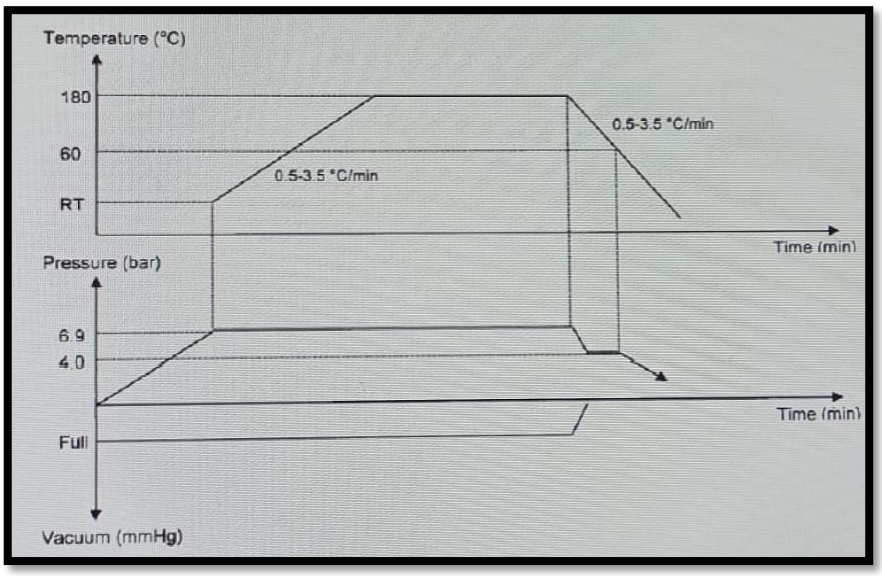

Figure 3.15 Autoclave cure cycle of prepreg

All material life times are noted again and control is provided. After the autoclave cycle, the tool is demolded and the resin residues are cleaned from the edges (Figure 3.16).

Figure 3.16 Demolded samples (Base & Fiber configurations)

Samples are directly sent to composite cutter machine to adjust width-length according to DCB standards (40 mm initial crack zone, 250 mm total length, 25 mm width).

3.5. Mechanical Test for Mode I Fracture Toughness

After composite cutting operations, DCB test coupons are marked as “base” or “fiber”. For every single fiber configuration, another base is cured in the same bag and the same cure cycle. The reasons of that are:

i) Elimination of outside conditions such as cure cycle differences, compaction differences, temperature and pressure differences which are already controlled.

ii) Elimination of UD prepreg batch differences (Every batch of prepregs have their own mechanical properties even though they are dependent the same material specifications)

iii) Elimination of prepreg out-time conditions (Every samples (Base + Fiber) are removed from refrigerator at the same time.)

Marked coupons are sent to test laboratory for Mode I (G_{IC}) fracture toughness testing process. Header is prepared for every test operation (See table 3.2 for example).

Table 3.2 Header for DCB test

Test Method	AITM 1-0053
Test Equipment	Instron 5966
Test Speed	5 mm and 10 mm per min
Part Number	A35-AITM 10053-THINUD
SOIR Number	ALICAN TEZ-D
Temperature	23°C
Humidity	48 %
Date	23.12.2022
Operator	C.M.Gundes & A. Kara

Then, piano hinges are located to precrack one of the specimens (Figure 3.17).

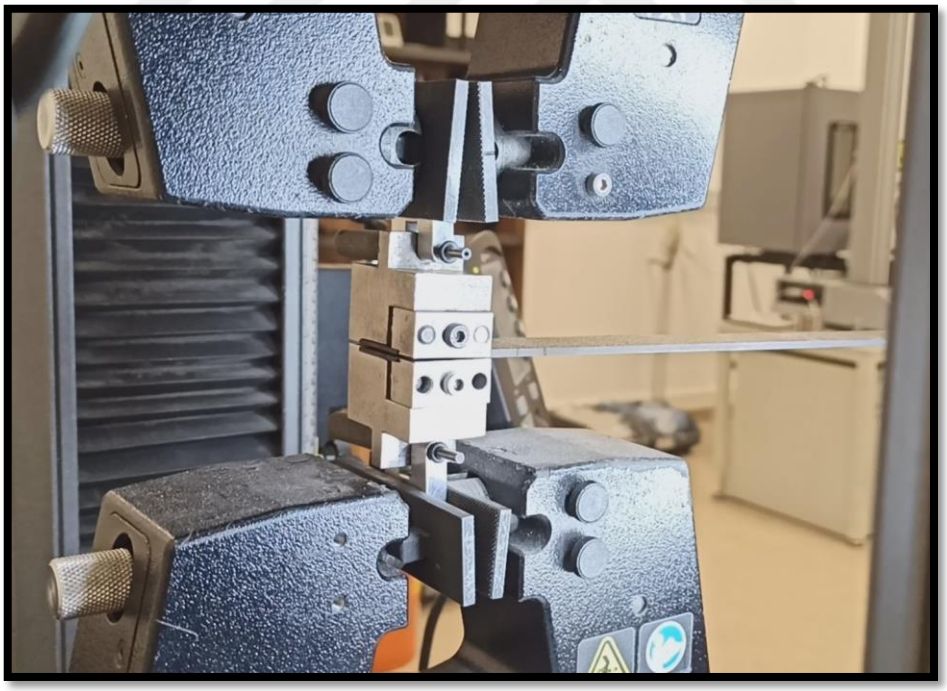

Figure 3.17 Piano hinges with DCB coupon

According to DCB documents all points are marked and examined under professional Smartzoom Zeiss PlanApo D 0.5x/0.03 FWD 78 mm machine (Figure 3.18).

Figure 3.18 DCB test & Smartzoom machine

Thanks to Bluehill Universal Software, all results can be get directly from the program with only simple operator inputs (Figure 3.19).

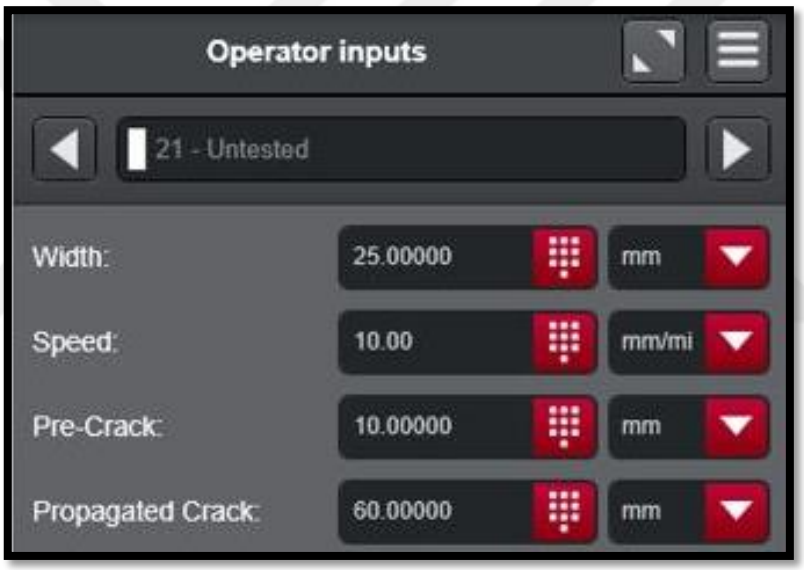

Figure 3.19 DCB test inputs

Test standard AITM 1-0053 cannot be shared due to legal obligations however it is quite similar with ASTM 5528 test standard.

3.6. Material Characterization

After solution preparation and electrospinning processes, a micro-nanofiber veil has been prepared on collector. SEM (FEI Quanta 200F) was used to examine the content of this veil structure and to detect the differences and similarities in the microstructure. On a black background, tiny samples are located for SEM as shown on Figure 3.20.

Figure 3.20 SEM sample

Then all samples are examined under SEM and prepared their images under certain magnification values. (Figure 3.21)

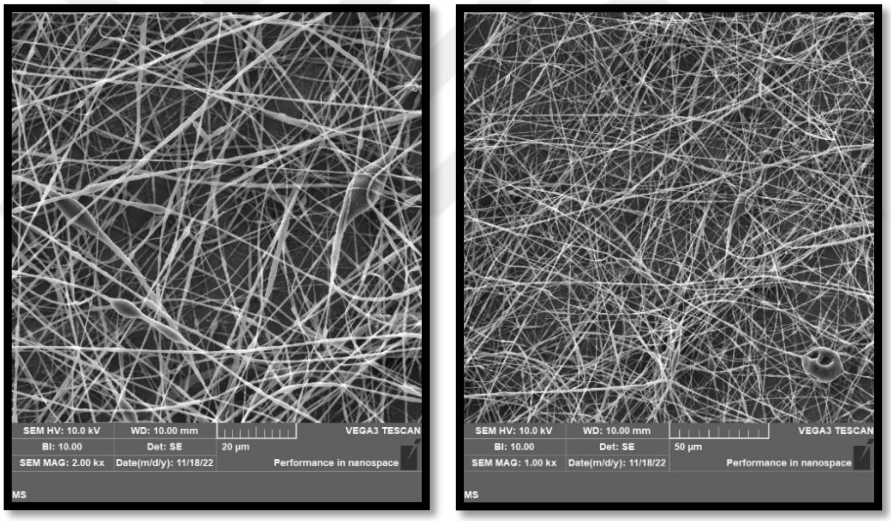

Figure 3.21 Example of SEM data with different scale values

Also Beads and all orientations can be examined from SEM data. On the other hand, fiber diameters can be detected with the help of the ImageJ program.

The spectra of the samples were recorded utilizing a Thermo Scientific Nicolet 6700 (USA) with Attenuated Total Reflectance (ATR). Each collected spectrum is the average of 64 scans in the range of 500 – 4000 cm-1 and collected at a resolution of 4 cm-1. FT-IR analyzes were used to examine the comparison of ST-PA 6,6 and PA 6,6.

4. RESULTS AND DISCUSSION

4.1. Solvent Studies

As detailed in Section 3.1 Electrospinning Solution Preparation, various solvents were tested in various combinations. The main challenge was to find the solvent combination that dissolves the part that makes PA 6,6 “super tough” so that it can be electrospun. In addition, due to the fact that solvents are not cheap and are available in limited quantities in our laboratory, a wide spectrum of dissolution tests were not performed for each concentration. Instead, by observing the gradual effects, sometimes the concentration was increased or decreased, sometimes the ratios of solvents were increased or decreased, and sometimes both parameters were changed at once, taking into account the situations in previous studies and trials.

FTIR & DSC Results are also showed that ST-PA 6,6 mechanism is different than standard PA 6,6.

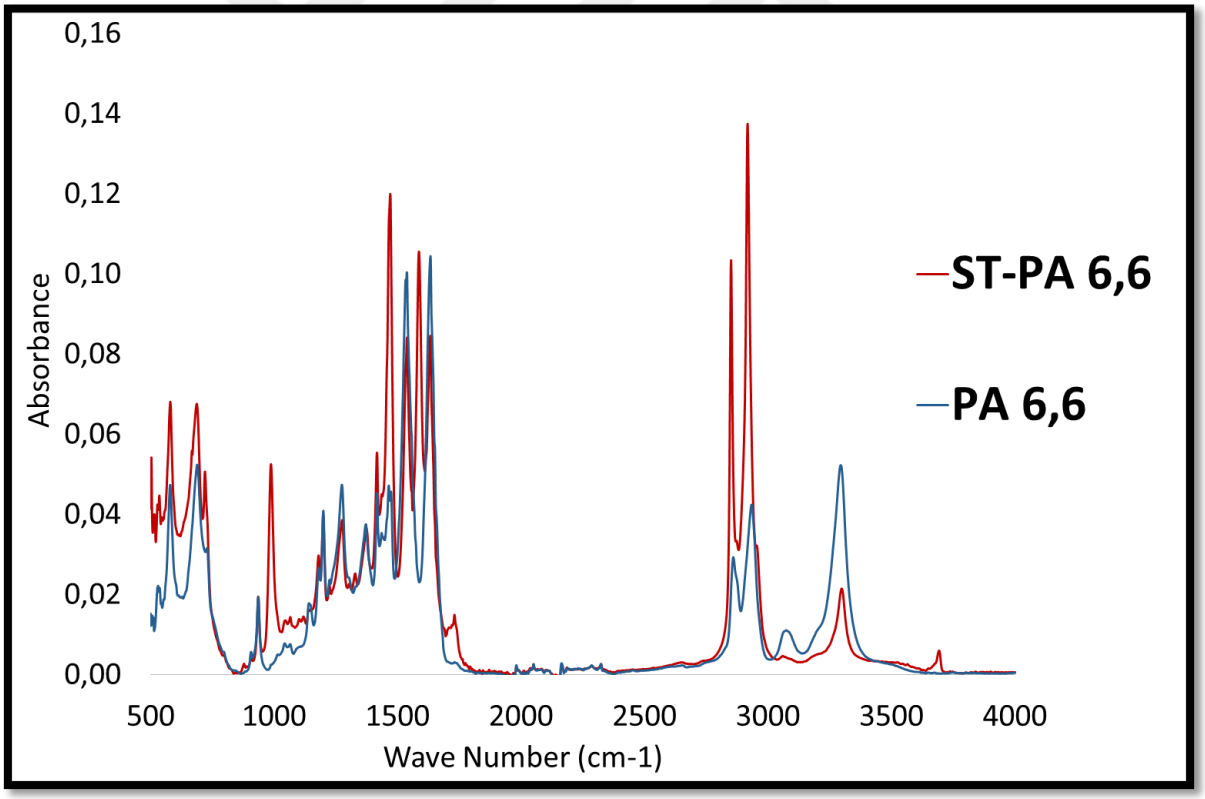

Figure 4.1 FTIR results of ST-PA 6,6 and PA 6,6

In Figure 4.1, around wave number 1050 cm^{-1},1750 cm^{-1} and 3750 cm^{-1}, difference can be seen clearly. That difference shows that ST-PA 6,6 has different type of chemical bond other than PA 6,6. So it can be interpreted as ST-PA 6,6 has another toughening material addition such an elastomer.

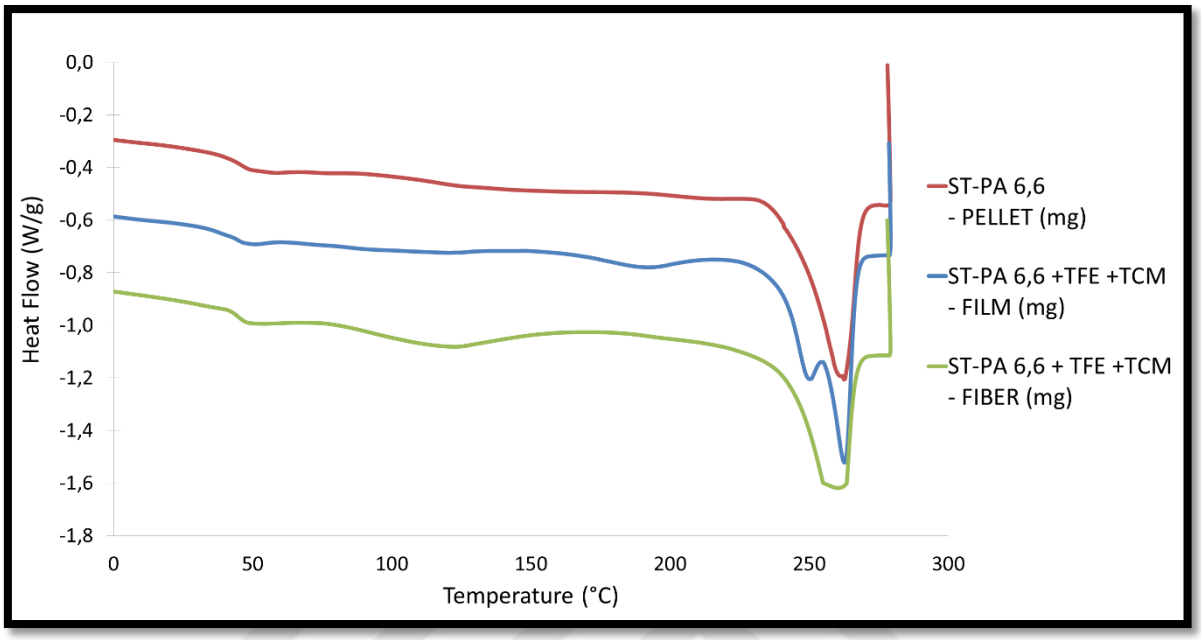

Figure 4.2 DSC results of ST-PA 6,6 Pellet, Film & Fiber

As seen in Figure 4.2 at 250 °C, the DSC taken from the dissolved and dried film detected another material on the surface.

The reason why this curve does not appear in the pellet is because these elastomers are not present on the surface of the pellet. Likewise, the reason why it is not visible on the fiber graph shows that the surface of the well dissolved and spun veil can be spun homogeneously.

Considering all these studies, the ST-PA 6,6 could not be dissolved in any combination until transparency. However, since some of the mixtures (For example D-59: ST-PA 6,6 + TFE:XYL 3:1) obtained from the studies can be electrospun, the fiber structures were investigated under SEM (see Appendix D). Based on this, it can be concluded that the fibers with beads and aggregations were not well dissolved. (Figure 4.3)

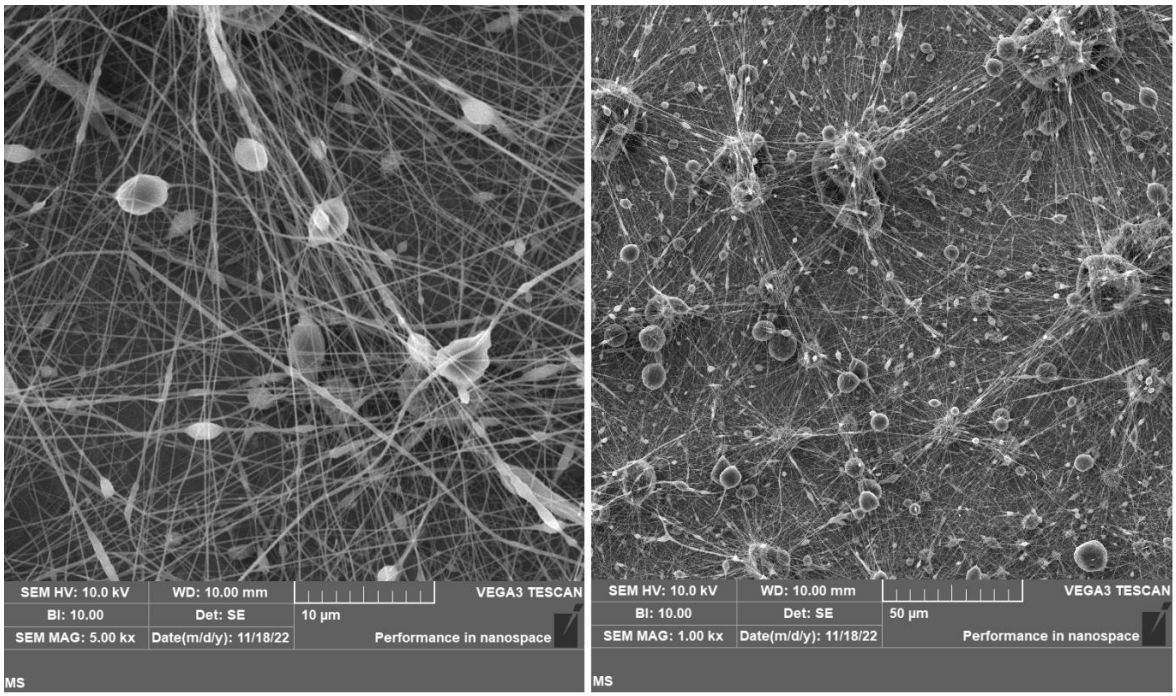

a b

Figure 4.3 SEM image with a)5.00 kx b)1.00 kx of D59

The 3 solutions that give the best SEM results are experiments D56, D57 & D58 shown in the chart in appendix B. SEM results of D57 are shown on Figure 4.4 which are way better than D59 about beads. SEM results of D58 are shown on Figure 4.5 which are also quite better.

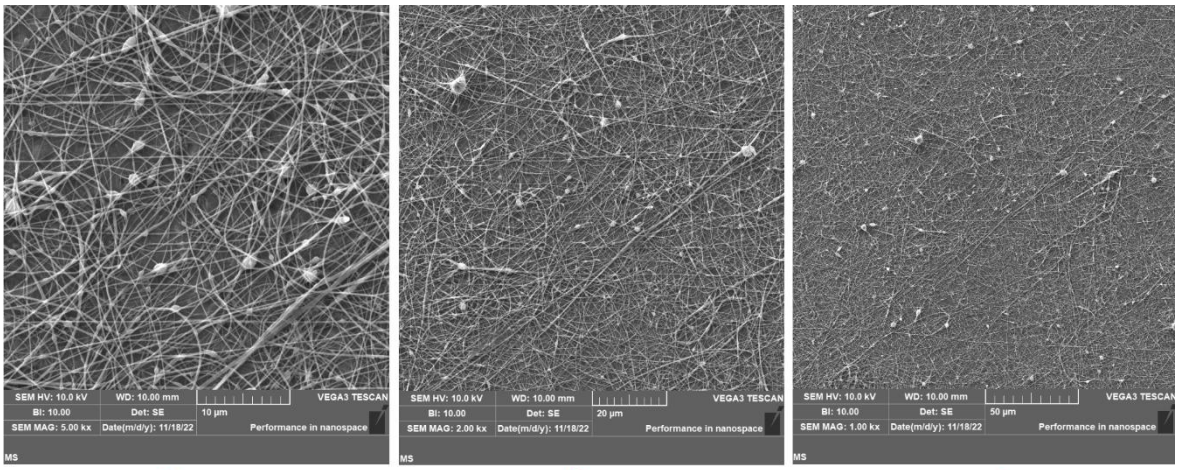

a b c

Figure 4.4 SEM micrographs with a)5.00 kx b)2.00 kx c)1.00 kx of D57

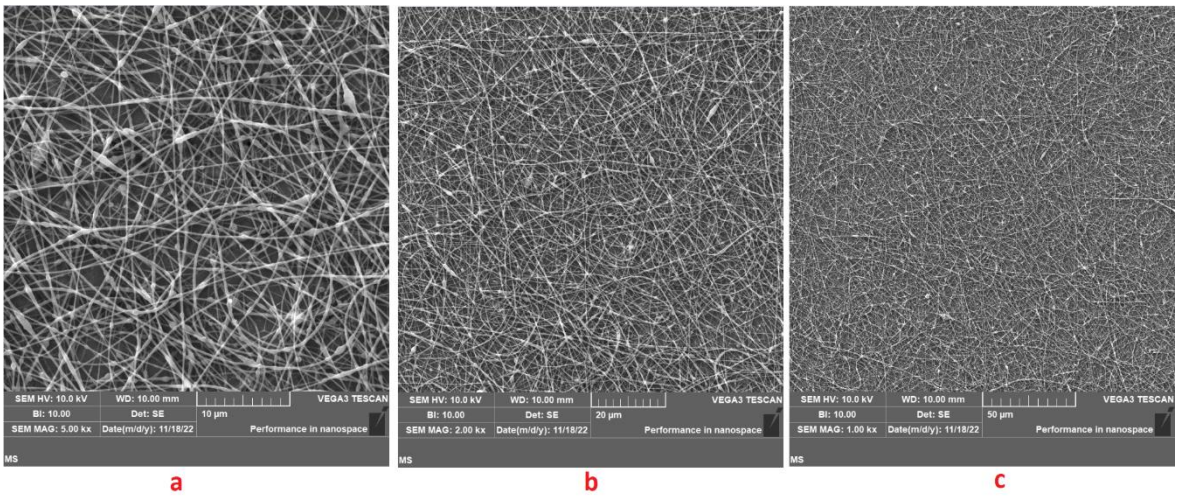

Figure 4.5 SEM micrographs with a)5.00 kx b)2.00 kx c)1.00 kx of D58

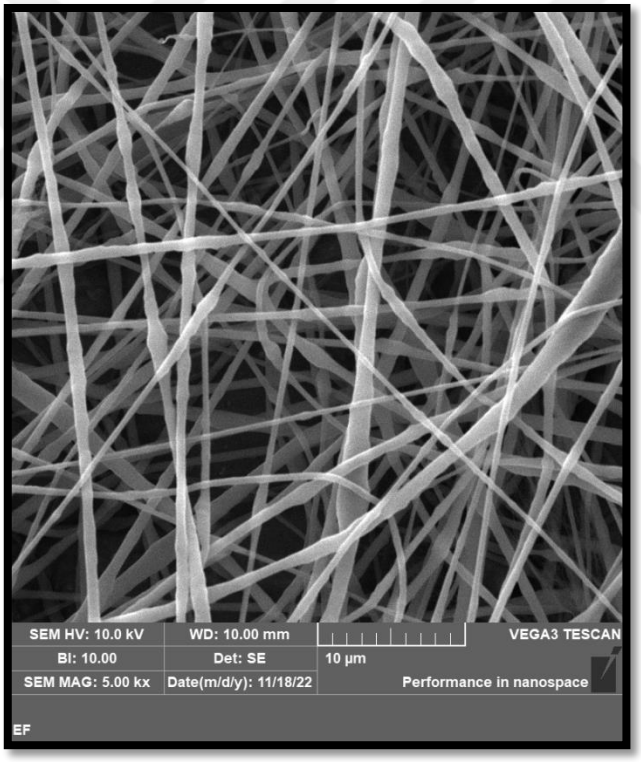

Figure 4.6 SEM micrograph with 5.00 kx of D56

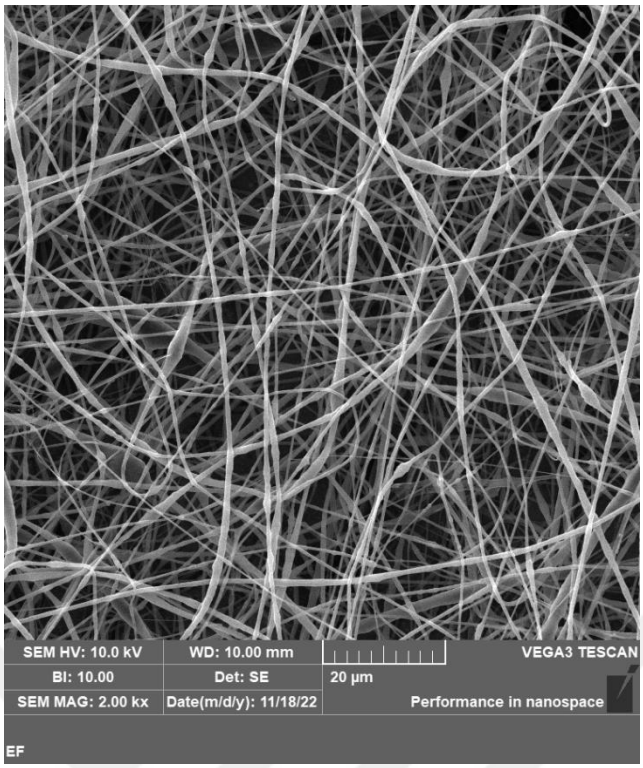

Figure 4.7 SEM micrograph with 2.00 kx of D56

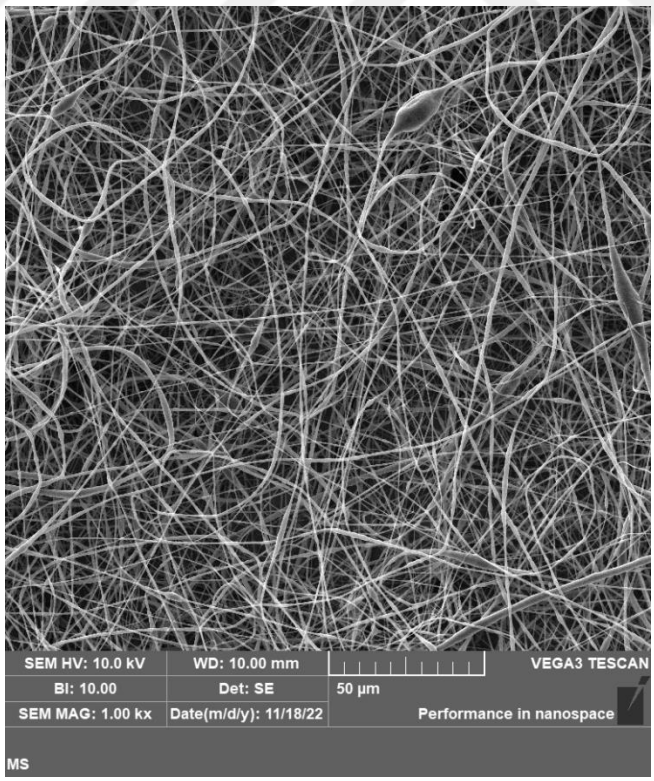

Figure 4.8 SEM micrograph with 1.00 kx of D56

SEM results of D56 is shown on Figure 4.6, 4.7, 4.8 which are given by their magnification values 5.00kx-2.00kx-1.00kx. Those were good enough to continue with. On the other hand, the concentration by mass for D-56 was 8%. The solvents used were added to the mixture at a ratio of TFE:TCM 3:1. Due to the rapid evaporation of TFE, mixing could not be achieved at high temperature values. It was mixed at 35 °C at 500 rpm for 48 hours. The concentration by mass for D-57 was 8%. The solvents used were added to the mixture in a ratio of FA:XYL:TCM 65:21:14. These solvents were mixed overnight at 500 rpm at 50 °C. The concentration by mass for D-58 was 8%. The solvents used were added to the mixture at the ratio of TFE:FA:TCM 55:30:15. Since TFE was present in the mixture as in D56, it was mixed at 35 °C at 500 rpm for 48 hours.

The reason for continuing these experiments with D-56 is not related to its solvents. While D-56 can be spun with a flow rate of approximately 2.8-3.2 ml/hr, since the other two mixtures are spun with 0.1-0.15 ml/hr, the interleaving experiments were continued with the D-56 mixture in order not to make it 30 times slower.
In addition to all these, calibrating the pipettes used while preparing the mixture, with the help of the parafilm, closing the caps of the glass bottles in which the mixture takes place, keeping the mixture temperature as constant as possible are some of the most important precautions in these processes.

4.2. Electrospinning

4.2.1. Setup Improvements

In our laboratory, a rotating copper collector was used in similar previous electrospinning studies. Although copper was originally preferred for its electrical conductivity, the transfer of spun tulle over the collector to the interface has always been a problem. Since this problem may even prevent probing the direct effect of the experiments on the result, it was thought that this problem should be reevaluated and a permanent solution should be found. Thus, the same mixture was spun onto copper collector, aluminum collector (Figure 4.9) and titanium collector (Figure 4.10) for trial purposes. As a result, the collector was chosen as titanium for the veil, which can be peeled off and transferred much more easily over the titanium collector.(Figure 4.11) With the improvements in the lay-up process (double-sided

vacuuming), the best transfer ever made had been achieved in our laboratory.

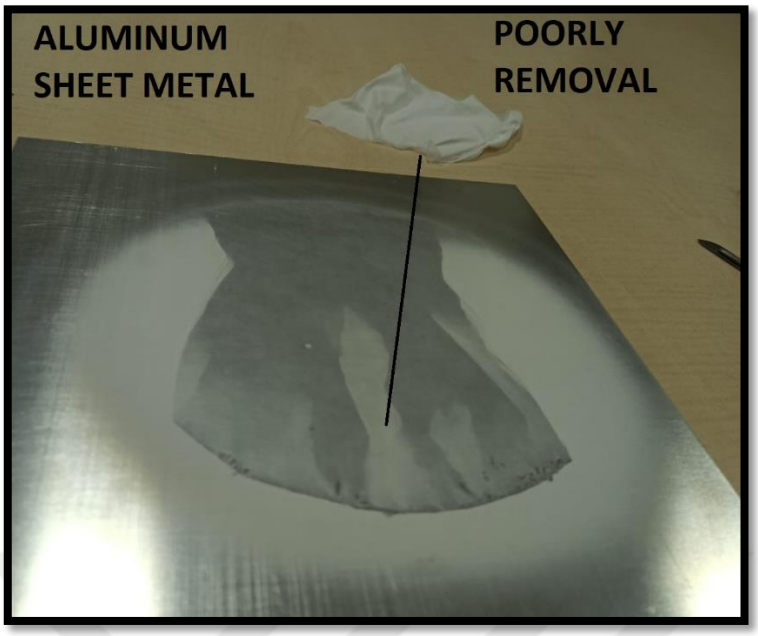

Figure 4.9 Veil removal process with aluminum collector

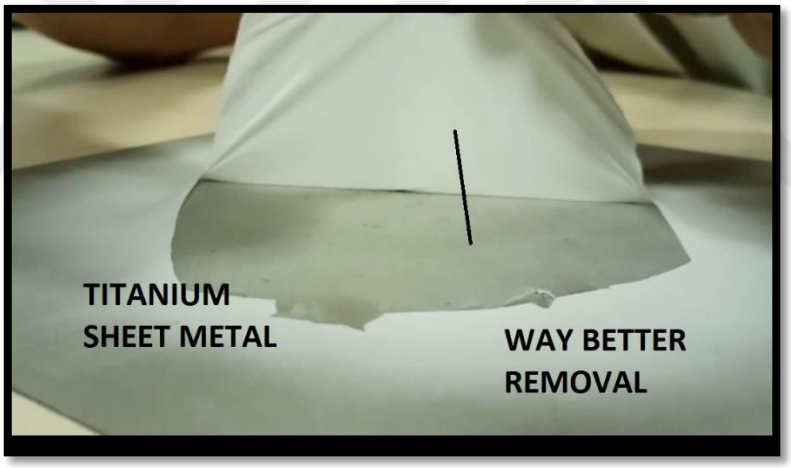

Figure 4.10 Veil removal process with titanium collector

Figure 4.11 Result of veil removal process with titanium collector

4.2.2. Distance, Voltage & Flowrate

Apart from the collector material, other important parameters are distance, voltage and flowrate. During an experiment, the distance values between the needle and the collector were increased by 1 cm from 16 cm to 23 cm and spinning was observed. While spinning could be done with less voltage at 16 cm, it was necessary to increase the voltage value to 23 cm. In general, results at a distance of 18 cm were more optimal. Likewise, this value was kept constant in the electrospinning processes made with different materials in the literature and in the laboratory. Although the voltage value is generally used between 18-26 kV during all the experiments, when we keep the other parameters constant, increasing the voltage causes thinning in the fiber diameters, but when the flowrate is not increased together, it dries at the needle tip. Likewise, when the voltage is reduced without changing other parameters, the fiber diameters become larger and dripping problem occurs in a short time.

Flowrate, on the other hand, is usually set observationally according to the other two parameters and left constant. For a mixture to be tried for the first time, it may be insignificant to set a starting value because the flow rate should be decreased when

it drips, and the flow rate should be increased when it freezes. The flow rate in our selected mixture (D-56) varies between 2.8-3.2 ml/hr. From the position of the hose to the condition of the stabilizer, all of them affect the flow rate. In addition, since the electric field decreases due to the spun veil in the long-term spinning process, either the flow rate in the device should be reduced gradually or the voltage should be increased gradually. In this way, freezing and dripping can be prevented.

4.3. Mode I Fracture Toughness Tests of Laminates

4.3.1. Reference (Base) Laminates

Reference plates (Base) were prepared in factory clean room-autoclave conditions as described in Section 3.3 between 3 different batch prepregs and the same cure cycle min-max values at 3 different time intervals. From each of these plates, 4 Mode I test specimens were cut with 0.5 mm precision. Testing of each was done according to AITM 1-0053 Airbus Standards similar to ASTM 5528 standard which is mostly used in literature.

G_{IC} values are respectively (A:C:E) in the initiation part (55.7 J/m^2: 58.5 J/m^2: 76.1 J/m^2) in the propagation part (239.1 J/m^2: 269. 8 J/m^2: 281.5 J/m^2) is calculated as an average. (Figure 4.12, 4.13, 4.14)

The increase in each of these values, especially in the 3rd, indicates that the prepregs have different structures among their own batches, so the fact that each interface addition has its own reference sample gave a better evaluation.
Summary results are shown in the table 4.1.
The detailed table is shown in appendix 1.

Table 4.1 Reference panel (base) results

A (BASE)	TOTAL ENERGY J	G_{IC} J/ m^2	C (BASE)	TOTAL ENERGY J	G_{IC} J/ m^2	E (BASE)	TOTAL ENERGY J	G_{IC} J/ m^2
1	0.41	267.5	1	0.42	280	1	0.39	262.2
2	0.34	221.5	2	0.41	265.5	2	0.42	291.1
3	0.34	222.2	3	0.41	272.7	3	0.43	287
4	0.37	245.1	4	0.39	261	4	0.43	285.6
AVG	**0.37**	**239.1**	**AVG**	**0.41**	**269.8**	**AVG**	**0.42**	**281.5**

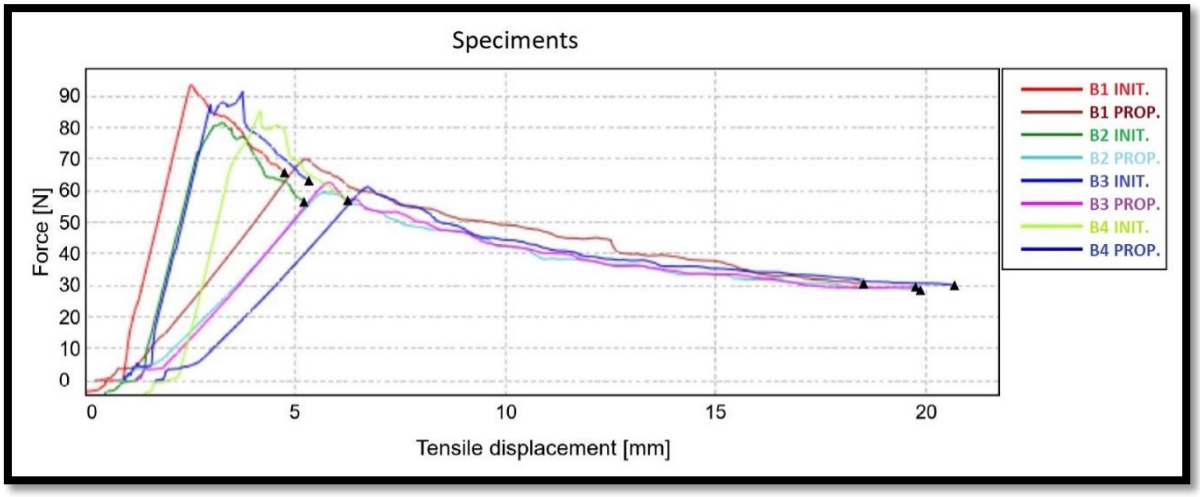

Figure 4.12 DCB graph for experiment A (Reference of B-3.5 g/m^2)

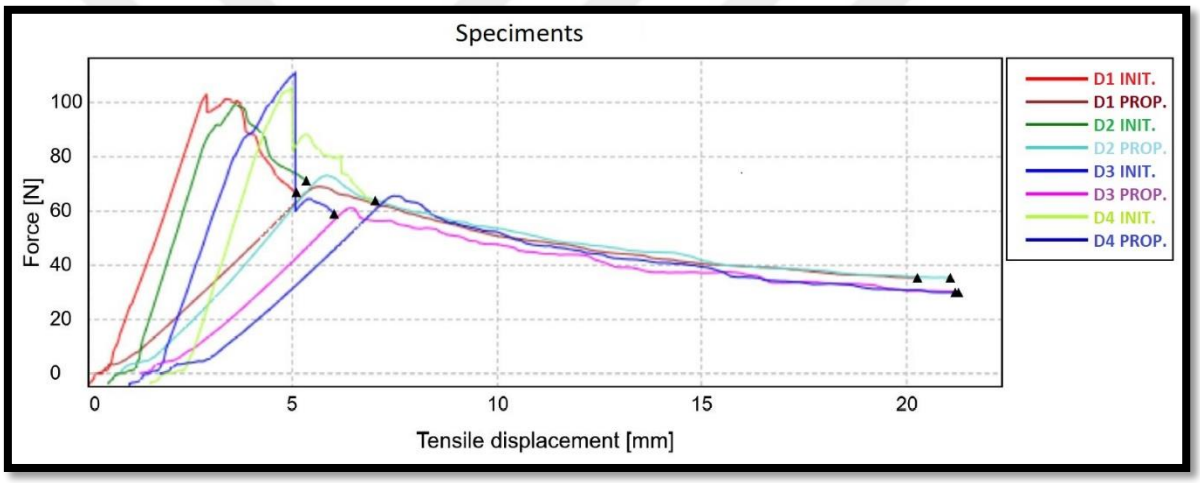

Figure 4.13 DCB graph for experiment C (Reference of D-7 g/m^2)

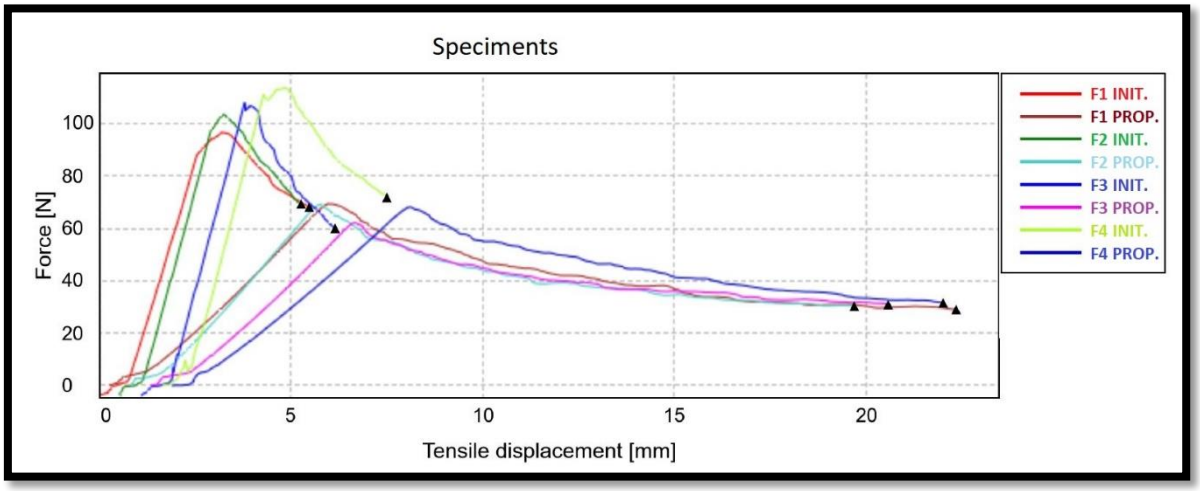

Figure 4.14 DCB graph for experiment E (Reference of D-10 g/m^2)

4.3.2. ST-PA 6,6 Interleaved Composites

Interleaved ST-PA 6,6 electrospun composite plates (coded as “Fiber”) were also prepared in factory clean room-autoclave conditions as described in section 3.3 between 3 different batch prepregs and the same cure cycle min-max values at 3 different time intervals. From each of these plates, 4 Mode I test specimens were cut with 0.5 mm precision. Testing of each was done according to AITM 1-0053 Airbus Standards similar to ASTM 5528 standard which is mostly used in literature.

G_{IC} values are respectively B:D:F in the initiation part 67.5 J/m^2 : 87.8 J/m^2: 103 J/m^2 in the propagation part 274.9 J/m^2: 317.8 J/m^2: 308.9 J/m^2 is calculated as an average. (Figure 4.15, 4.16, 4.17)

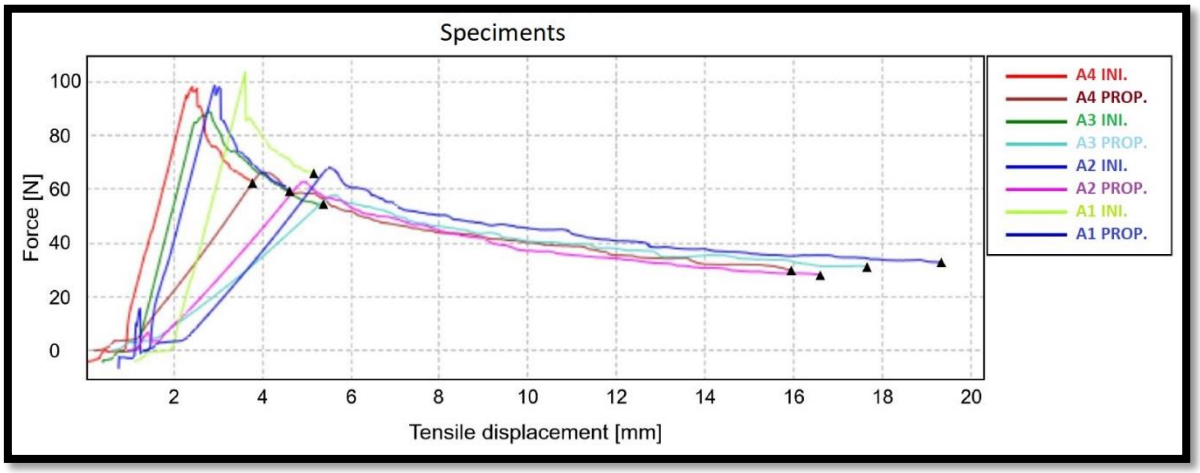

Figure 4.15 DCB graph for experiment B (3.5 g/m^2)

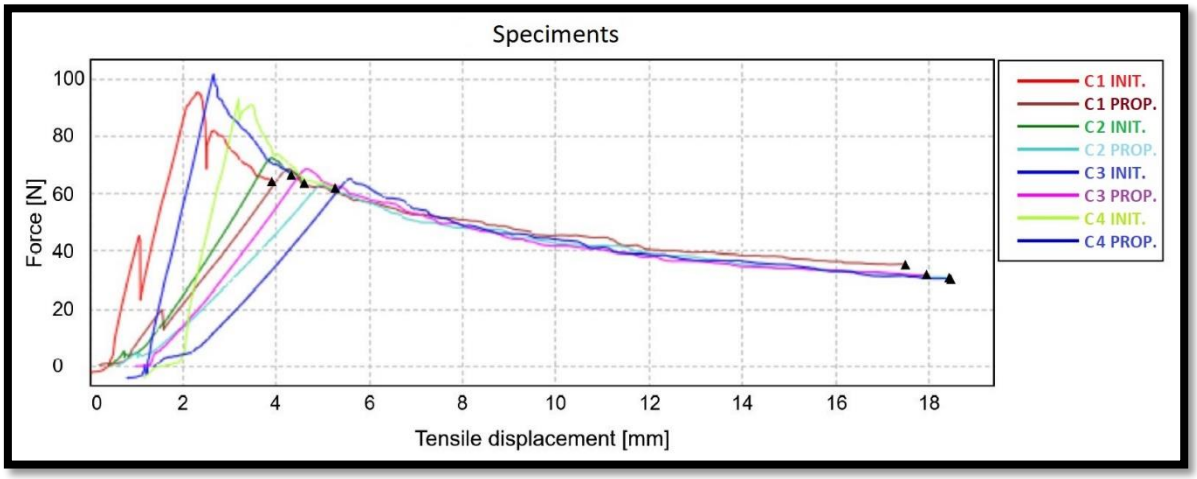

Figure 4.16 DCB graph for experiment D (7 g/m^2)

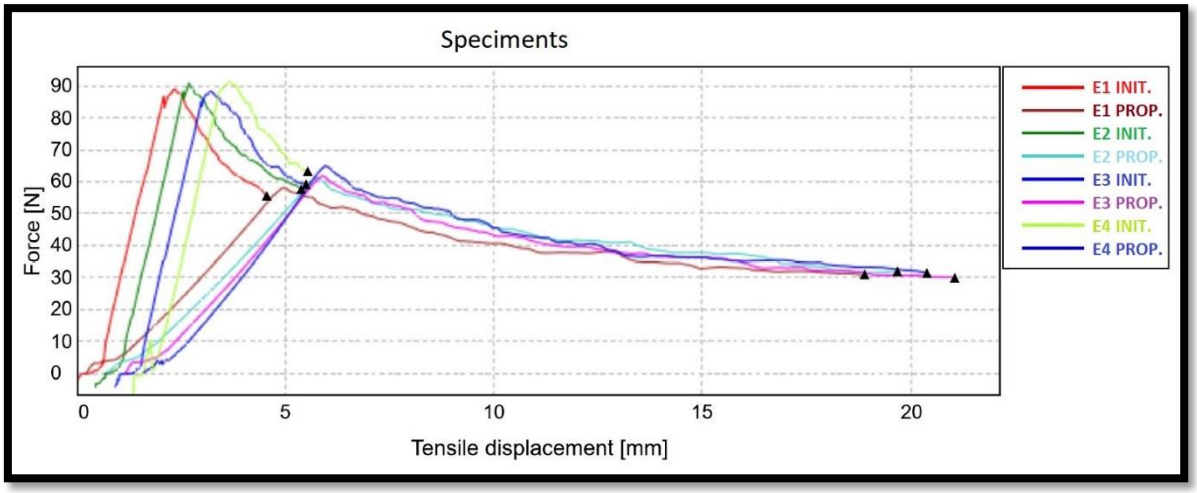

Figure 4.17 DCB graph for experiment F (10 g/m^2)

When compared according to their own references (base), all samples of the three test sets seem to increase the fracture toughness (Figure 4.18) both in the initiation and propagation regions. However, the highest increase was observed in the samples (Sample D) whose interface was toughened with veil with a areal density of 7 g/m^2 (G_{IC} i : 50% , G_{IC} p : 18%).

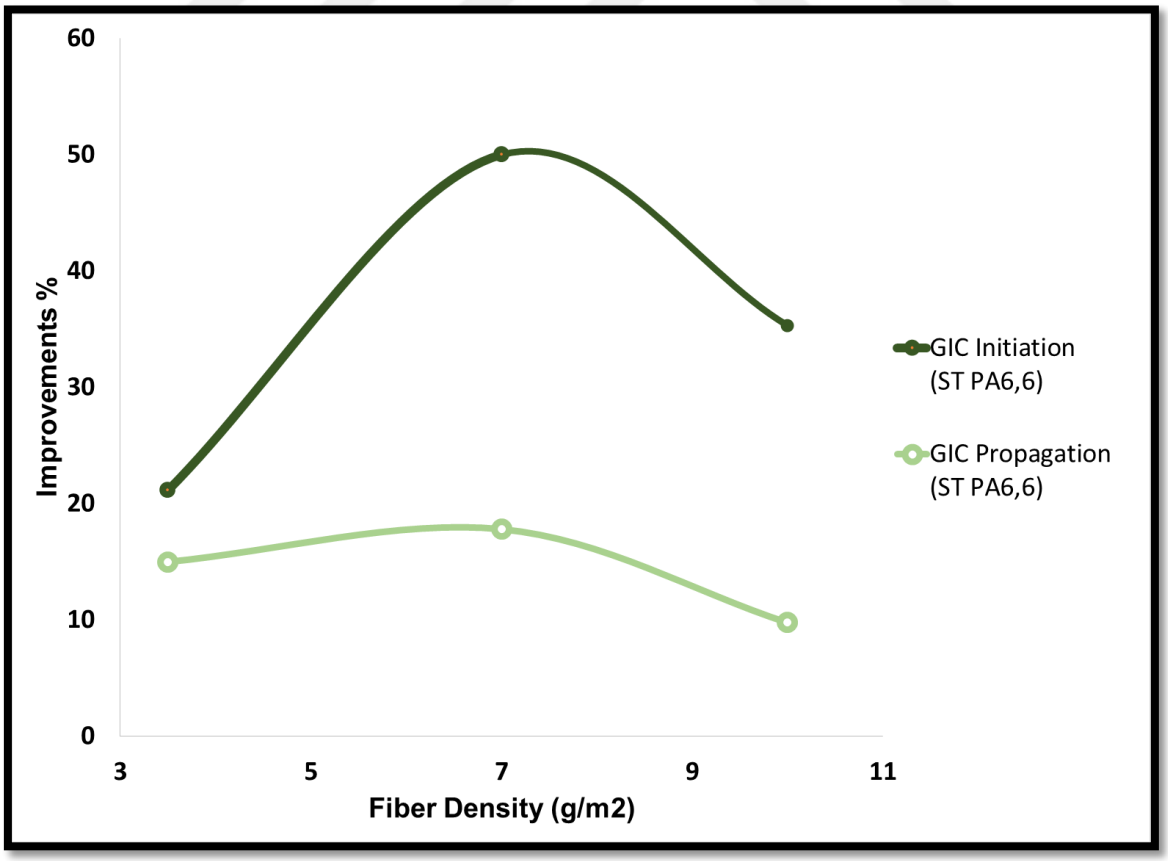

Figure 4.18 % Improvements due to fiber densities

When the data of the two samples, which compare the thickness differences by making various additions to the veil previously produced by the electrospinning method, are examined in the same graphic (Figure 4.19), it is seen that there is a thickness optimization for each interface toughening study. This explains why the percentage of improvement accelerated first and then decreased in the experiments conducted in this thesis. At the same time, it was observed that the fracture toughness of PA 6,6 veil with added NBR was higher in percentage. This showed that rubber-based polymers added after spinning can be even more effective at similar densities [27] [33].

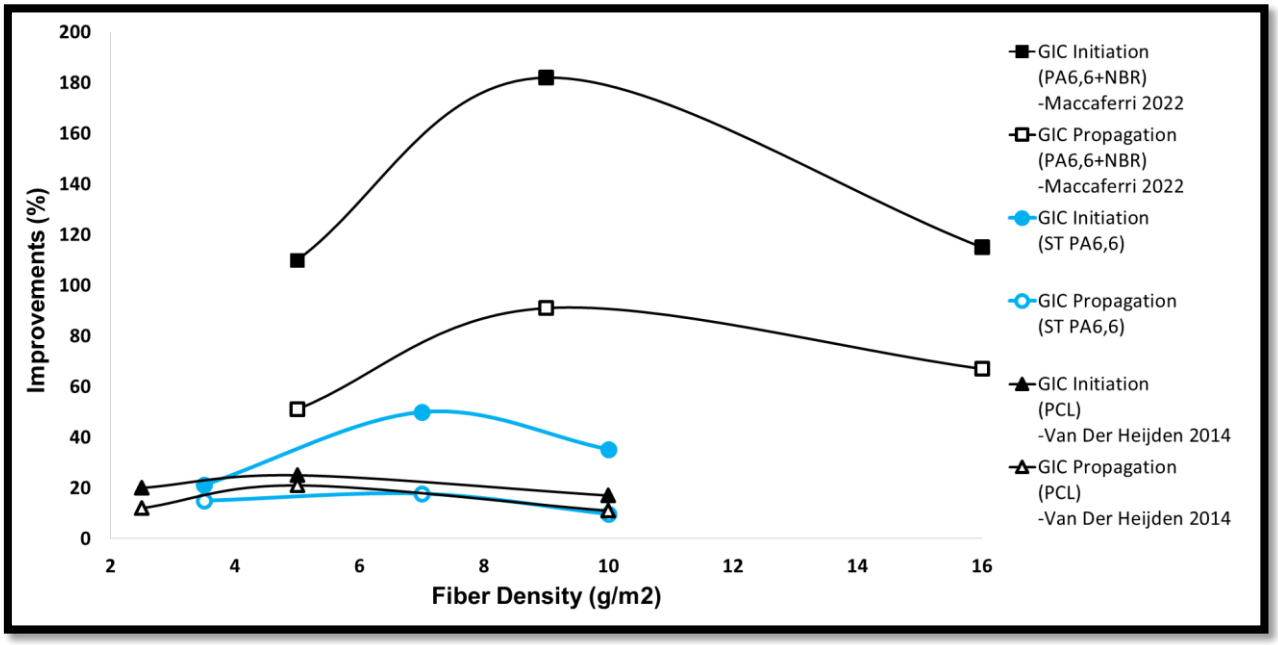

Figure 4.19 % Improvements due to fiber densities (Comparison) (PA 6,6+PCL[33], PA 6,6+NBR [27])

This improvement on ST-PA 6,6 alone has shown that it can be much more effective with different polymers (NBR, PCL etc.) that can be added on it. It even showed the potential to create a much more effective structure with a different solvent mixture that can be prepared for super tough blend.

5. CONCLUSIONS

1. Placing nanofiber veil produced by electrospinning from thermoplastic polymer mixtures between layers in CFRP composites increases G_{IC} (Mod I) interface toughness values at both crack initiation and propagation stages.
2. Best SEM results were seen with D-56 solvent combination (TFE:TCM 3:1) because of its electrospinability.
3. When the veil produced by electrospinning the ST-PA 6,6 blend was transferred to the interface, it provided 50% improvement for crack initiation and 18% for crack propagation. This improvement was achieved by adding a tulle of only 7 g/m^2 areal density in the composite structure.
4. In situations requiring instant toughness (Demolding), crack initiation stability is a more important indicator. The produced veil can be used for such situations thanks to the 50% improvement.
5. The reason why the improvement percentage is lower than expected is because ST-PA 6,6 does not show much different properties from other nylon 6,6. There may be various reasons for this;
   i) ST-PA 6,6 is not fully dissolved. Accordingly, the spun fibers did not create a bridging effect.
   ii) ST-PA 6,6 pellets taken in blended form do not fully contain the epoxy adhesion feature in standard PA 6,6.
6. Choosing titanium metal as the collector made it easier to peel the veil off the surface.
7. Laying up in factory conditions and using autoclaves made the processes more standardized.
8. Generating each fiber sample with its own reference (base) has increased the accuracy in comparison.
9. By carrying out a thickness/density study, it was concluded that the areal density should be optimized in this method.

6. REFERENCES

[1] Kılıcoglu, M., *Use Of Nano-Hybrid Systems In Carbon Fiber Reinforced Polymer Matrix Composites (CFRP) For Interfacial Toughening,* **2018**.

[2] Dzenis, Y.A. and J. Qian, *Analysis of microdamage evolution histories in composites.* International Journal of Solids and Structures, **2001**. 38(10-13): p. 1831-1854.

[3] Abdelhady, S.S., et al., *Electrospinning process optimization for Nylon 6, 6/Epoxy hybrid nanofibers by using Taguchi method.* Materials Research Express, **2019**. 6(9): p. 095314.

[4] Ashby, M.F. and D. Cebon, *Materials selection in mechanical design.* Le Journal de Physique IV, **1993**. 3(C7): p. C7-1-C7-9.

[5] Jabbari, M., et al., *New Solvent for Polyamide 66 and Its Use for Preparing a Single-Polymer Composite-Coated Fabric.* International Journal of Polymer Science, **2018**. 2018.

[6] Biber, E., et al., *Effects of electrospinning process parameters on nanofibers obtained from Nylon 6 and poly (ethylene-n-butyl acrylate-maleic anhydride) elastomer blends using Johnson S B statistical distribution function.* Applied Physics A, **2010**. 99(2): p. 477-487.

[7] Kılıçoğlu, M., *Nano-Melez Sistemlerin Karbon Fiber Takviyeli Polimer Matris Kompozitlerde (KFTP) Arayüz Toklaştırma Amacıyla Kullanımı,* **07/2017**.

[8] Campbell, F.C., *Structural composite materials*, **2010**: ASM international.

[9] Yıldırım, M.U., *Improvement of Interfacıal Toughness of Layered Composıtes By Usıng Electrostatıc Flockıng Technıque,* **2021**.

[10] Wu, X.-F., *Fracture of advanced polymer composites with nanofiber reinforced interfaces*. **2003**, PhD, Department of Engineering Mechanics,University of Nebreska.

[11] Nejati, H.R., et al., *Monitoring of fracture propagation in brittle materials using acoustic emission techniques-A review.* Comput. Concr, **2020**. 25: p. 15-27.

[12] Airbus, A., *AITM 1-0053.* Carbon fiber reinforced plastics. Determination of fracture toughness energy of bonded joints. Mode I. GIC test, **2015**.

[13] Internat., A., *Standard test method for mode I interlaminar fracture toughness of unidirectional fiber-reinforced polymer matrix composites*. Vol. **2013**. 2013: ASTM Internat.

[14] ASTM-International, *Standard Test Method for Mode I Interlaminar Fracture Toughness of Unidirectional Fiber-Reinforced Polymer Matrix Composites,* **2013**.

[15] Gunavathi, P., T. Ramachandran, and K.P. Chellamani, *Characterization of nanomembrane using nylon-6 and nylon-6/poly (e-caprolactine) blend.* Indian Journal of Fibre and Textile Research, **2012**. 37(3): p. 211-216.

[16] Sun, Y., et al., *Study on the Toughening Mechanism of Rubber Toughened Epoxy.* Chinese Journal of Polymer Science **1986**. 4(3): p. 229-234.

[17] Fu, Z. and Y. Sun, *Epoxy Resin Toughened by Thermoplastics.* Chinese Journal of Polymer Science **1989**. 7(4): p. 367-378.

[18] Kawaguchi, T. and R.A. Pearson, *The effect of particle–matrix adhesion on the mechanical behavior of glass filled epoxies. Part 2. A study on fracture toughness.* Polymer, **2003**. 44(15): p. 4239-4247.

[19] Kinloch, A.J., et al. *Toughening mechanisms in novel nano-silica epoxy polymers*. in *5th Australasian Congress on Applied Mechanics (ACAM 2007)*. **2007**. Brisbane, Australia.

[20] Sprenger, S., A.J. Kinloch, and A.C. Taylor, *Fibre Reinforced Composites Optimized by the Synergy Between Rubber-Toughening and Sio2-Nanoparticles*. **2009**.

[21] Mirmohseni, A. and S. Zavareh, *Preparation and characterization of an epoxy nanocomposite toughened by a combination of thermoplastic, layered and particulate nano-fillers.* Materials & Design, **2010**. 31(6): p. 2699-2706.

[22] Sager, R., *A Characterization of the Interfacial and Interlaminar Properties of Carbon Nanotube Modified Carbon Fiber/Epoxy Composites*. **2008**, Texas A&M University.

[23] Jiang, W., et al., *Interlaminar Fracture Properties of Carbon Fibre/Epoxy Matrix Composites Interleaved with Polyethylene Terephthalate (PET) Films.* Polymers and Polymer Composites, **2001**. 9(2): p. 141-145.

[24] McGarry, F.J., B. Zhu, and D.E. Katsoulis, *Silicone Resin Based Composites Interleaved for Improved Toughness*. **2003**, Dow Corning Corporation: United States.

[25] White, K.L. and H.-J. Sue, *Delamination toughness of fiber-reinforced composites containing a carbon nanotube/polyamide-12 epoxy thin film interlayer.* Polymer, **2012**. 53(1): p. 37-42.

[26] Meireman, T., et al., *Delamination resistant composites by interleaving bio-based long-chain polyamide nanofibers through optimal control of fiber diameter and fiber morphology.* Composites Science and Technology, **2020**. 193: p. 108126.

[27] Maccaferri, E., et al., *Rubber-enhanced polyamide nanofibers for a significant improvement of CFRP interlaminar fracture toughness.* Scientific Reports, **2022**. 12(1): p. 1-16.

[28] Beckermann, G.W. and K.L. Pickering, *Mode I and Mode II interlaminar fracture toughness of composite laminates interleaved with electrospun nanofibre veils.* Composites Part A: Applied Science and Manufacturing, **2015**. 72: p. 11-21.

[29] Palazzetti, R. and A. Zucchelli, *Electrospun nanofibers as reinforcement for composite laminates materials–a review.* Composite Structures, **2017**. 182: p. 711-727.

[30] Biber, E., et al., *Compatibility analysis of Nylon 6 and poly (ethylene-n-butyl acrylate-maleic anhydride) elastomer blends using isothermal crystallization kinetics.* Materials Chemistry and Physics, **2010**. 122(1): p. 93-101.

[31] Saghafi, H., et al., *The effect of interleaved composite nanofibrous mats on delamination behavior of polymeric composite materials.* Composite Structures, **2014**. 109: p. 41-47.

[32] Larrondo, L. and R. St. John Manley, *Electrostatic fiber spinning from polymer melts. I. Experimental observations on fiber formation and properties.* Journal of Polymer Science: Polymer Physics Edition, **1981**. 19(6): p. 909-920.

[33] Van Der Heijden, S., et al., *Interlaminar toughening of resin transfer moulded glass fibre epoxy laminates by polycaprolactone electrospun nanofibres,* **2014**.

[34] van der Heijden, S., et al., *Interlaminar toughening of resin transfer molded laminates by electrospun polycaprolactone structures: Effect of the interleave morphology.* Composites Science and Technology, **2016**. 136: p. 10-17.

[35] De Schoenmaker, B., et al., *Effect of electrospun polyamide 6 nanofibres on the mechanical properties of a glass fibre/epoxy composite.* Polymer testing, **2013**. 32(8): p. 1495-1501.

[36] Saghafi, H., et al., *The effect of PVDF nanofibers on mode-I fracture toughness of composite materials.* Composites Part B: Engineering, **2015**. 72: p. 213-216.

[37] Saghafi, H., G. Minak, and A. Zucchelli, *Effect of preload on the impact response of curved composite panels.* Composites Part B: Engineering, **2014**. 60: p. 74-81.

[38] van Der Heijden, S., et al., *Novel composite materials with tunable delamination resistance using functionalizable electrospun SBS fibers.* Composite Structures, **2017**. 159: p. 12-20.

[39] Kelkar, A.D., et al., *Effect of nanoparticles and nanofibers on Mode I fracture toughness of fiber glass reinforced polymeric matrix composites.* Materials Science and Engineering: B, **2010**. 168(1-3): p. 85-89.

[40] Li, G., et al., *Inhomogeneous toughening of carbon fiber/epoxy composite using electrospun polysulfone nanofibrous membranes by in situ phase separation.* Composites Science and Technology, **2008**. 68(3-4): p. 987-994.

[41] Phong, N.T., et al., *Improvement in the mechanical performances of carbon fiber/epoxy composite with addition of nano-(Polyvinyl alcohol) fibers.* Composite structures, **2013**. 99: p. 380-387.

[42] Zhang, J., et al., *Phase morphology of nanofibre interlayers: Critical factor for toughening carbon/epoxy composites.* Composites Science and Technology, **2012**. 72(2): p. 256-262.

[43] Shivakumar, K., et al., *Polymer nanofabric interleaved composite laminates.* AIAA journal, **2009**. 47(7): p. 1723-1729.

[44] Brugo, T. and R. Palazzetti, *The effect of thickness of Nylon 6, 6 nanofibrous mat on Modes I–II fracture mechanics of UD and woven composite laminates.* Composite Structures, **2016**. 154: p. 172-178.

[45] Daelemans, L., et al., *Nanofibre bridging as a toughening mechanism in carbon/epoxy composite laminates interleaved with electrospun polyamide nanofibrous veils.* Composites Science and Technology, **2015**. 117: p. 244-256.

[46] Brugo, T., et al., *An investigation on the fatigue based delamination of woven carbon-epoxy composite laminates reinforced with polyamide nanofibers.* Procedia Engineering, **2015**. 109: p. 65-72.

[47] Palazzetti, R., et al., *Influence of electrospun Nylon 6,6 nanofibrous mats on the interlaminar properties of Gr–epoxy composite laminates.* Composite Structures, **2012**. 94(2): p. 571-579.

[48] Hamer, S., et al., *Mode I interlaminar fracture toughness of Nylon 66 nanofibrilmat interleaved carbon/epoxy laminates.* Polymer composites, **2011**. 32(11): p. 1781-1789.

[49] Magniez, K., T. Chaffraix, and B. Fox, *Toughening of a Carbon-Fibre Composite Using Electrospun Poly(Hydroxyether of Bisphenol A) Nanofibrous Membranes Through Inverse Phase Separation and Inter-Domain Etherification.* Materials, **2011**. 4(12): p. 1967-1984.

[50] Zhang, H., et al., *Localized toughening of carbon/epoxy laminates using dissolvable thermoplastic interleaves and electrospun fibres.* Composites Part A: Applied Science and Manufacturing, **2015**. 79: p. 116-126.

[51] Beylergil, B., M. Tanoğlu, and E. Aktaş, *Modification of carbon fibre/epoxy composites by polyvinyl alcohol (PVA) based electrospun nanofibres.* Advanced Composites Letters, **2016**. 25(3): p. 096369351602500303.

[52] Magniez, K., C. De Lavigne, and B. Fox, *The effects of molecular weight and polymorphism on the fracture and thermo-mechanical properties of a carbon-fibre composite modified by electrospun poly (vinylidene fluoride) membranes.* Polymer, **2010**. 51(12): p. 2585-2596.

[53] Brugo, T., et al. *A study on fatigue behavior of nanointerleaved woven CFRP*. in *European Conference on Composite Materials-ECCM 17*, **2016**.

[54] Saghafi, H., et al., *The effect of nanofibrous membrane thickness on fracture behaviour of modified composite laminates–A numerical and experimental study.* Composites Part B: Engineering, **2016**. 101: p. 116-123.

[55] Alessi, S., et al., *Effects of Nylon 6, 6 nanofibrous mats on thermal properties and delamination behavior of high performance CFRP laminates.* Polymer Composites, **2015**. 36(7): p. 1303-1313.

[56] Kılıçoğlu, M., et al., *Fibers of thermoplastic polymer blends activate multiple interlayer toughening mechanisms.* Composites Part A: Applied Science and Manufacturing, **2022**. 158: p. 106982.

[57] Ognibene, G., et al., *Interlaminar toughening of epoxy carbon fiber reinforced laminates: soluble versus non-soluble veils.* Polymers, **2019**. 11(6): p. 1029.

[58] Aljarrah, M.T. and N.R. Abdelal, *Improvement of the mode I interlaminar fracture toughness of carbon fiber composite reinforced with electrospun nylon nanofiber.* Composites Part B: Engineering, **2019**. 165: p. 379-385.

[59] Ahmadloo, E., et al., *How fracture toughness of epoxy-based nanocomposite is affected by PA66 electrospun nanofiber yarn.* Engineering Fracture Mechanics, **2017**. 182: p. 62-73.

[60] Daelemans, L., et al., *Damage-resistant composites using electrospun nanofibers: a multiscale analysis of the toughening mechanisms.* ACS applied materials & interfaces, **2016**. 8(18): p. 11806-11818.

[61] Daelemans, L., et al., *Improved fatigue delamination behaviour of composite laminates with electrospun thermoplastic nanofibrous interleaves using the Central Cut-Ply method.* Composites Part A: Applied Science and Manufacturing, **2017**. 94: p. 10-20.

[62] Palazzetti, R., *Flexural behavior of carbon and glass fiber composite laminates reinforced with Nylon 6, 6 electrospun nanofibers.* Journal of composite materials, **2015**. 49(27): p. 3407-3413.

[63] Saghafi, H., et al., *Influence of electrospun nanofibers on the interlaminar properties of unidirectional epoxy resin/glass fiber composite laminates.* Journal of Reinforced Plastics and Composites, **2015**. 34(11): p. 907-914.

[64] Daelemans, L., et al., *Using aligned nanofibres for identifying the toughening micromechanisms in nanofibre interleaved laminates.* Composites Science and Technology, **2016**. 124: p. 17-26.

[65] Zhao, Y., et al., *Hybrid multi-scale epoxy composites containing conventional glass microfibers and electrospun glass nanofibers with improved mechanical properties.* Journal of Applied Polymer Science, **2015**. 132(44).

[66] Manh, C.V. and H.J. Choi, *Enhancement of interlaminar fracture toughness of carbon fiber/epoxy composites using silk fibroin electrospun nanofibers.* Polymer-Plastics Technology and Engineering, **2016**. 55(10): p. 1048-1056.

[67] Brugo, T., et al., *Study on Mode I fatigue behaviour of Nylon 6, 6 nanoreinforced CFRP laminates.* Composite Structures, **2017**. 164: p. 51-57.

[68] Daelemans, L., et al., *Toughening mechanisms responsible for excellent crack resistance in thermoplastic nanofiber reinforced epoxies through in-situ optical and scanning electron microscopy.* Composites Science and Technology, **2021**. 201: p. 108504.

7. APPENDIXES

A. TABLES OF LITERATURE BASED ON ITS TEST RESULTS

Papers on Mode I tests.							
Ref #	**Polymer**	**Solution**	**Fiber Diameter**	**Fiber Amount**	**Manuf.**	**Layup**	**Results**
(a) Glass fibers - Papers on Mode I							
[34]	PCL	12% in 9:1 FA:AA	343 ± 150	5-15 g/m^2	VARTM	[0]8	GI,C : +50%
	PA6	16% in 1:1 FA:AA	195 ± 35	4-20 g/m^2			GI,C : No variation
[35]	PA6	16% in 1:1 FA:AA	150 ± 19	5 g/m^2	VARTM	[0,90 2	GI,C : +14%
			230 ± 26	10 g/m^2			GI,C : −12%
[36]	PA6,6	14% in 1:1 FA:CLF	150 ± 15	25 ± 8 µm (25 g/m^2)	PrP	[0]10	GI,C : +62%
[37]	PA6,6	14% in 1:1 FA:CLF	270	27 µm	PrP	[0]14	GI,C : +25%
	PCL	15% in 1:1 FA:AA	150	31 µm			GI,C : +4.5%
	PA6,6 + PCL			30 µm			GI,C : +21%
[33]	PCL	14 wt% in 1:1 FA:AA	400 ± 100	30-176 µm single layer	PrP	[0]8	GI,C/GI,R:+20/+12%
				17-89 µm double layer			GI,C/GI,R: +94/+27%
[38]	SBS	BuAc:SBS :MTI-TAD :LiCl	2000 ± 500	12-22 g/m^2	VARTM	[0]8	GI,C : +90%

		100:13 :0.0585:1.3					
[39]	TEOS	[109]	500	NA	VARTM	[0/90]10	GI,C : −12%
(b) Carbon fibers - Papers on Mode I							
[40]	Epoxy 609	18-25% in 3:1 MEK :PGME	NA	90, 128, 144, 216μm	PrP	[0]24	No significant effects
[41]	nPVA	16, 18, 20, 22% in H2O	40-80	NA	VARTM	[0/90]?	at 0.1 % nPVA:
							GI,C/GI,R: +65/+73%
[28]	PA6,6	15% in 68:17 FA:AA	150-300	1.5, 4.5, 9 g/m^2	PrP	[0]12	GI,C/GI,R: +33/−6%
	PVB	10% in ETH	400-700	4.5 g/m^2			GI,C/GI,R: +13/+4%
		10.6 in ETH	700-1000	4.3 g/m^2			GI,C/GI,R: +16/+11%
	PCL	13% in 70:17 FA:AA	150-300	4.2 g/m^2			GI,C/GI,R: +3/+12%
	PES	20% in DMA	150-300	3.6 g/m^2			GI,C/GI,R: −52/−52%
	PAI	15% in 77:8 DMA:DMF	150-300	4.1 g/m^2			GI,C/GI,R: −58/−68%
[42]	PCL	12-15-20% in 1:1 DMF:CHL	103-125 -210		PrP	[0/90]4	GI C , : +92% with 125 nm PCL
	PVDF	16% in 1:1 DMF:AC	542	0.2%			GI,R: +37% with 125 nm PCL
	PAN	13% in DMF	607				
[43]	PA6,6	12% in 3:1 FA:AA	75-250	1.6-2.0 g/m^2	PrP	[0]20	KI: +150%

							GI,C/GI,R: +152/+31%
[44]	PA6,6	20% in 70:30 TFA:FA	350-400	40, 90 µm	PrP	[0]20	GI,C/GI,R: +56/+11%
						[0/90]14	GI,C/GI,R: +250/+122%
[45]	PA6,6	14% 7:3 in FA:AA	158 ± 19	3, 18 g/m^2	PrP	[0]10	GI,C/GI,R: +28/−41%
	PA6,9	16% 1:1 in FA:AA	245 ± 28			[0/90]20	GI,C/GI,R: +48/+62%
[46]	PA	20% in 1:1 FA:CLF	400-650	40 µm (1.8 g/m^2)	PrP	[0/90]14	GI,C/GI,R: +137/+124%
[47]	PA6,6	14% in 1:1 FA:CLF	150 ± 20	25 ± 8 µm	PrP	[0/90]12	GI,C : +5% - Energy absorbed: +23%
[48]	PA6,6	20% in 7:3 TFE:FA	500	70-100 µm (8-12 g/m^2)	PrP	[0/90]18	GI,C : 280-340% - GI,R: 255-322%
[31]	PA6,6	14, 25% in 1:1 FA:CLF	150.500	25, 50 µm	PrP	[0/90]20	Best with thin nanoreinforce, random Nanofibers, small fiber diameter
[49]	Phenoxy	30% in 3:7 DMF:THF	909 ± 126	70 µm	PrP	[0/90]8	GI,C/GI,R: +98/+106%
[50]	Phenoxy	15% in 4:1 DMF:CHL	700	35-150 µm	RTM	[0/90]10	GI,C/GI,R: +325/+300%
[40]	PSF	25% in 9:1 DMAC:AC	230	1, 3, 5% resin content	PrP	[0]24	GI,C : +158/+261/+281% with 1/3/5%

[40]	PSF	25% in 9:1 DMAC:AC	230	5% resin content	PrP	NA	GI,C : 280%
[51]	PVA	15% in H2O	329 ± 58	7.10 ± 0.70 g/m^2	VARTM	[0]4	GI,C : −27%
[52]	HMV PVDF	25% in NA	213 ± 70	5% resin content	PrP	[0/90]8	GI,C/Fmax : −20/+6.0%
	LMW PVDF	30% in NA	340±150				GI,C/Fmax : −20 + 3.6%
[53]	PVDF	15% in 7:3 DMSO:AC	500 ± 110	45 ± 5	PrP	[0/90]14	GI,C/GI,R/Fmax : +98/+73/+36%
[36]	PVDF	15% in 3:7 DMSO:AC	500 ± 110	30 ± 3 µm	PrP	[0/90]14	GI,C/GI,R: +43/+36%
[54]	PVDF	15% in 3:7 DMSO:AC	500 ± 110	30 ± 3 µm	PrP	[0/90]14	GI,C : +44%
				60 ± 5 µm			GI,C : +88%
[55]	PA6,6	14% in 1:1 FA:CLF	170 ± 30	70-100 µm	PrP	[0]10	GI,C/GI,R: +23/−22%
[1, 56]	PCL/PA6	3,7 PCL + 5,6 Nylon % TFE	150 ± 25	NA	PrP	[0]18	GI,C/GI,R: +69/+59%
[57]	PES	5 gr in 5.00 mL DMF and 5.00 mL of Toluene	168	1,68 g/m^2	PrP	[0]6	GI,C : 78%
[58]	PA66	10% in FA	106 ± 9	30-80 µm	VARTM	[0]10	GI,C : 25%
[59]	PA66	14% in FA	262 ± 81	NA			GI,C : 15%
[27]	PA66	10% in FA + TCM	232 ± 44	25-27 g/m^2	PrP	[0]14	GI,C : 64%

	PA66	10% in FA + TCM + TFA	259 ± 53	10-11 g/m^2	PrP	[0]14	GI,C : 53%
	PA66+ NBR	10% in FA + TCM	-	9-10 g/m^2	PrP	[0]14	GI,C : 180%

Papers on Mode II tests.							
Ref #	**Polymer**	**Solution**	**Fiber Diameter**	**Fiber Amount**	**Manuf.**	**Layup**	**Results**
(a) Glass fibers - Papers on Mode II							
[40]	Epoxy	18-25% in 3:1 MEK:PGME		80-257 µm	PrP	[0]24	GII,C from −41% to +17%
							GII,C,F max at 0.1281 mm nanomat thick
[60]	PCL	12% in 9:1 FA:AA	343 ± 150	5-15 g/m^2	VARTM	[0]8	GII,C : +81%
	PA6	16% in 1:1 FA:AA	195 ± 35	4-20 g/m^2			GII,C : +76%
[61]	PCL	1:1 FA:AA	650 ± 150	14 ± 0.5 g/m^2	VARTM	[0]8	GII,C : +25/+42% CCP/ENF
	PA6		195 ± 35				GII,C : +28/+30% CCP/ENF
	PA6,9		250 ± 30				GII,C : +31/+46% CCP/ENF
[62]	PA6,6	14% in 1:1 FA:CLF	100	9 g/m^2	PrP	[0]10	GII,C : +85%
						[0]16	GII,C : +75%
						[0]18	No effect
[63]	PA6,6	14% in 1:1 FA:CLF	150 ± 15	25 ± 8 µm (25 g/m^2)	PrP	[0]10	GII,C : +109%
[31]	PA6,6	14% in 1:1 FA:CLF	270	27 µm	PrP	[0]16	GII,C : +24%

	PCL	15% in 1:1 FA:AA	150	31 µm			GII,C : +68%
	PA6,6 + PCL			30 µm			GII,C : +56%
[64]	PA6,9	20% in 1:1 FA:AA	457 ± 53 random	11 ± 0.5 g/m^2	PrP	[0]12	GII,C : +400%
			464 ± 110 aligned				
[38]	SBS	BuAc:SBS :MTI-TAD:LiCl in 100:13 :0.0585:1.3	2000 ± 500	12-22 g/m^2	VARTM	[0]8	GII,C : +100%
[65]	TEOS	see reference	200	6 µm (2.5 g/m^2)	VARTM	[0/90]6	GII,C : +56.1%
(b) Carbon fibers - Papers on Mode II							
[28]	PA6,6	15% in 68:17 FA:AA	150-300	1.5, 4.5, 9 g/m^2	PrP	[0]12	GII,C : +29, 69, 54% with NFamount
	PVB	10% in ETH	400-700	4.5 g/m^2			GII,C : −6%
		10% in ETH	700-1000	4.3 g/m^2			GII,C : −8%
	PCL	13% in 70:17 FA:AA	150-300	4.2 g/m^2			GII,C : +7%
	PES	20% in DMA	150-300	3.6 g/m^2			GII,C : +20%
	PAI	15% in 77:8 DMA:DMF	150-300	4.1 g/m^2			GII,C : +56%
[62]	PA6,6	14% in 1:1 FA:CLF	100	9 g/m^2	PrP	[0]18	no significant effect

[44]	PA6,6	20% in 70:30 TFA:FA	350-400	40, 90 µm	PrP	[0]20	GII,C : +62%
						[0/90]14	GII,C/GII,R: +99/+34%
[45]	PA6,6	14% 7:3 in FA:AA	158 ± 19	3, 18 g/m^2	PrP	[0]10	GII,C/GII,R: +20/+211%
	PA6,9	16% 1:1 in FA:AA	245±28			[0/90]20	GII,C/GI,R: +211/+65%
[47]	PA6,6	14% in 1:1 FA:CLF	150 ± 20	25 ± 8 µm	PrP	[0/90]12	σmax : +6.5% - Absorbed energy:
							+8.1%
[31]	PA6,6	14, 25% in 1:1 FA:CLF	150,500	25, 50 µm	PrP	[0/90]20	No thickness effect, aligned nanofibers, Smaller nanofibers improved absorbed energy,Bigger diameters improved the maximum tension
[49]	Phenoxy	30% in 3:7 DMF:THF	909 ± 126	70 µm	PrP	[0/90]8	GII,C : +31%
[52]	HMV PVDF	25% in 8:2 DMF:AC	213 ± 70	5% resin content	PrP	[0/90]8	GII,C : +57%
	LMW PVDF		340 ± 150				
[66]	Silk	13% in FA	50-100	0, 3, 5, 10% resin content	VARTM	[0/90]10	GII,C : +30% at 5%
	PA69	16 wt%, 1:1 FA/AA	200 ± 25	6 g/m^2	PrP	[0]4	0,65

	PA6	16 wt%, 1:1 FA/AA	150 ± 20	6 g/m^2	PrP	[0]4	GII C , 30%
	PA66	20% w/v nylon 6,6 pellets dissolved in 30/70 v/v of FA and TFE	250 ± 50	70 ± 5 µm	PrP	[0/90]24	GIIC 161%

Papers on Mode I/II fatigue tests.							
Ref #	**Polymer**	**Solution**	**Fiber Diameter**	**Fiber Amount**	**Manuf.**	**Layup**	**Results**
(a) Glass fibers - Papers on Fatigue Mode II							
[61]	PCL	NA% in 1:1 FA:AA	650 ± 150	14 ± 0.5 g/m^2	VARTM	[0]8	CCP: PCL best results
	PA6		195 ± 35				ENF: Growth rate: −15 times
	PA6,9		250 ± 30				
[26]	PA11/ PEBA	8 wt%, 60:40 FA/An	50-800	6 g/m^2		[0] 3mm	GI,C : 78% GIIC : 96%
(b) Carbon fibers - Papers on Fatigue Mode I							
[41]	nPVA	16, 18, 20, 22% in H2O	40-80	Mixed into epoxy	VARTM	[0/90]?	at 0.1% nPVA
							Fatigue life: 10–30 times longer
[43]	PA6,6	12% in 3:1 FA:AA	75-250	1.6-2.0 g/m^2	PrP	[0]20	Delamination onset life: improved
							Fatigue GI C , : +66%

[46]	PA	20% in 1:1 FA:CLF	400-650	40 µm (1.8 g/m^2)	PrP	[0/90]14	GI,threshold: +90%
[67]	PA6,6	20% in 1:1 FA:CLF	520 ± 100	18 g/m^2	PrP	[0/90]14	Fatigue life: +96%.
(c) Other composite materials							
[68]	PA6,9	6%PA69 6%PCL in 1:1 FA:AA	100-200	100 µm	-	[0] 3mm	increased the fracture energy by 50–100%

B. SOLVENT EXPERIMENTS DETAILED FLOW CHART

In between D5-D12, same solvent mixture is used.

- Since 7th experiment, clean room is used (cylindrical collector).
- Used for set-up optimization.
- In 8th , removal process was made easier.
- In 9th , transfer was failed due to lack of bonding of fiber veil. DCB results were differed.
- In 10th , transfer was successful (2 sided vacuuming). DCB results were stabil (15% improvement) however SEM results showed too much beads.
- In 11th & 12th , needle-collector dimension is controlled in between 16 cm -23 cm. Vaporising ↓ Beads ↑

D12 → D15 Alternate solvent mixtures are studied from literature.

D15 → D17 Too much beads are observed in SEM in D15. Tried to decrease concentration and add some trichloromethane (TCM).

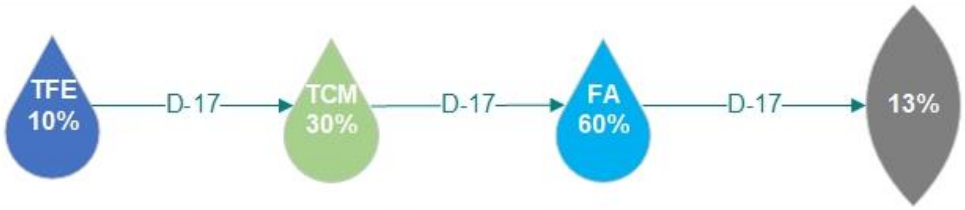

D17 → D22 Fully dissolving has not seen in D17. Partial dissolving experiments have been started. ST801-NC010A code has been learnt from Supertough Nylon 66 producer.

D22 : Zussman's Solvent Formula was repeated. Freezing under needle has been observed. Tried to decrease concentration. → D23

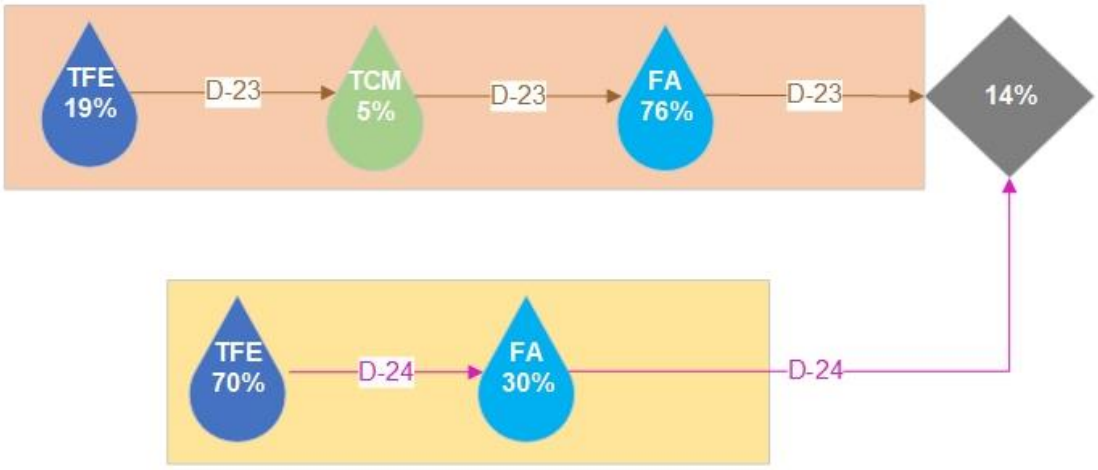

D23 & D24 : Can not spinned. Electrical sizzle has been heard . Tried to increase concentration. → D25 & D26

D25: Has been frozen on needle.

D26: Scanning electron microscope (SEM) results were far better. Tried to spin continiously for an hour. → D27
D27: Solution has been dropped. Can not spinned. (May be electrical contact issue?)
D27 → D28 Zuccelli's formula for PA 66 XXX-NC010A has been tried.

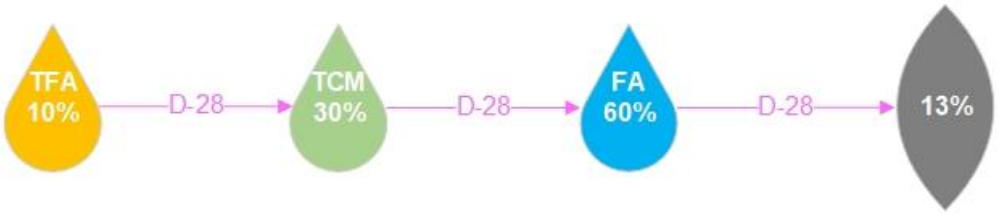

D28 : Can not spinned. Electrical sizzle has been heard .

D28 → D42 Here, there were many experiments done with low concentrations. Also film has been taken from solvent mixtures for Differential scanning calorimetry (DSC) analysis.
On the other hand, study of M.T.Hahn for impact modifier Nylon 6,6 has been examined at the same time. For that reason, it was thought that supertough nylon 6,6 was formed from the blending of paritally cross-linked elastomers with Nylon 6,6. Several paritally dissolving experiments are performed with THF,Xylene & Formic acid.
In D38 concentration has been referenced from Kilicoglu's PA 6,6 formula but prepared with different solvents for adjusting it to supertough. Solution mixture has been observed. There were a bit of a residue, however it has ben seem more clearer. It has been tried to spin, however solution has been dropped.

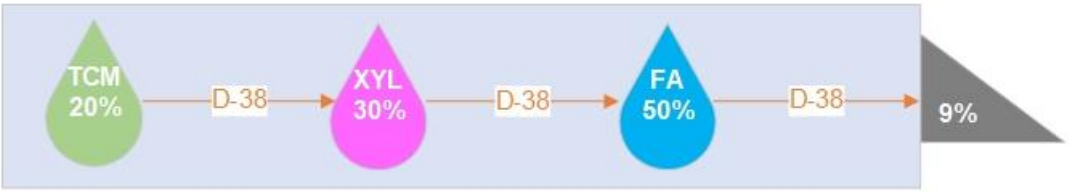

D38 → D42 : Concentration was increased.

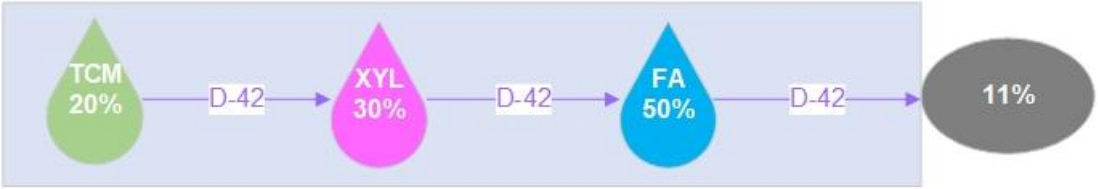

D42 : Solution has been dropped either frozen while optimizing voltage .
D42 → D45 Concentration was decreased.

D45 : Drops were decreased. Partially spinning was observed.
D45 → D48 FA ratio & concentration was increased.

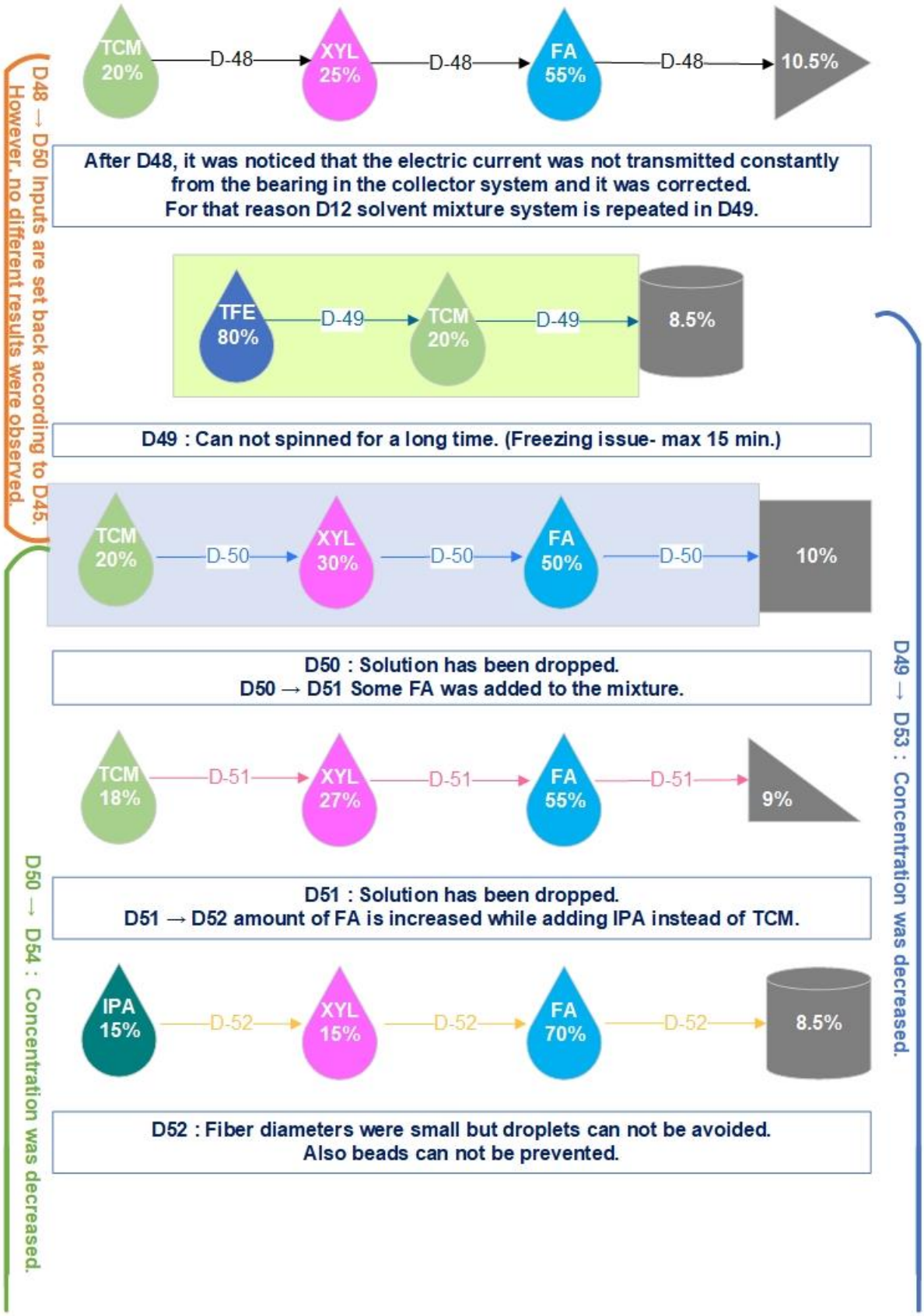
TCM 20%
D-48
XYL 25%
D-48
FA 55%
D-48
10.5%
After D48, it was noticed that the electric current was not transmitted constantly from the bearing in the collector system and it was corrected.
For that reason D12 solvent mixture system is repeated in D49.
TFE 80%
D-49
TCM 20%
D-49
8.5%
D49 : Can not spinned for a long time. (Freezing issue- max 15 min.)
TCM 20%
D-50
XYL 30%
D-50
FA 50%
D-50
10%
D50 : Solution has been dropped.
D50 → D51 Some FA was added to the mixture.
TCM 18%
D-51
XYL 27%
D-51
FA 55%
D-51
9%
D51 : Solution has been dropped.
D51 → D52 amount of FA is increased while adding IPA instead of TCM.
IPA 15%
D-52
XYL 15%
D-52
FA 70%
D-52
8.5%
D52 : Fiber diameters were small but droplets can not be avoided.
Also beads can not be prevented.
D48 → D50 Inputs are set back according to D45.
However, no different results were observed.
D50 → D54 : Concentration was decreased.
D49 → D53 : Concentration was decreased.

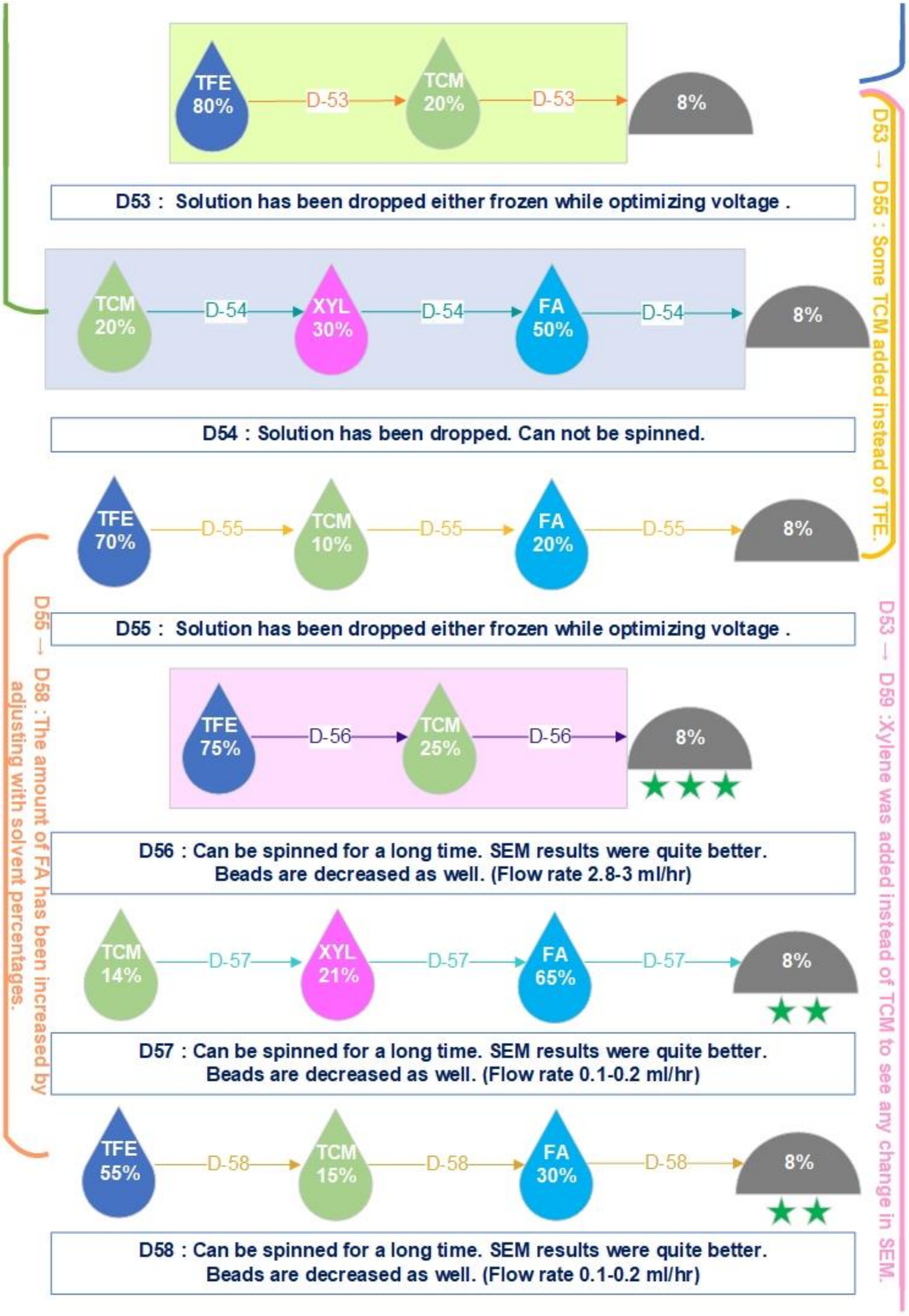
TFE 80%
D-53
TCM 20%
D-53
8%
D53 : Solution has been dropped either frozen while optimizing voltage .
TCM 20%
D-54
XYL 30%
D-54
FA 50%
D-54
8%
D54 : Solution has been dropped. Can not be spinned.
TFE 70%
D-55
TCM 10%
D-55
FA 20%
D-55
8%
D55 : Solution has been dropped either frozen while optimizing voltage .
TFE 75%
D-56
TCM 25%
D-56
8%
D56 : Can be spinned for a long time. SEM results were quite better.
Beads are decreased as well. (Flow rate 2.8-3 ml/hr)
TCM 14%
D-57
XYL 21%
D-57
FA 65%
D-57
8%
D57 : Can be spinned for a long time. SEM results were quite better.
Beads are decreased as well. (Flow rate 0.1-0.2 ml/hr)
TFE 55%
D-58
TCM 15%
D-58
FA 30%
D-58
8%
D58 : Can be spinned for a long time. SEM results were quite better.
Beads are decreased as well. (Flow rate 0.1-0.2 ml/hr)
D53 → D55 : Some TCM added instead of TFE.
D53 → D59 :Xylene was added instead of TCM to see any change in SEM.
D55 → D58 :The amount of FA has been increased by adjusting with solvent percentages.

D59 : Solution has been frozen. SEM results were not convenient.

Same as D56, spinned and transferred to the interface. Only difference is their densities. (3.5 g/m^2, 7 g/m^2, 10 g/m^2)

C. DCB RESULTS ON TABLE

i. Comparison of 3.5 g/m^2 fiber & its own base in crack initiation improvements

A (BASE)	Width [mm]	Pre-Crack [mm]	Propagated Crack [mm]	Load @ Final Crack Length [N]	Disp.@ Final Crack Length [mm]	Area Under Curve [J]	Area Under Line [J]	TOTAL ENERGY [J]	G_{IC} N/M
1	24.96	10.6	60	65.92	4.04	0.20	0.13	0.07	44.52
2	25	10.4	60	59.46	3.85	0.20	0.11	0.09	56.77
3	24.98	10.5	60	54.28	4.99	0.25	0.14	0.12	78.28
4	24.96	10.4	60	62.55	3.78	0.18	0.12	0.06	43.28
AVG								**0.08**	**55.71**

B (FIBER)	Width [mm]	Pre-Crack [mm]	Propagated Crack [mm]	Load @ Final Crack Length [N]	Disp.@ Final Crack Length [mm]	Area Under Curve [J]	Area Under Line [J]	TOTAL ENERGY [J]	G_{IC} N/M
1	24.98	10.1	60	65.75	4.75	0.25	0.16	0.1	65.73
2	25	11.1	60	56.7	4.75	0.23	0.13	0.09	62.48
3	25.01	10.8	60	63.39	4.36	0.25	0.14	0.11	75.22
4	25	10.5	60	57.23	4.84	0.24	0.14	0.1	66.48
AVG								**0.1**	**67.48**

% IMP TOTAL ENERGY (J)	% IMP G_{IC} (N/m)
21.23	**21.12**

ii. **Comparison of 3.5 g/m^2 fiber & its own base in crack propagation improvements**

A (BASE)	Width [mm]	Pre-Crack [mm]	Propagated Crack [mm]	Load @ Final Crack Length [N]	Disp.@ Final Crack Length [mm]	Area Under Curve [J]	Area Under Line [J]	TOTAL ENERGY [J]	G_{IC} [N/m]
1	24.96	10	61.5	32.84	18.01	0.70	0.30	0.41	267.49
2	25	10	61.7	28.39	15.66	0.56	0.22	0.34	221.47
3	24.98	10	61.5	31.16	17.1	0.61	0.27	0.34	222.22
4	24.96	10	60.4	30.03	15.75	0.61	0.24	0.37	245.1
AVG								**0.37**	**239.07**

B (FIBER)	Width [mm]	Pre-Crack [mm]	Propagated Crack [mm]	Load @ Final Crack Length [N]	Disp.@ Final Crack Length [mm]	Area Under Curve [J]	Area Under Line [J]	TOTAL ENERGY [J]	G_{IC} [N/m]
1	24.98	10	61.6	30.7	18.28	0.75	0.28	0.47	306.43
2	25	10	61.5	28.68	19.17	0.68	0.27	0.41	263.8
3	25.01	10	61	29.49	18.56	0.68	0.27	0.4	264.97
4	25	10	60.6	30	19.04	0.69	0.29	0.4	264.25
AVG								**0.42**	**274.86**

% IMP TOTAL ENERGY (J)	% IMP G_{IC} (N/m)
14.95	**14.97**

iii. Comparison of 7 g/m^2 fiber & its own base in crack initiation improvements

C (BASE)	Width [mm]	Pre-Crack [mm]	Propagated Crack [mm]	Load @ Final Crack Length [N]	Disp.@ Final Crack Length [mm]	Area Under Curve [J]	Area Under Line [J]	TOTAL ENERGY [J]	G_{IC} N/M
1	24.9	11.7	60.3	64.57	3.91	0.22	0.13	0.09	59.3
2	24.85	11.5	60	63.73	4.21	0.16	0.13	0.02	14.74
3	24.75	11.8	60	66.57	3.55	0.21	0.12	0.088	58.99
4	24.8	11.8	60	62.35	4.09	0.21	0.13	0.085	57.29
AVG								**0.087**	**58.53**

*2nd Base Value is not taken account for average calculation.

D (FIBER)	Width [mm]	Pre-Crack [mm]	Propagated Crack [mm]	Load @ Final Crack Length [N]	Disp.@ Final Crack Length [mm]	Area Under Curve [J]	Area Under Line [J]	TOTAL ENERGY [J]	G_{IC} N/M
1	24.9	12.1	60	66.67	5.08	0.31	0.17	0.14	96.84
2	24.95	12.4	60	71.24	4.82	0.29	0.17	0.12	77.05
3	24.9	11.6	60	59.08	5	0.28	0.15	0.13	86.15
4	24.75	10.7	60	63.52	5.51	0.31	0.17	0.14	91.08
AVG								**0.13**	**87.78**

% IMP TOTAL ENERGY (J)	% IMP G_{IC} (N/m)
50.06	**49.98**

iv. Comparison of 7g/m^2 fiber & its own base in crack propagation improvements

C (BASE)	Width [mm]	Pre-Crack [mm]	Propagated Crack [mm]	Load @ Final Crack Length [N]	Disp.@ Final Crack Length [mm]	Area Under Curve [J]	Area Under Line [J]	TOTAL ENERGY [J]	G_{IC} N/M
1	24.9	10	60	35.61	17.31	0.73	0.31	0.42	280.06
2	24.85	10	61.9	30.77	17.85	0.68	0.27	0.41	265.48
3	24.75	10	60.8	31.77	16.96	0.68	0.27	0.41	272.73
4	24.8	10	60.5	30.47	17.09	0.65	0.26	0.39	260.99
AVG								**0.41**	**269.81**

D (FIBER)	Width [mm]	Pre-Crack [mm]	Propagated Crack [mm]	Load @ Final Crack Length [N]	Disp.@ Final Crack Length [mm]	Area Under Curve [J]	Area Under Line [J]	TOTAL ENERGY [J]	G_{IC} N/M
1	24.9	10	60.6	35.21	20.2	0.86	0.35	0.51	336.59
2	24.95	10	60.6	35.26	20.32	0.89	0.36	0.53	349.62
3	24.9	10	60.4	30.12	19.92	0.74	0.3	0.44	293.57
4	24.75	10	61.7	29.81	19.47	0.74	0.29	0.45	291.35
AVG								**0.48**	**317.78**

% IMP TOTAL ENERGY (J)	% IMP G_{IC} (N/m)
18.09	**17.77**

v. **Comparison of 10 g/m^2 fiber & its own base in crack initiation improvements**

E (BASE)	Width [mm]	Pre-Crack [mm]	Propagated Crack [mm]	Load @ Final Crack Length [N]	Disp.@ Final Crack Length [mm]	Area Under Curve [J]	Area Under Line [J]	TOTAL ENERGY [J]	G_{IC} N/M
1	24.7	13.9	60	55.57	4.54	0.24	0.12	0.12	78.77
2	24.8	13.6	60	57.82	4.92	0.27	0.14	0.13	84.48
3	24.85	12.2	60.2	59.08	4.57	0.25	0.14	0.11	74.34
4	24.8	13.4	60	63.43	4.19	0.23	0.13	0.1	66.93
AVG								**0.11**	**76.13**

F (FIBER)	Width [mm]	Pre-Crack [mm]	Propagated Crack [mm]	Load @ Final Crack Length [N]	Disp.@ Final Crack Length [mm]	Area Under Curve [J]	Area Under Line [J]	TOTAL ENERGY [J]	G_{IC} N/M
1	24.9	13.6	60	68.09	5.47	0.32	0.18	0.14	91.78
2	24.8	13.5	60	69.22	4.74	0.29	0.16	0.13	88.28
3	24.85	13.8	60	59.88	5.08	0.3	0.15	0.14	97.17
4	24.8	13.7	60	72.02	5.87	0.41	0.21	0.20	134.74
AVG								**0.15**	**102.99**

% IMP TOTAL ENERGY (J)	% IMP G_{IC} (N/m)
35.46	**35.28**

vi. Comparison of 10 g/m^2 fiber & its own base in crack propagation improvements

E (BASE)	Width [mm]	Pre-Crack [mm]	Propagated Crack [mm]	Load @ Final Crack Length [N]	Disp.@ Final Crack Length [mm]	Area Under Curve [J]	Area Under Line [J]	TOTAL ENERGY [J]	G_{IC} N/M
1	24.7	10	59.8	30.74	18.67	0.67	0.29	0.39	262.18
2	24.8	10	58.6	31.86	19.01	0.73	0.30	0.42	291.09
3	24.85	10	60.5	30.08	19.92	0.73	0.29	0.43	286.97
4	24.8	10	60.4	31.49	18.78	0.72	0.29	0.43	285.6
AVG								**0.42**	**281.46**

F (FIBER)	Width [mm]	Pre-Crack [mm]	Propagated Crack [mm]	Load @ Final Crack Length [N]	Disp.@ Final Crack Length [mm]	Area Under Curve [J]	Area Under Line [J]	TOTAL ENERGY [J]	G_{IC} N/M
1	24.9	10	61.1	29.05	22.05	0.85	0.32	0.52	344.82
2	24.8	10	60.2	30.56	18.86	0.72	0.29	0.44	292.04
3	24.85	10	58.6	31.08	19.21	0.70	0.3	0.4	275.2
4	24.8	10	60.2	31.77	20.8	0.8	0.32	0.48	323.44
AVG								**0.46**	**308.87**

% IMP TOTAL ENERGY (J)	% IMP G_{IC} (N/m)
10.46	**9.74**

D. SEM RESULTS OF EXPERIMENTS

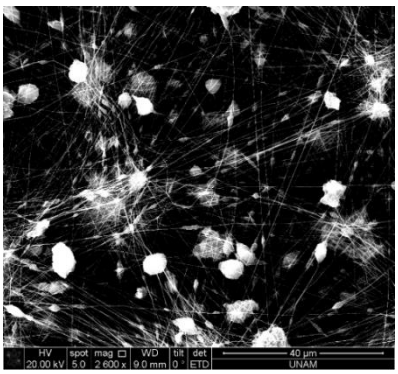

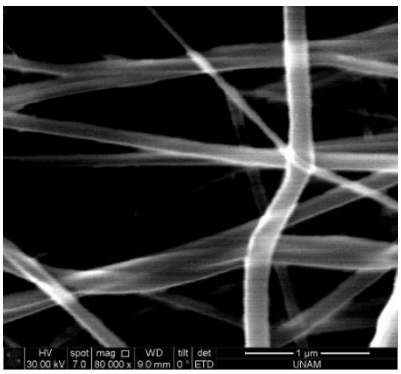

EXPERIMENT NO	SOLVENT MIXTURE	WEIGHT % OF POLYMER	VOLTAGE (kV)	DISTANCE (cm)	FLOW RATE (ml/hr)
D2	TFE	10.85	10	10	1

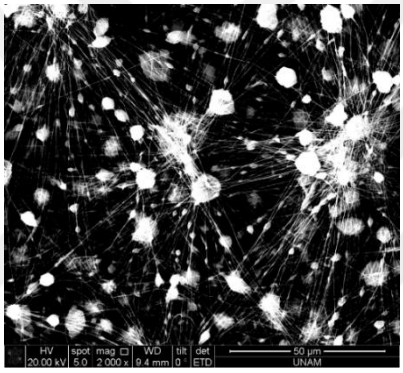

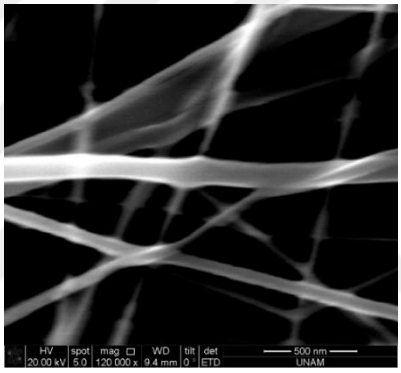

EXPERIMENT NO	SOLVENT MIXTURE	WEIGHT % OF POLYMER	VOLTAGE (kV)	DISTANCE (cm)	FLOW RATE (ml/hr)
D2	TFE	10.85	12	10	1

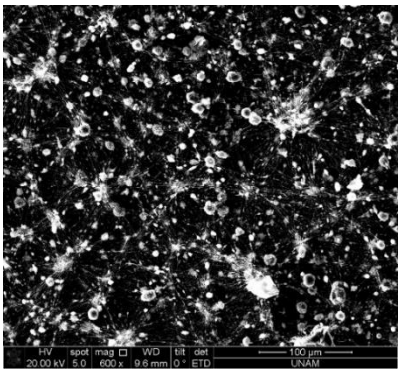

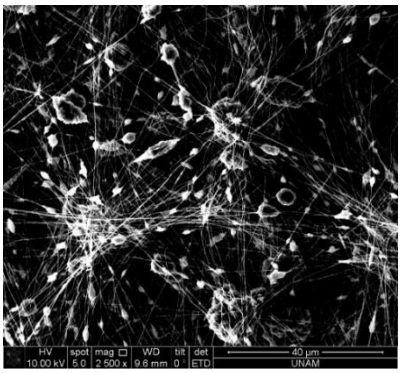

EXPERIMENT NO	SOLVENT MIXTURE	WEIGHT % OF POLYMER	VOLTAGE (kV)	DISTANCE (cm)	FLOW RATE (ml/hr)
D2	TFE	10.85	14	10	1

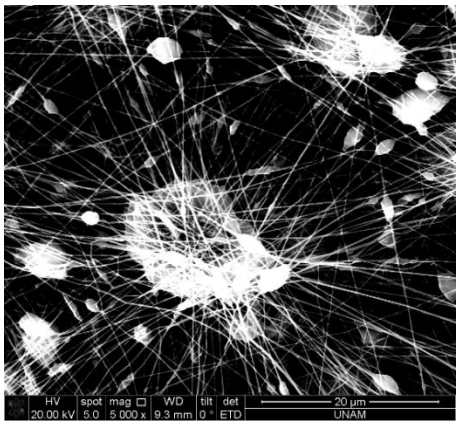

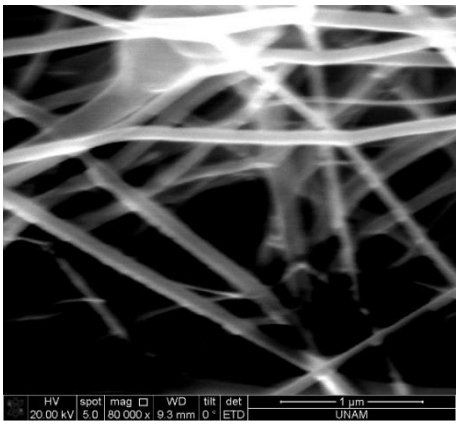

EXPERIMENT NO	SOLVENT MIXTURE	WEIGHT % OF POLYMER	VOLTAGE (kV)	DISTANCE (cm)	FLOW RATE (ml/hr)
D2	TFE	10.85	8	10	1

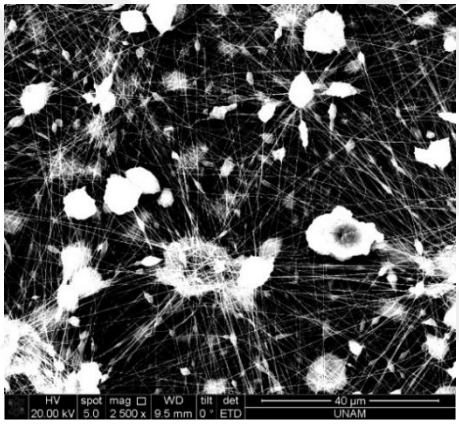

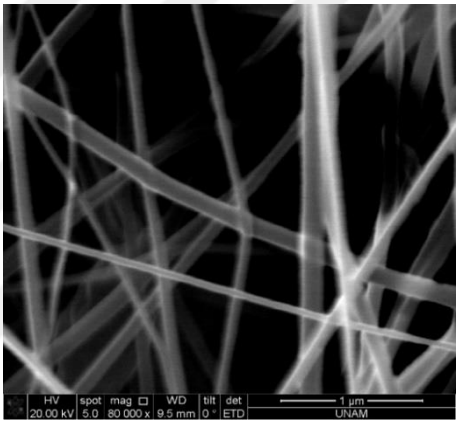

EXPERIMENT NO	SOLVENT MIXTURE	WEIGHT % OF POLYMER	VOLTAGE (kV)	DISTANCE (cm)	FLOW RATE (ml/hr)
D2	TFE	10.85	10	10	0.8

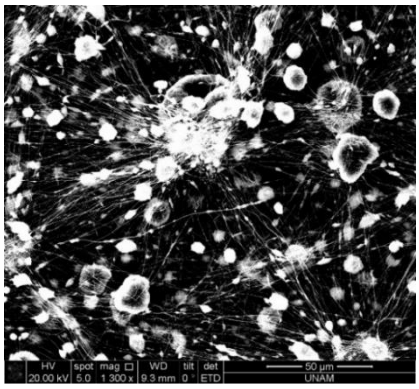

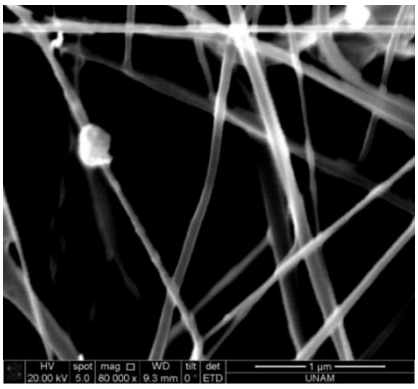

EXPERIMENT NO	SOLVENT MIXTURE	WEIGHT % OF POLYMER	VOLTAGE (kV)	DISTANCE (cm)	FLOW RATE (ml/hr)
D2	TFE	10.85	10	10	0.9

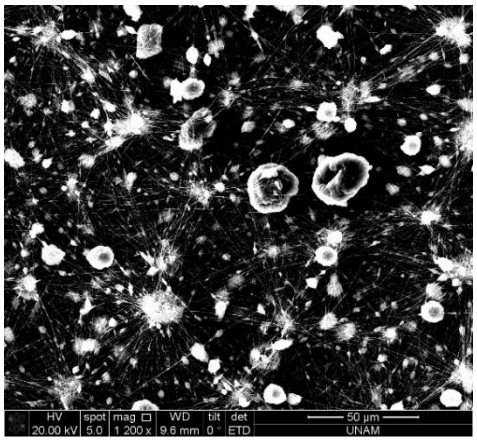

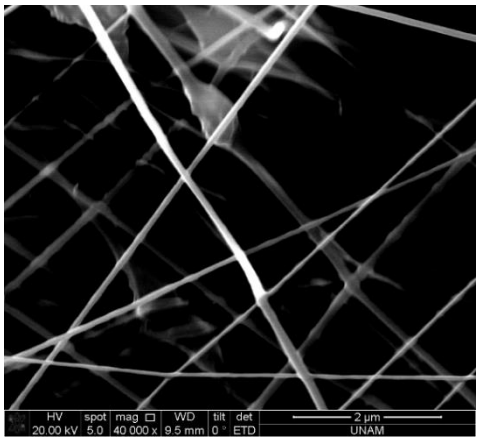

EXPERIMENT NO	SOLVENT MIXTURE	WEIGHT % OF POLYMER	VOLTAGE (kV)	DISTANCE (cm)	FLOW RATE (ml/hr)
D2	TFE	10.85	10	10	1.1

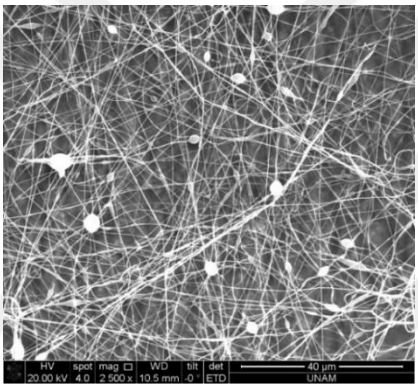

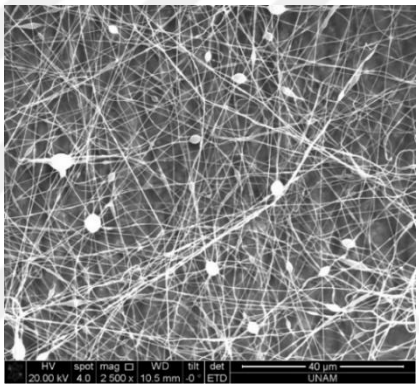

EXPERIMENT NO	SOLVENT MIXTURE	WEIGHT % OF POLYMER	VOLTAGE (kV)	DISTANCE (cm)	FLOW RATE (ml/hr)
D4	TFE:TCM 4:1	8.5	20	18	2

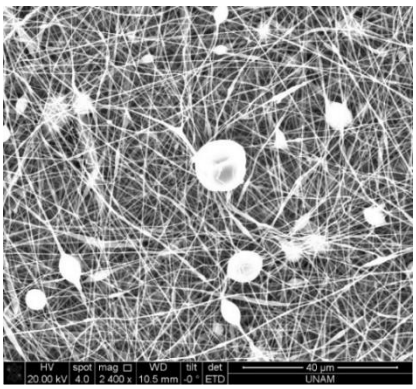

EXPERIMENT NO	SOLVENT MIXTURE	WEIGHT % OF POLYMER	VOLTAGE (kV)	DISTANCE (cm)	FLOW RATE (ml/hr)
D4	TFE:TCM 4:1	8.5	19	18	2

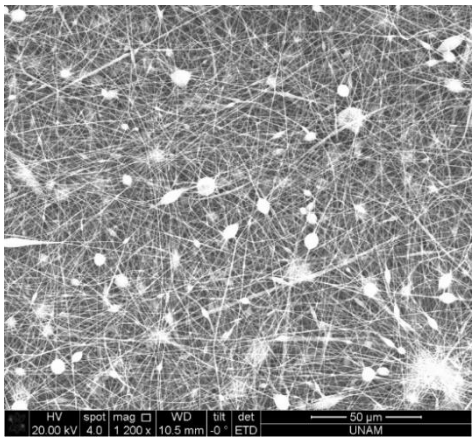

EXPERIMENT NO	SOLVENT MIXTURE	WEIGHT % OF POLYMER	VOLTAGE (kV)	DISTANCE (cm)	FLOW RATE (ml/hr)
D4	TFE:TCM 4:1	8.5	18	18	2

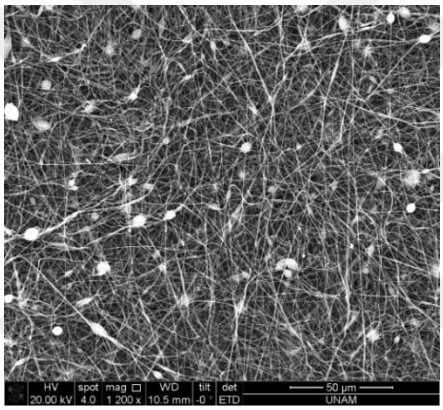

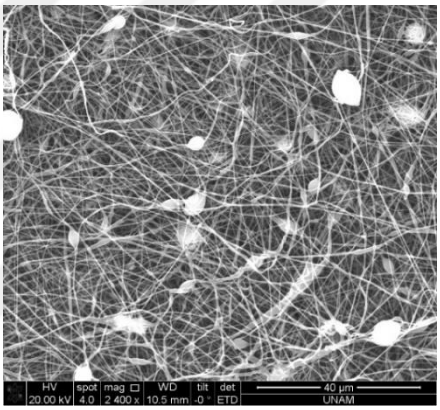

EXPERIMENT NO	SOLVENT MIXTURE	WEIGHT % OF POLYMER	VOLTAGE (kV)	DISTANCE (cm)	FLOW RATE (ml/hr)
D4	TFE:TCM 4:1	8.5	21	18	2

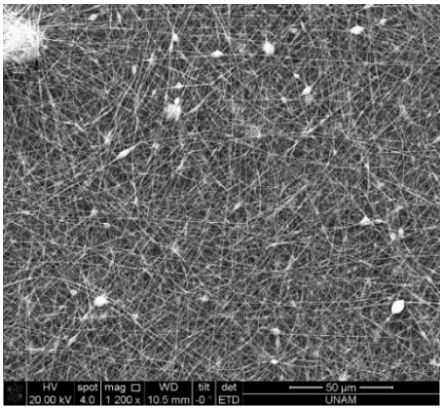

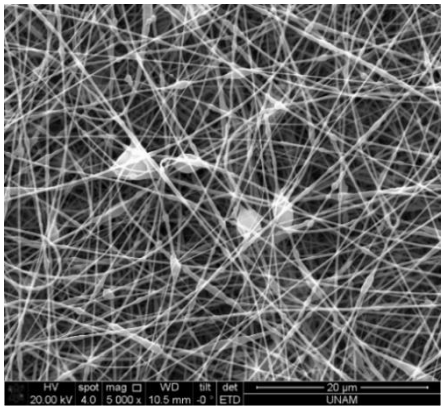

EXPERIMENT NO	SOLVENT MIXTURE	WEIGHT % OF POLYMER	VOLTAGE (kV)	DISTANCE (cm)	FLOW RATE (ml/hr)
D4	TFE:TCM 4:1	8.5	20	18	1.7

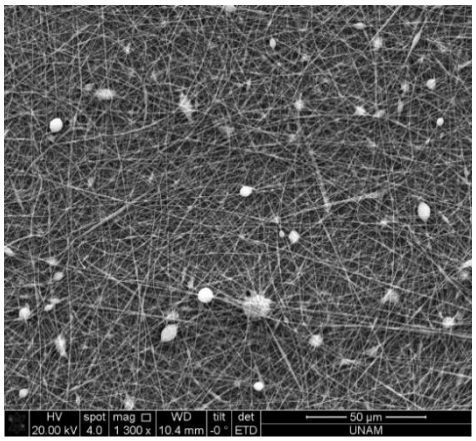

EXPERIMENT NO	SOLVENT MIXTURE	WEIGHT % OF POLYMER	VOLTAGE (kV)	DISTANCE (cm)	FLOW RATE (ml/hr)
D4	TFE:TCM 4:1	8.5	20	18	1.8

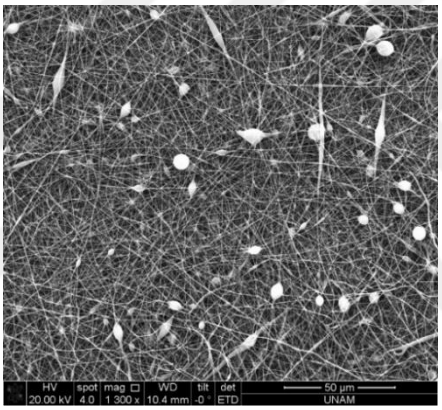

EXPERIMENT NO	SOLVENT MIXTURE	WEIGHT % OF POLYMER	VOLTAGE (kV)	DISTANCE (cm)	FLOW RATE (ml/hr)
D4	TFE:TCM 4:1	8.5	20	18	1.9

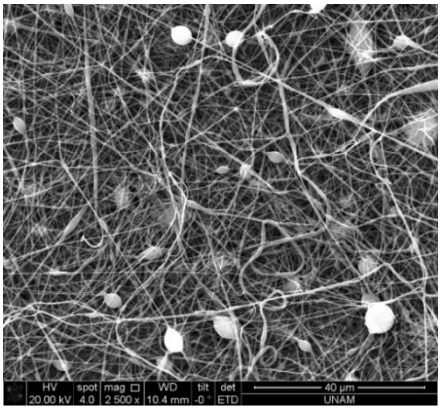

EXPERIMENT NO	SOLVENT MIXTURE	WEIGHT % OF POLYMER	VOLTAGE (kV)	DISTANCE (cm)	FLOW RATE (ml/hr)
D4	TFE:TCM 4:1	8.5	20	18	2.1

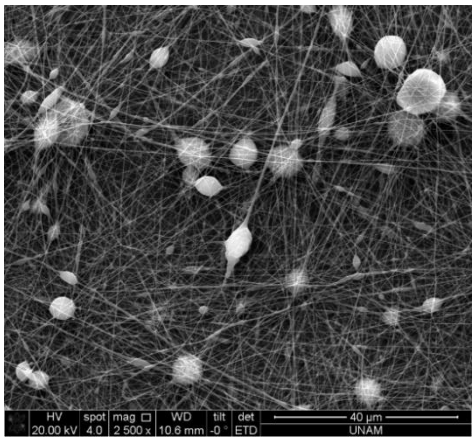

EXPERIMENT NO	SOLVENT MIXTURE	WEIGHT % OF POLYMER	VOLTAGE (kV)	DISTANCE (cm)	FLOW RATE (ml/hr)
D5	TFE:TCM 4:1	10	20	18	2

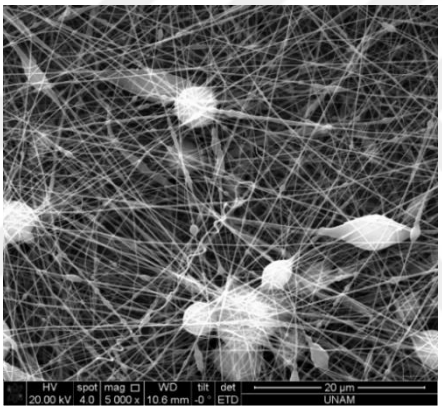

EXPERIMENT NO	SOLVENT MIXTURE	WEIGHT % OF POLYMER	VOLTAGE (kV)	DISTANCE (cm)	FLOW RATE (ml/hr)
D5	TFE:TCM 4:1	10	19	18	2

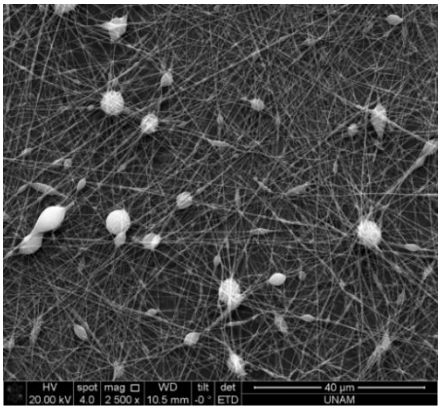

EXPERIMENT NO	SOLVENT MIXTURE	WEIGHT % OF POLYMER	VOLTAGE (kV)	DISTANCE (cm)	FLOW RATE (ml/hr)
D5	TFE:TCM 4:1	10	18	18	2

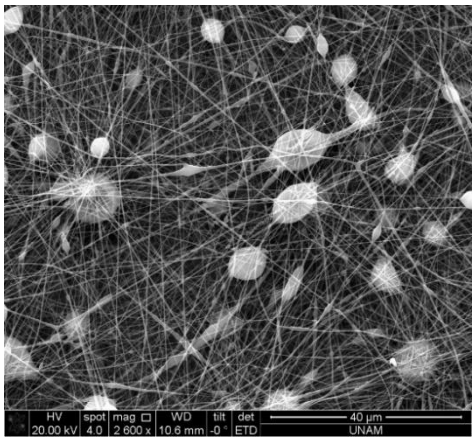

EXPERIMENT NO	SOLVENT MIXTURE	WEIGHT % OF POLYMER	VOLTAGE (kV)	DISTANCE (cm)	FLOW RATE (ml/hr)
D5	TFE:TCM 4:1	10	21	18	2

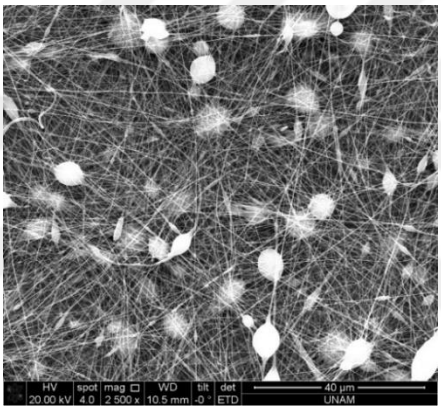

EXPERIMENT NO	SOLVENT MIXTURE	WEIGHT % OF POLYMER	VOLTAGE (kV)	DISTANCE (cm)	FLOW RATE (ml/hr)
D5	TFE:TCM 4:1	10	20	18	1.7

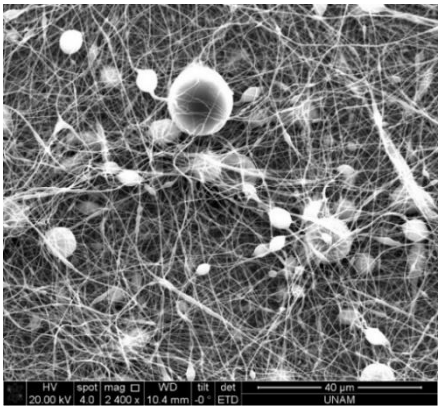

EXPERIMENT NO	SOLVENT MIXTURE	WEIGHT % OF POLYMER	VOLTAGE (kV)	DISTANCE (cm)	FLOW RATE (ml/hr)
D5	TFE:TCM 4:1	10	20	18	1.8

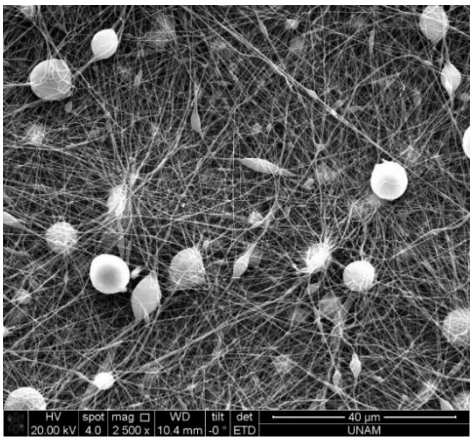

EXPERIMENT NO	SOLVENT MIXTURE	WEIGHT % OF POLYMER	VOLTAGE (kV)	DISTANCE (cm)	FLOW RATE (ml/hr)
D5	TFE:TCM 4:1	10	20	18	1.9

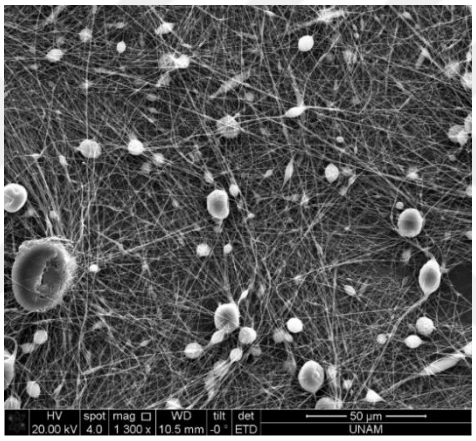

EXPERIMENT NO	SOLVENT MIXTURE	WEIGHT % OF POLYMER	VOLTAGE (kV)	DISTANCE (cm)	FLOW RATE (ml/hr)
D5	TFE:TCM 4:1	10	20	18	2.1

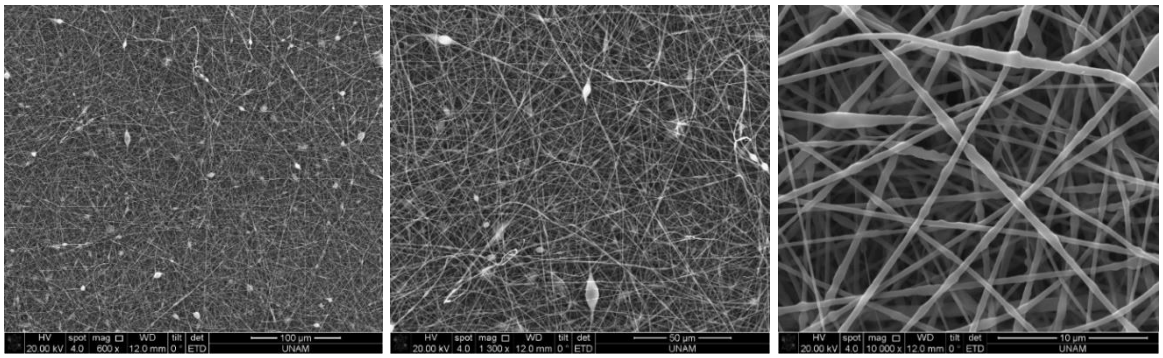

EXPERIMENT NO	SOLVENT MIXTURE	WEIGHT % OF POLYMER	VOLTAGE (kV)	DISTANCE (cm)	FLOW RATE (ml/hr)
D6	TFE:TCM 4:1	8.5	20	18	1.5

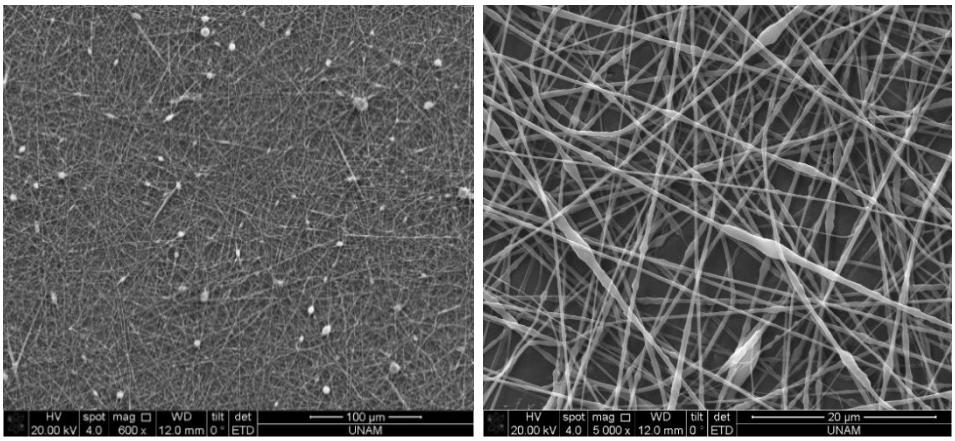

EXPERIMENT NO	SOLVENT MIXTURE	WEIGHT % OF POLYMER	VOLTAGE (kV)	DISTANCE (cm)	FLOW RATE (ml/hr)
D6	TFE:TCM 4:1	8.5	20	18	1.6

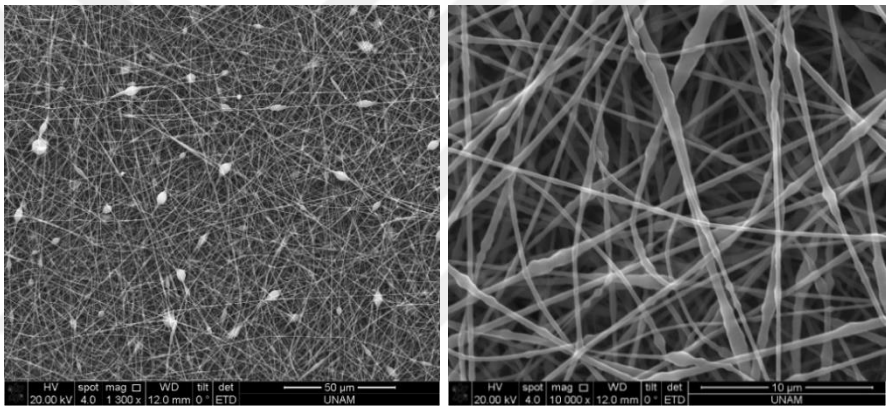

EXPERIMENT NO	SOLVENT MIXTURE	WEIGHT % OF POLYMER	VOLTAGE (kV)	DISTANCE (cm)	FLOW RATE (ml/hr)
D6	TFE:TCM 4:1	8.5	20	18	1.8

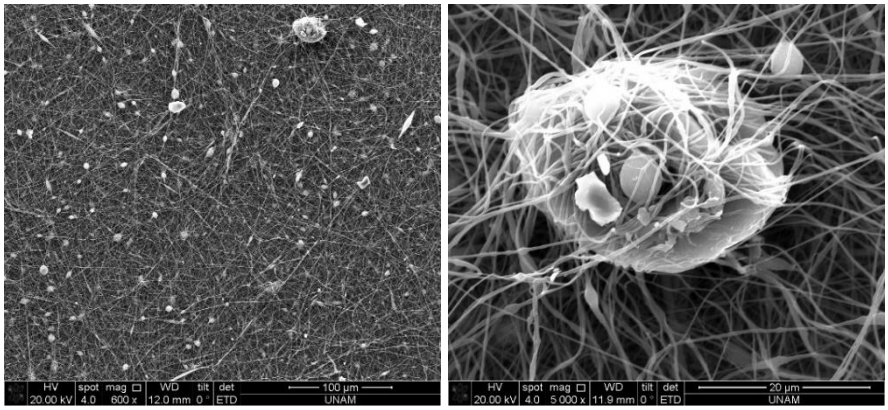

EXPERIMENT NO	SOLVENT MIXTURE	WEIGHT % OF POLYMER	VOLTAGE (kV)	DISTANCE (cm)	FLOW RATE (ml/hr)
D6	TFE:TCM 4:1	8.5	20	18	1.9

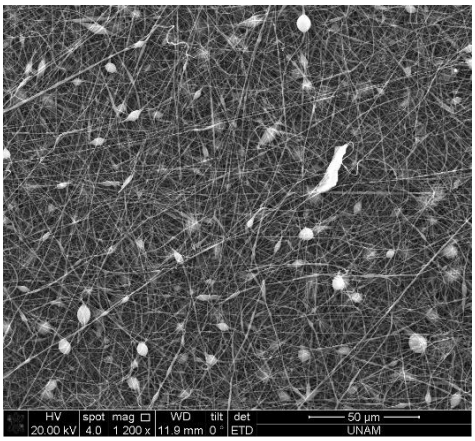

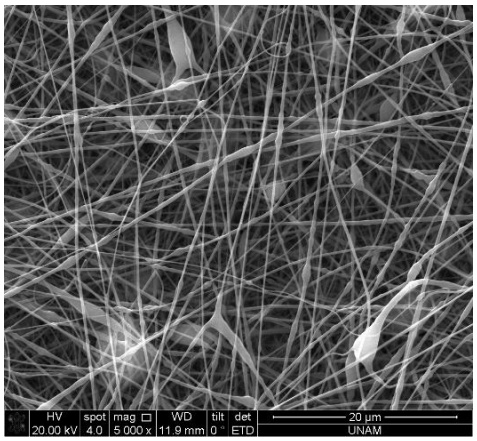

EXPERIMENT NO	SOLVENT MIXTURE	WEIGHT % OF POLYMER	VOLTAGE (kV)	DISTANCE (cm)	FLOW RATE (ml/hr)
D6	TFE:TCM 4:1	8.5	18	18	1.7

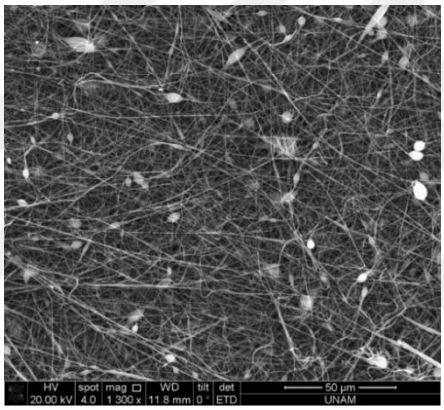

EXPERIMENT NO	SOLVENT MIXTURE	WEIGHT % OF POLYMER	VOLTAGE (kV)	DISTANCE (cm)	FLOW RATE (ml/hr)
D6	TFE:TCM 4:1	8.5	19	18	1.7

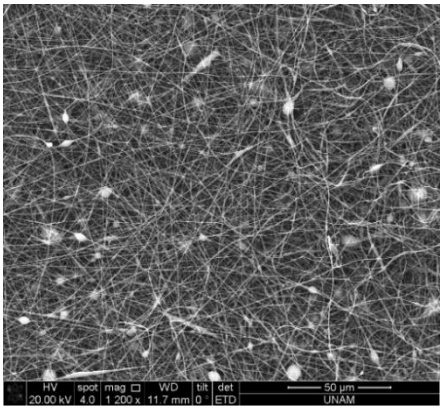

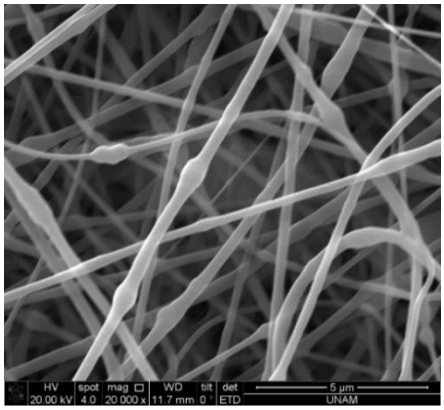

EXPERIMENT NO	SOLVENT MIXTURE	WEIGHT % OF POLYMER	VOLTAGE (kV)	DISTANCE (cm)	FLOW RATE (ml/hr)
D6	TFE:TCM 4:1	8.5	21	18	1.7

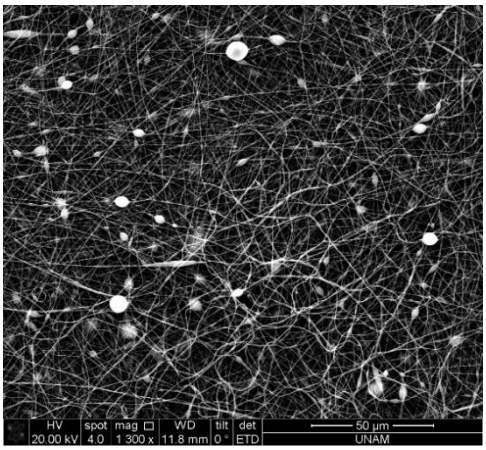

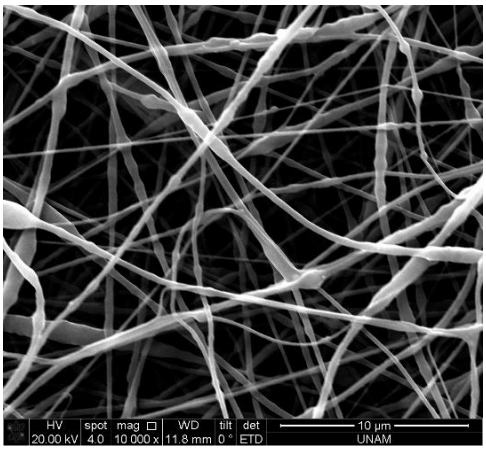

EXPERIMENT NO	SOLVENT MIXTURE	WEIGHT % OF POLYMER	VOLTAGE (kV)	DISTANCE (cm)	FLOW RATE (ml/hr)
D6	TFE:TCM 4:1	8.5	22	18	1.7

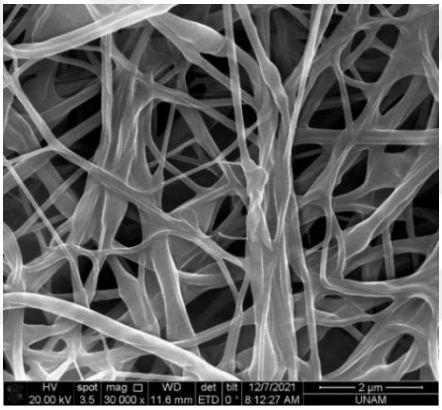

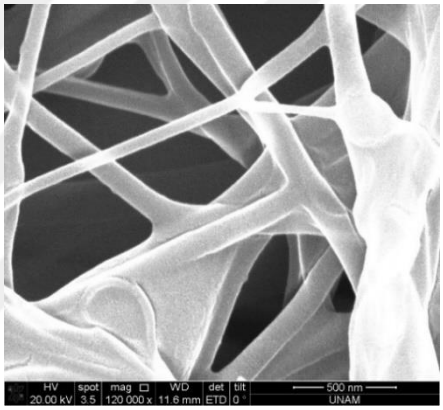

EXPERIMENT NO	SOLVENT MIXTURE	WEIGHT % OF POLYMER	VOLTAGE (kV)	DISTANCE (cm)	FLOW RATE (ml/hr)
D10	TFE:TCM 4:1	8.5	20	18	1.5

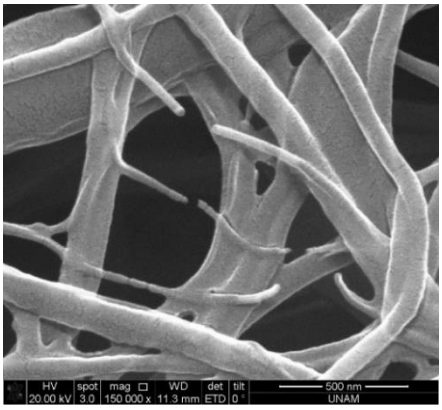

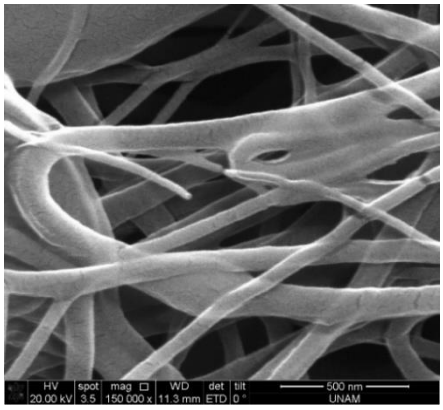

EXPERIMENT NO	SOLVENT MIXTURE	WEIGHT % OF POLYMER	VOLTAGE (kV)	DISTANCE (cm)	FLOW RATE (ml/hr)
D10	TFE:TCM 4:1	8.5	20	18	1.5

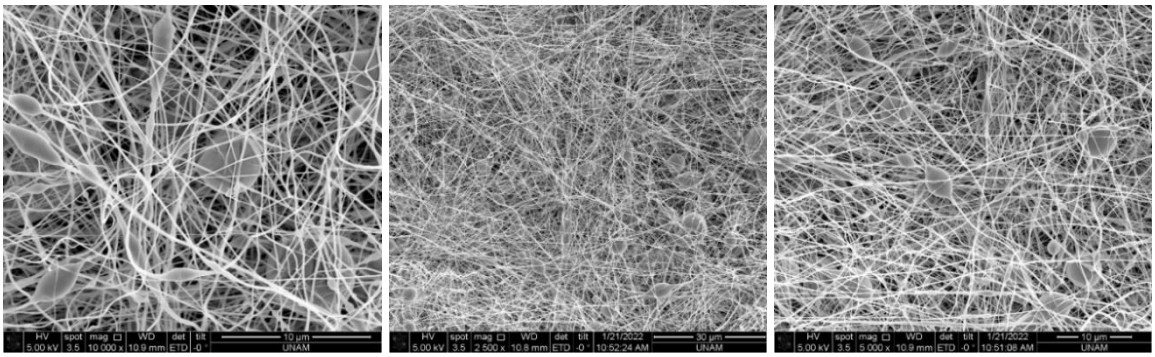

EXPERIMENT NO	SOLVENT MIXTURE	WEIGHT % OF POLYMER	VOLTAGE (kV)	DISTANCE (cm)	FLOW RATE (ml/hr)
D12	TFE:TCM 4:1	8.5	23	16	1.7

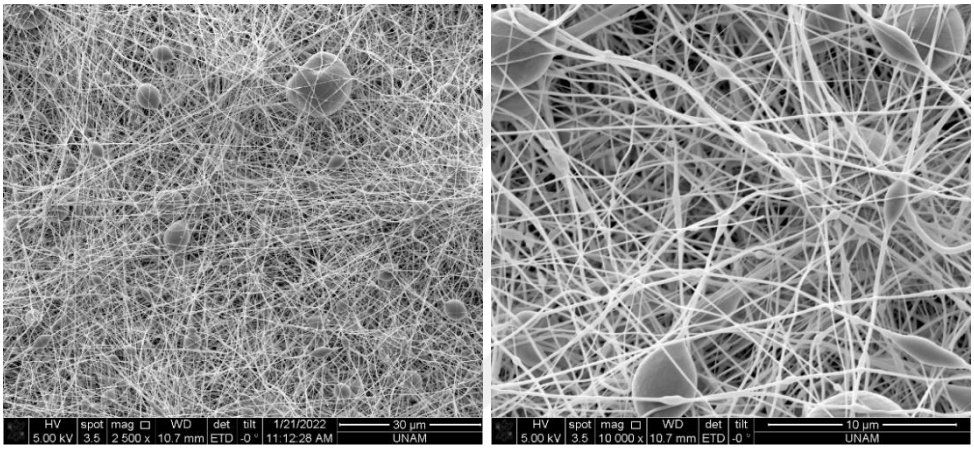

EXPERIMENT NO	SOLVENT MIXTURE	WEIGHT % OF POLYMER	VOLTAGE (kV)	DISTANCE (cm)	FLOW RATE (ml/hr)
D12	TFE:TCM 4:1	8.5	23	17	1.7

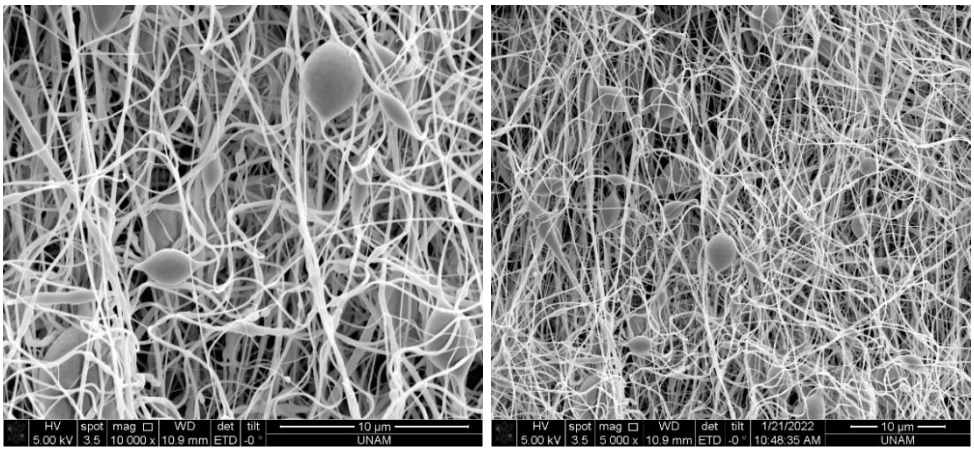

EXPERIMENT NO	SOLVENT MIXTURE	WEIGHT % OF POLYMER	VOLTAGE (kV)	DISTANCE (cm)	FLOW RATE (ml/hr)
D12	TFE:TCM 4:1	8.5	21	18	1.7

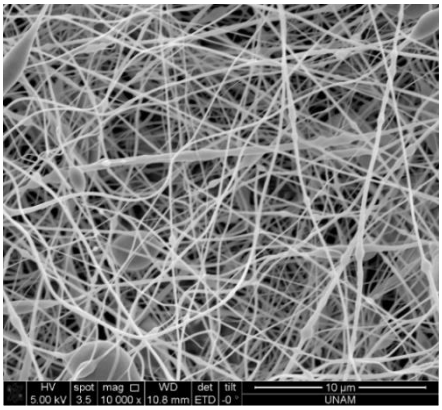

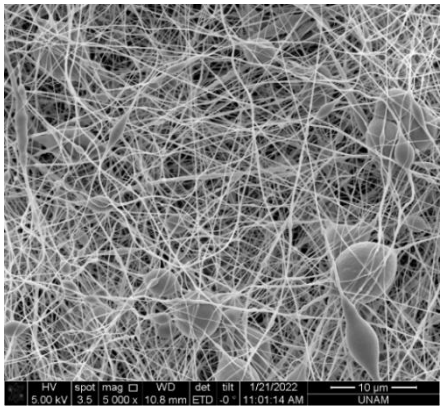

EXPERIMENT NO	SOLVENT MIXTURE	WEIGHT % OF POLYMER	VOLTAGE (kV)	DISTANCE (cm)	FLOW RATE (ml/hr)
D12	TFE:TCM 4:1	8.5	24	19	1.7

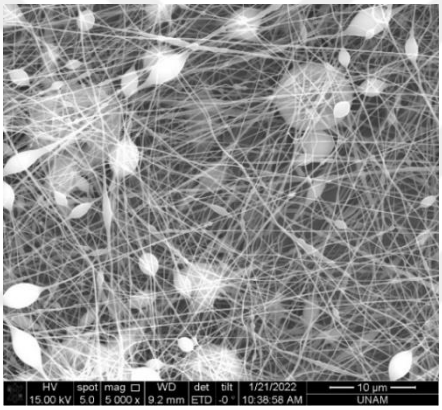

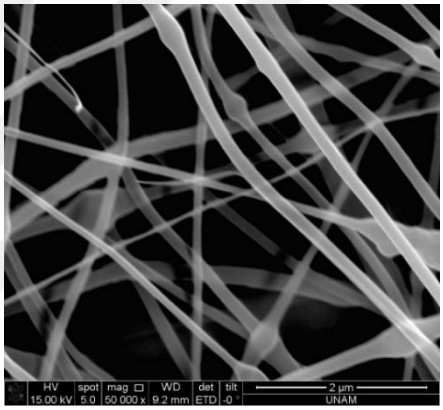

EXPERIMENT NO	SOLVENT MIXTURE	WEIGHT % OF POLYMER	VOLTAGE (kV)	DISTANCE (cm)	FLOW RATE (ml/hr)
D12	TFE:TCM 4:1	8.5	22	20	1.7

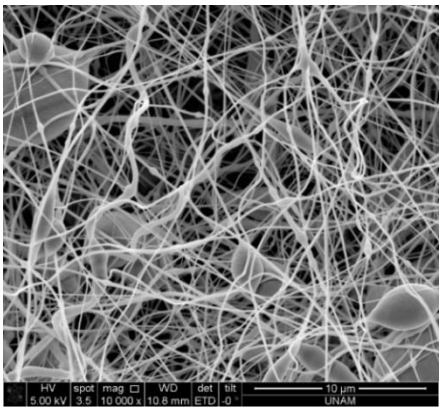

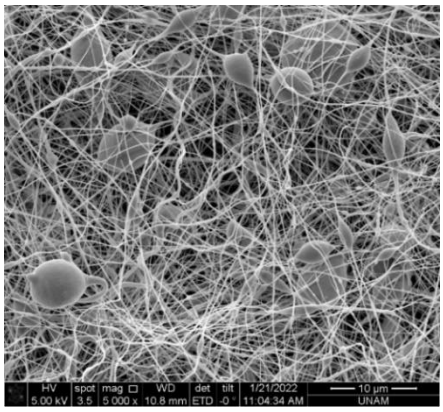

EXPERIMENT NO	SOLVENT MIXTURE	WEIGHT % OF POLYMER	VOLTAGE (kV)	DISTANCE (cm)	FLOW RATE (ml/hr)
D12	TFE:TCM 4:1	8.5	25	21	1.7

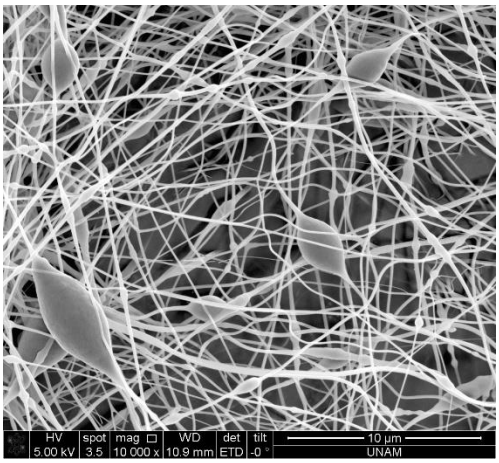

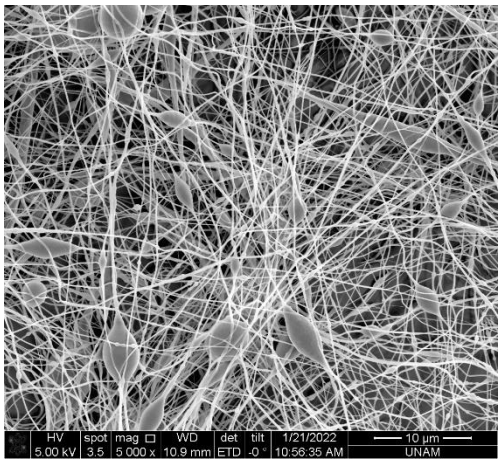

EXPERIMENT NO	SOLVENT MIXTURE	WEIGHT % OF POLYMER	VOLTAGE (kV)	DISTANCE (cm)	FLOW RATE (ml/hr)
D12	TFE:TCM 4:1	8.5	23	22	1.7

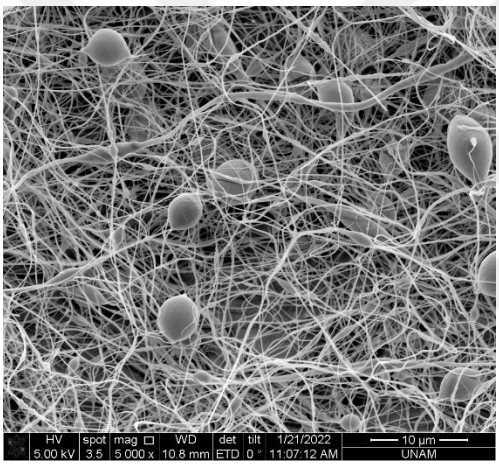

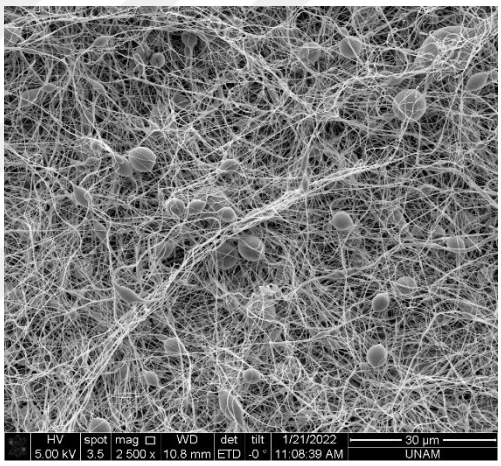

EXPERIMENT NO	SOLVENT MIXTURE	WEIGHT % OF POLYMER	VOLTAGE (kV)	DISTANCE (cm)	FLOW RATE (ml/hr)
D12	TFE:TCM 4:1	8.5	27	23	1.7

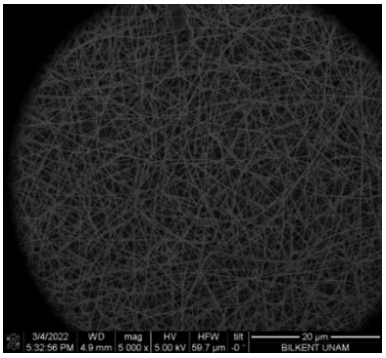

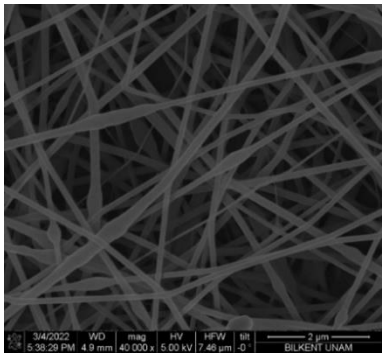

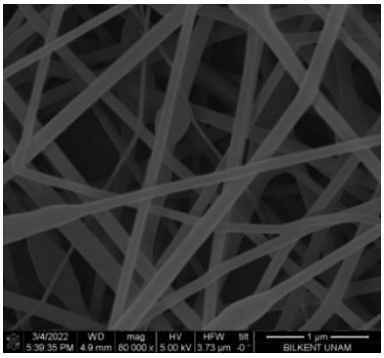

EXPERIMENT NO	SOLVENT MIXTURE	WEIGHT % OF POLYMER	VOLTAGE (kV)	DISTANCE (cm)	FLOW RATE (ml/hr)
D13	TFE:HFIP 1:1	20	21	18	1

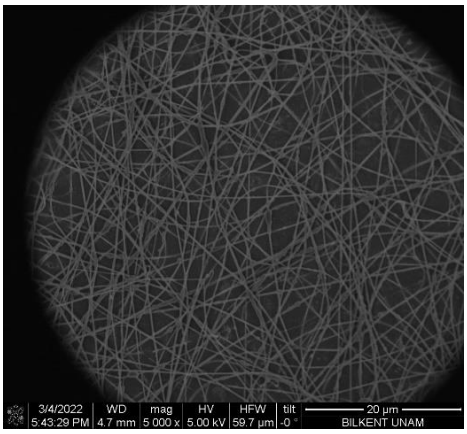

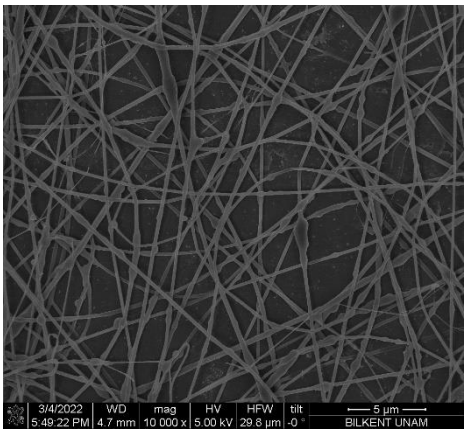

EXPERIMENT NO	SOLVENT MIXTURE	WEIGHT % OF POLYMER	VOLTAGE (kV)	DISTANCE (cm)	FLOW RATE (ml/hr)
D14	FA:HFIP 3:7	20	26	18	0.3

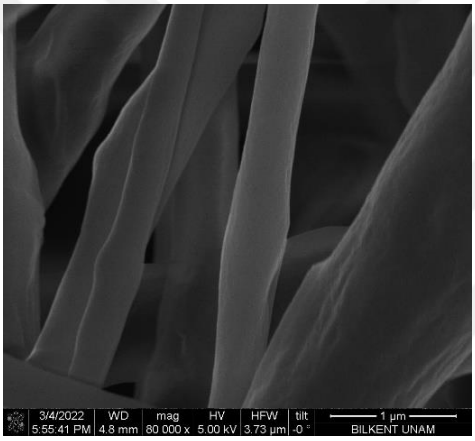

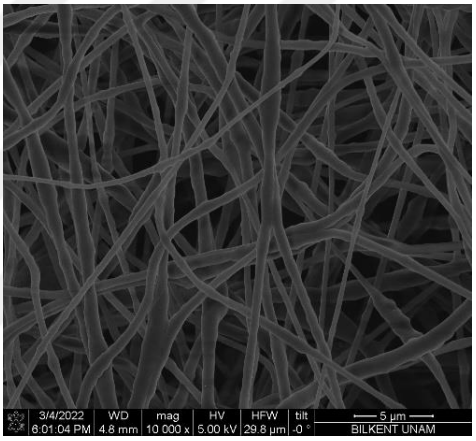

EXPERIMENT NO	SOLVENT MIXTURE	WEIGHT % OF POLYMER	VOLTAGE (kV)	DISTANCE (cm)	FLOW RATE (ml/hr)
D15	FA:TFE 7:3	20	27	18	0.7

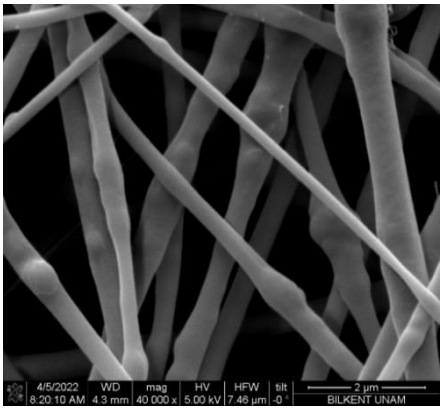

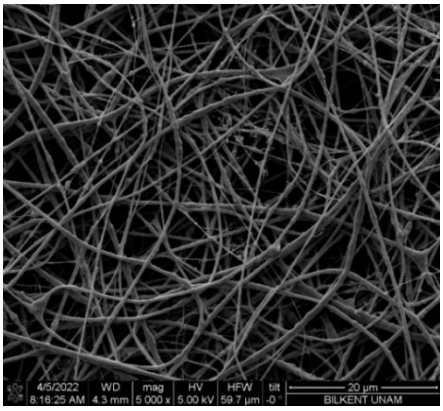

EXPERIMENT NO	SOLVENT MIXTURE	WEIGHT % OF POLYMER	VOLTAGE (kV)	DISTANCE (cm)	FLOW RATE (ml/hr)
D22	TFE:FA 7:3	20	21	18	1

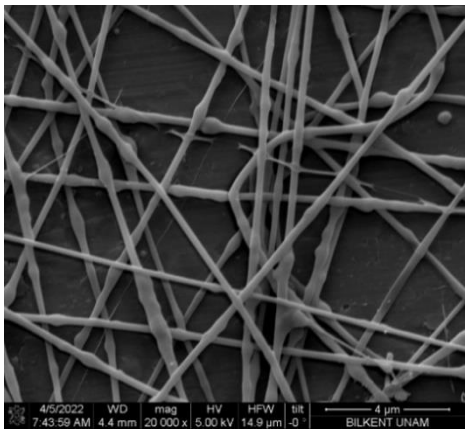

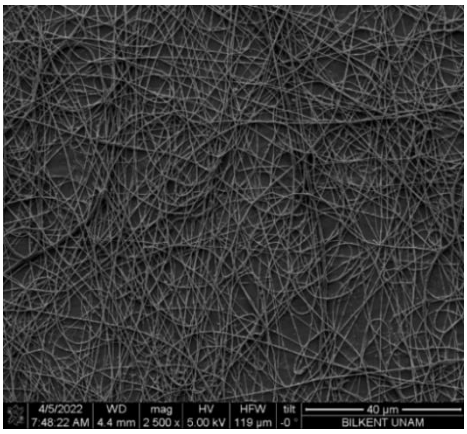

EXPERIMENT NO	SOLVENT MIXTURE	WEIGHT % OF POLYMER	VOLTAGE (kV)	DISTANCE (cm)	FLOW RATE (ml/hr)
D21	FA:TFE:THF 76:19:5	20	21	18	1

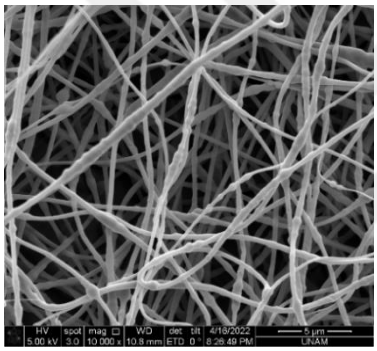
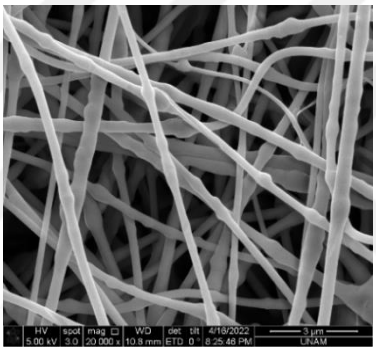
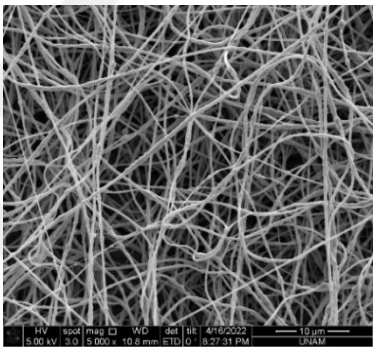

EXPERIMENT NO	SOLVENT MIXTURE	WEIGHT % OF POLYMER	VOLTAGE (kV)	DISTANCE (cm)	FLOW RATE (ml/hr)
D26	FA:TFE 3:7	20	24	18	0.75

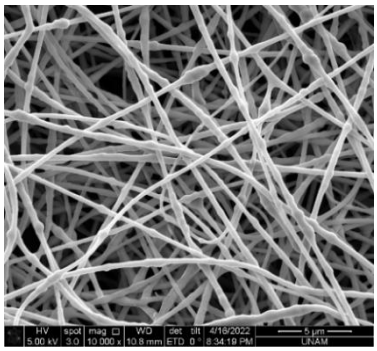
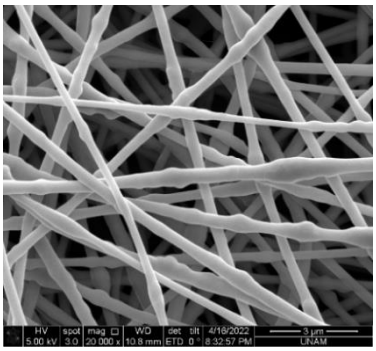
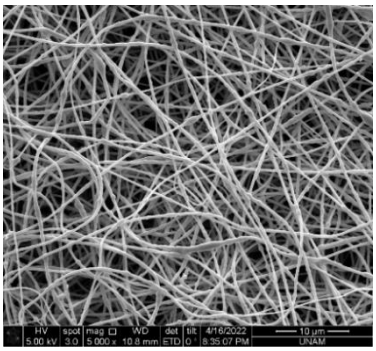

EXPERIMENT NO	SOLVENT MIXTURE	WEIGHT % OF POLYMER	VOLTAGE (kV)	DISTANCE (cm)	FLOW RATE (ml/hr)
D26	FA:TFE 3:7	20	25	18	0.75

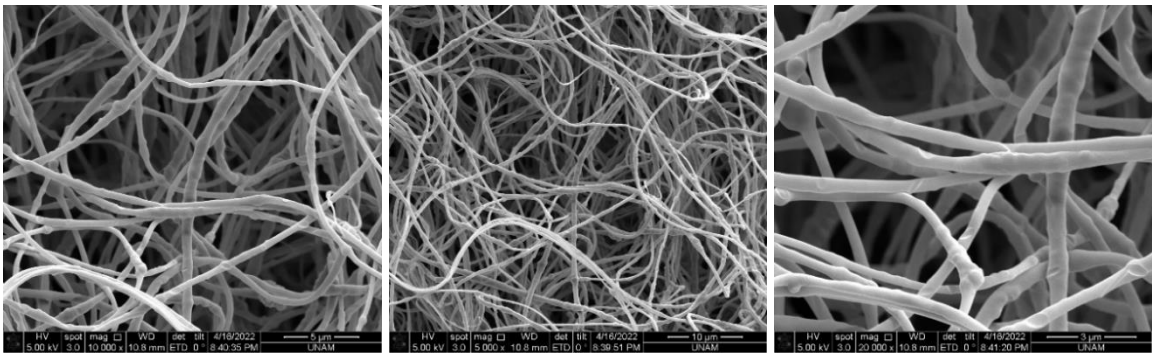

EXPERIMENT NO	SOLVENT MIXTURE	WEIGHT % OF POLYMER	VOLTAGE (kV)	DISTANCE (cm)	FLOW RATE (ml/hr)
D26	FA:TFE 3:7	20	23	17	0.75

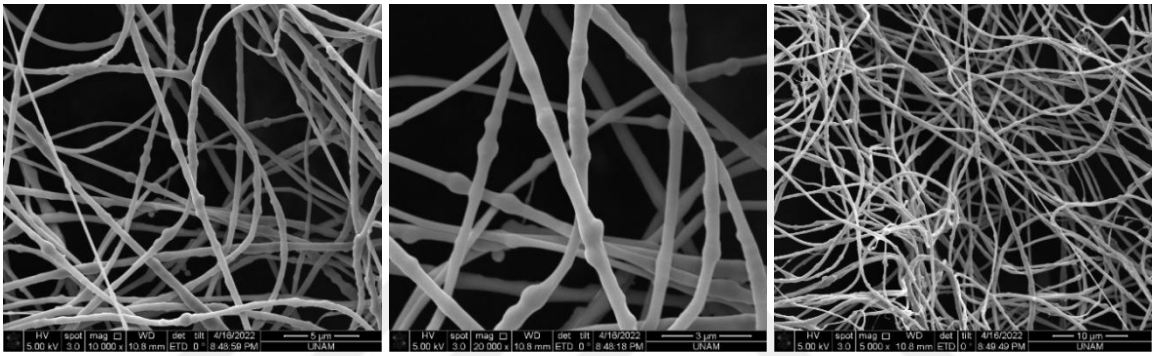

EXPERIMENT NO	SOLVENT MIXTURE	WEIGHT % OF POLYMER	VOLTAGE (kV)	DISTANCE (cm)	FLOW RATE (ml/hr)
D26	FA:TFE 3:7	20	24	20	0.75

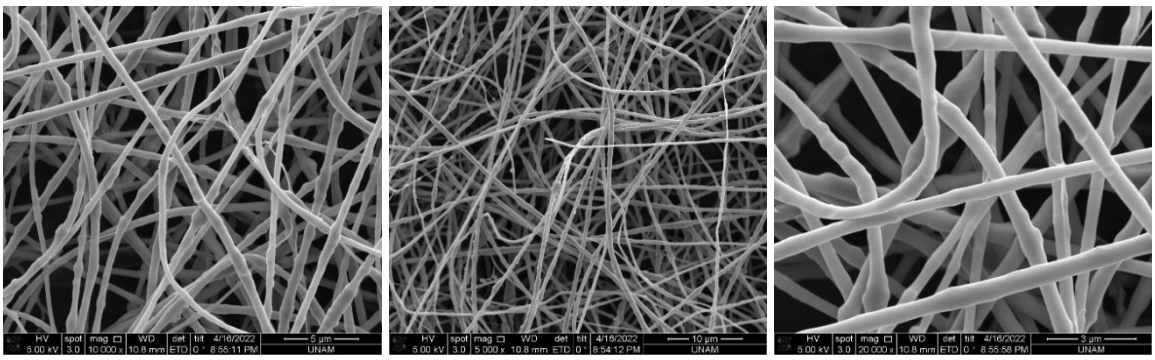

EXPERIMENT NO	SOLVENT MIXTURE	WEIGHT % OF POLYMER	VOLTAGE (kV)	DISTANCE (cm)	FLOW RATE (ml/hr)
D26	FA:TFE 3:7	20	23	18	0.75

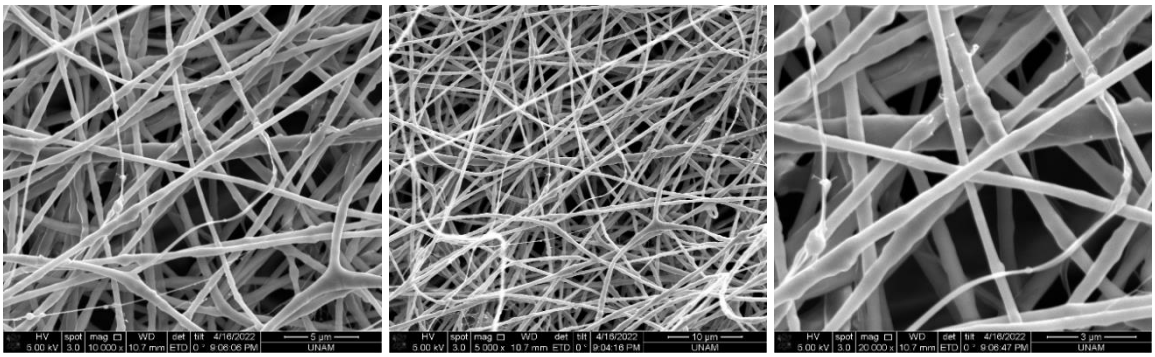

EXPERIMENT NO	SOLVENT MIXTURE	WEIGHT % OF POLYMER	VOLTAGE (kV)	DISTANCE (cm)	FLOW RATE (ml/hr)
D26	FA:TFE 3:7	20	25	18	0.75

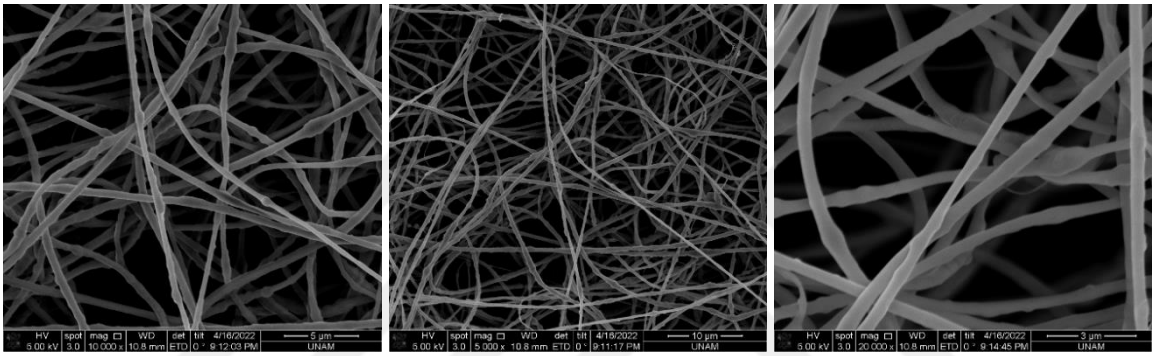

EXPERIMENT NO	SOLVENT MIXTURE	WEIGHT % OF POLYMER	VOLTAGE (kV)	DISTANCE (cm)	FLOW RATE (ml/hr)
D26	FA:TFE 3:7	20	23	18	0.65

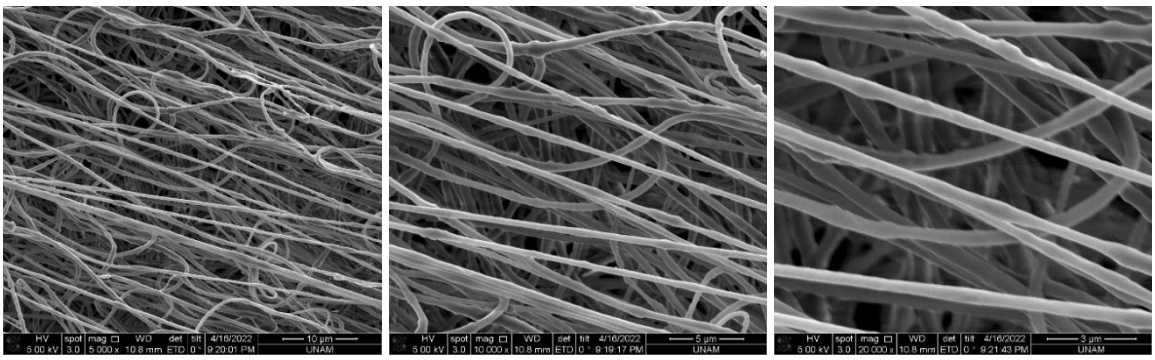

EXPERIMENT NO	SOLVENT MIXTURE	WEIGHT % OF POLYMER	VOLTAGE (kV)	DISTANCE (cm)	FLOW RATE (ml/hr)
D26	FA:TFE 3:7	20	25	18	0.85

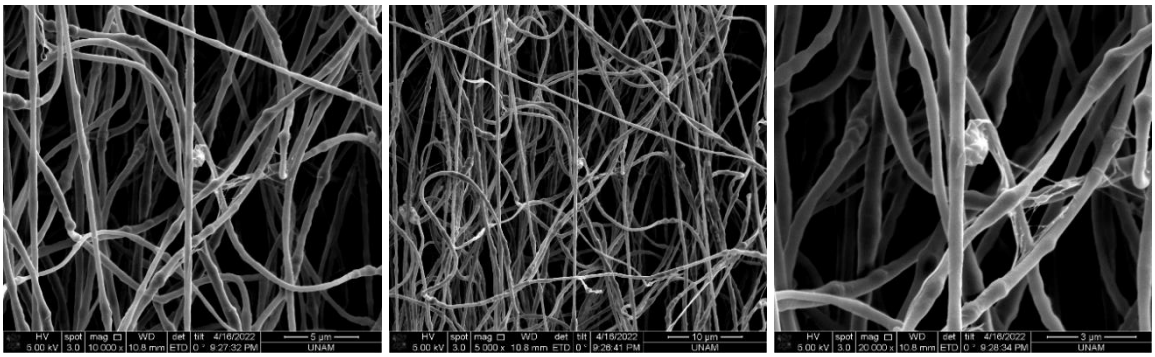

EXPERIMENT NO	SOLVENT MIXTURE	WEIGHT % OF POLYMER	VOLTAGE (kV)	DISTANCE (cm)	FLOW RATE (ml/hr)
D26	FA:TFE 3:7	20	25	18	1

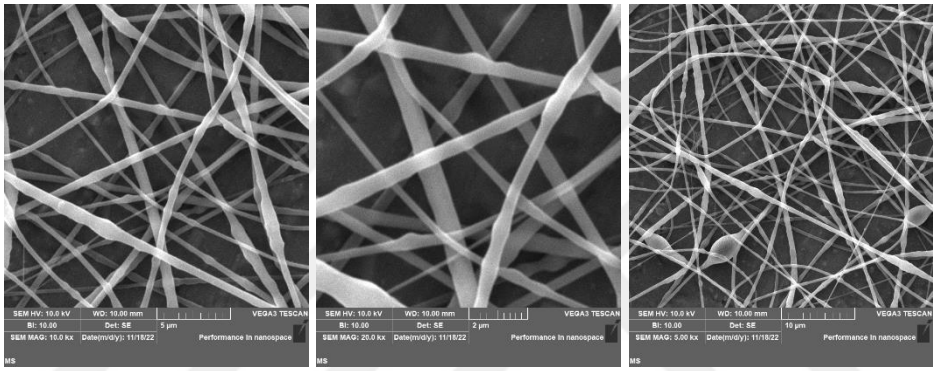

EXPERIMENT NO	SOLVENT MIXTURE	WEIGHT % OF POLYMER	VOLTAGE (kV)	DISTANCE (cm)	FLOW RATE (ml/hr)
D49	TFE:TCM 4:1	8.5	25	18	2

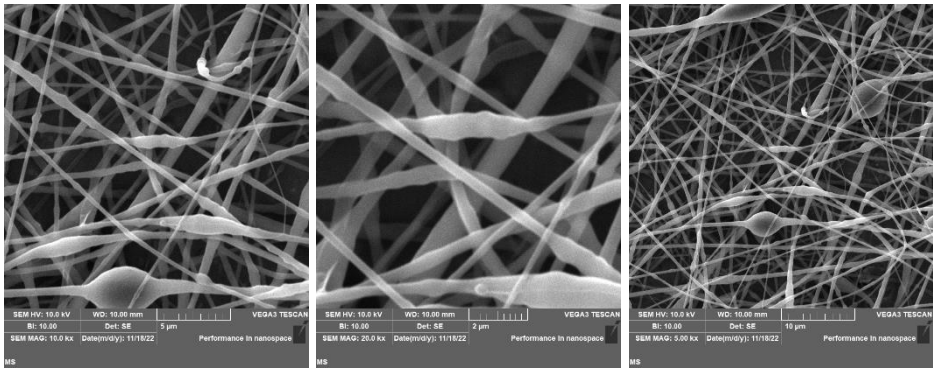

EXPERIMENT NO	SOLVENT MIXTURE	WEIGHT % OF POLYMER	VOLTAGE (kV)	DISTANCE (cm)	FLOW RATE (ml/hr)
D53	TFE:TCM 4:1	8	25	18	2

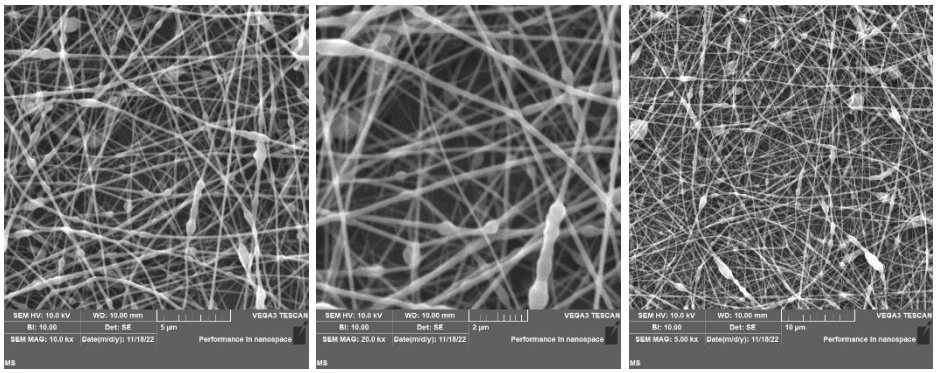

EXPERIMENT NO	SOLVENT MIXTURE	WEIGHT % OF POLYMER	VOLTAGE (kV)	DISTANCE (cm)	FLOW RATE (ml/hr)
D52	FA:XYL:IPA 70:15:15	8.5	25	18	2

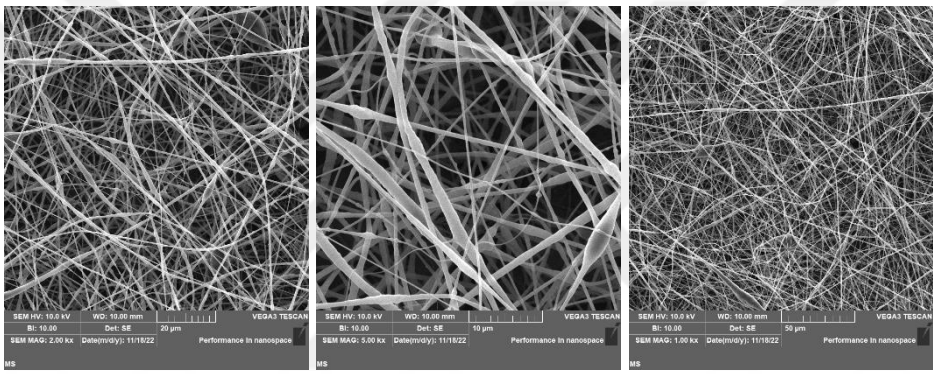

EXPERIMENT NO	SOLVENT MIXTURE	WEIGHT % OF POLYMER	VOLTAGE (kV)	DISTANCE (cm)	FLOW RATE (ml/hr)
D56	TFE:TCM 3:1	8	18	18	3

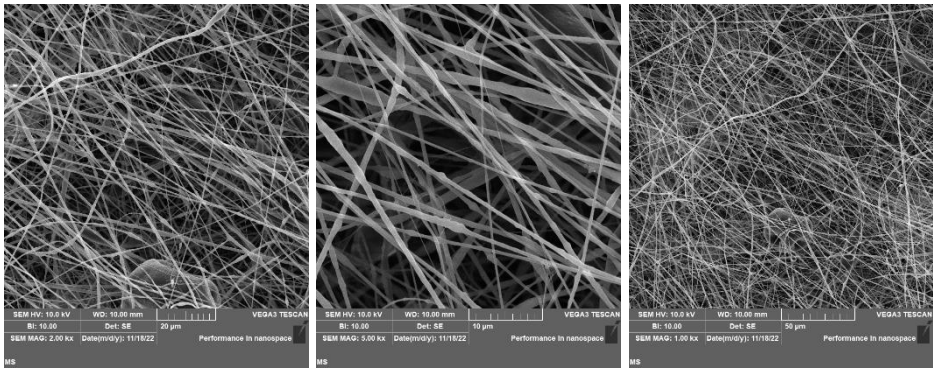

EXPERIMENT NO	SOLVENT MIXTURE	WEIGHT % OF POLYMER	VOLTAGE (kV)	DISTANCE (cm)	FLOW RATE (ml/hr)
D56	TFE:TCM 3:1	8	20	18	2

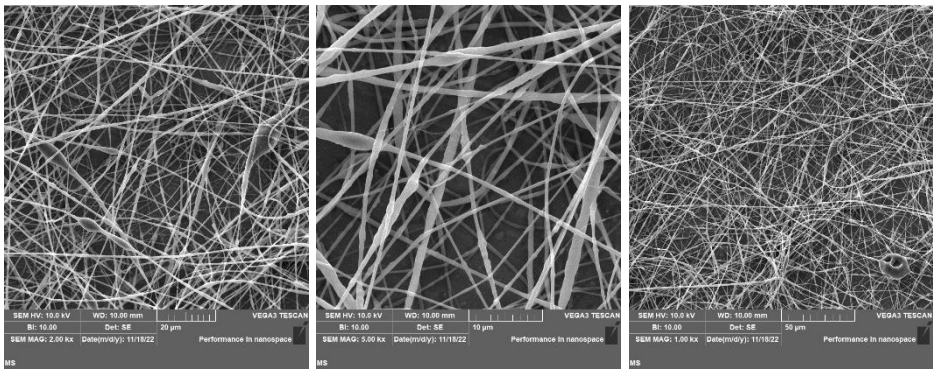

EXPERIMENT NO	SOLVENT MIXTURE	WEIGHT % OF POLYMER	VOLTAGE (kV)	DISTANCE (cm)	FLOW RATE (ml/hr)
D56	TFE:TCM 3:1	8	25	18	2.2

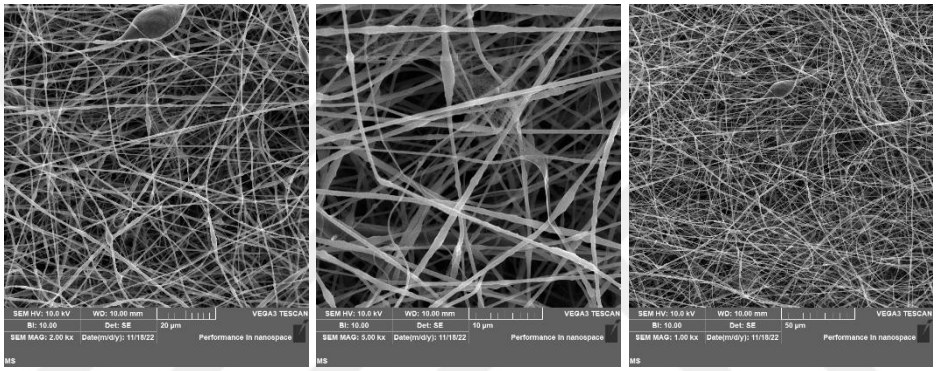

EXPERIMENT NO	SOLVENT MIXTURE	WEIGHT % OF POLYMER	VOLTAGE (kV)	DISTANCE (cm)	FLOW RATE (ml/hr)
D56	TFE:TCM 3:1	8	20	18	2.5

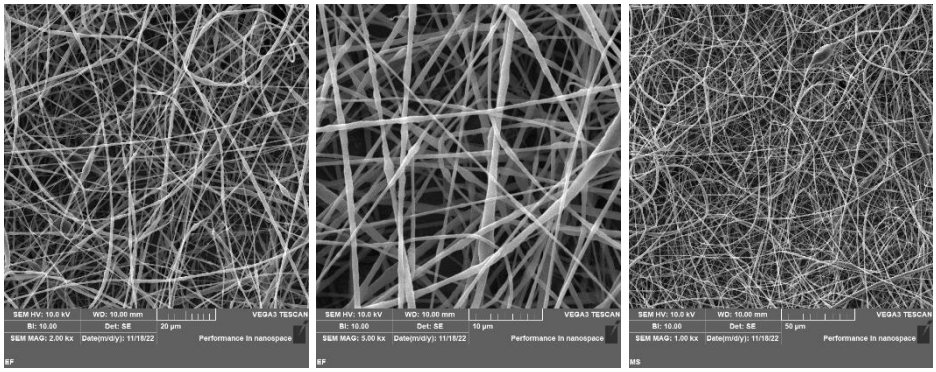

EXPERIMENT NO	SOLVENT MIXTURE	WEIGHT % OF POLYMER	VOLTAGE (kV)	DISTANCE (cm)	FLOW RATE (ml/hr)
D56	TFE:TCM 3:1	8	25	18	3

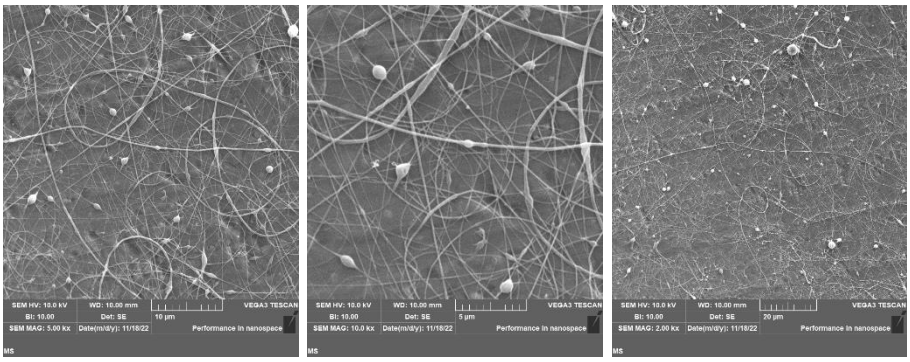

EXPERIMENT NO	SOLVENT MIXTURE	WEIGHT % OF POLYMER	VOLTAGE (kV)	DISTANCE (cm)	FLOW RATE (ml/hr)
D57	FA:XYL:TCM 65:21:14	8	25	18	0.25

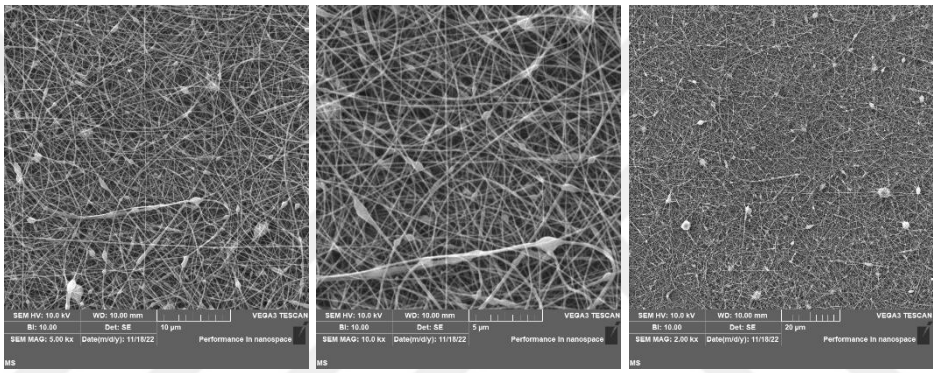

EXPERIMENT NO	SOLVENT MIXTURE	WEIGHT % OF POLYMER	VOLTAGE (kV)	DISTANCE (cm)	FLOW RATE (ml/hr)
D57	FA:XYL:TCM 65:21:14	8	27	18	0.15

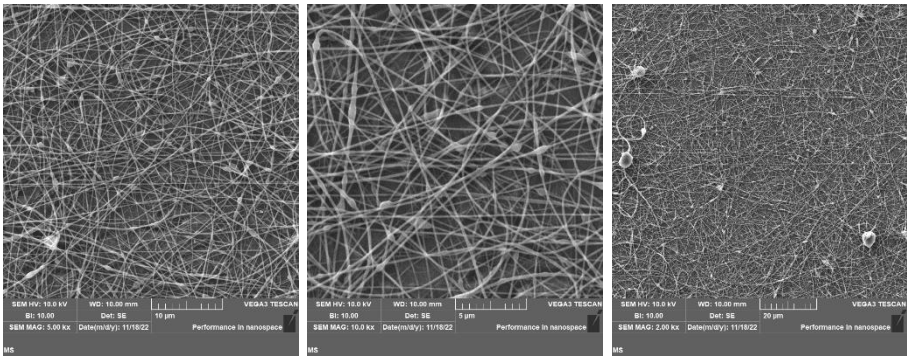

EXPERIMENT NO	SOLVENT MIXTURE	WEIGHT % OF POLYMER	VOLTAGE (kV)	DISTANCE (cm)	FLOW RATE (ml/hr)
D57	FA:XYL:TCM 65:21:14	8	25	18	0.1

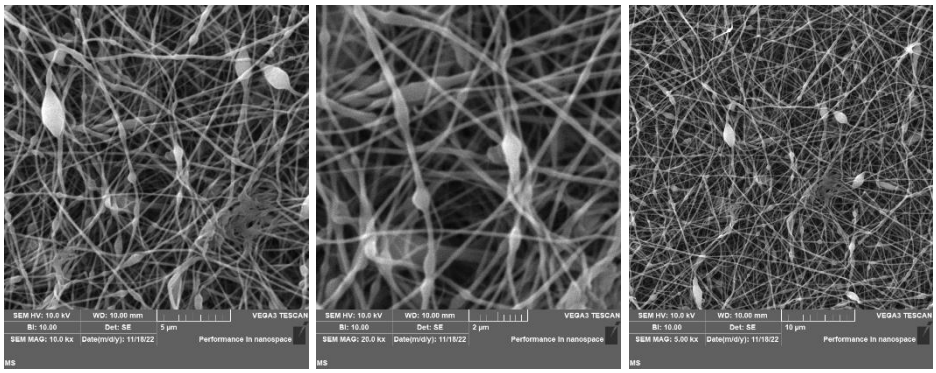

EXPERIMENT NO	SOLVENT MIXTURE	WEIGHT % OF POLYMER	VOLTAGE (kV)	DISTANCE (cm)	FLOW RATE (ml/hr)
D58	TFE:FA:TCM 55:30:15	8	23	18	0.3

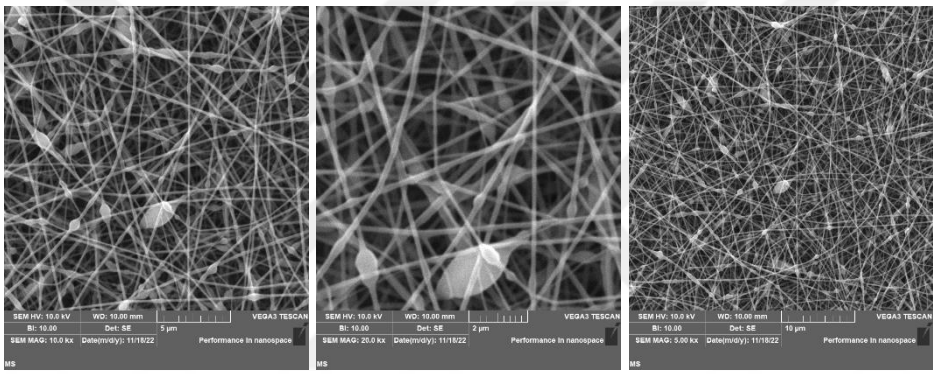

EXPERIMENT NO	SOLVENT MIXTURE	WEIGHT % OF POLYMER	VOLTAGE (kV)	DISTANCE (cm)	FLOW RATE (ml/hr)
D58	TFE:FA:TCM 55:30:15	8	24	18	0.25

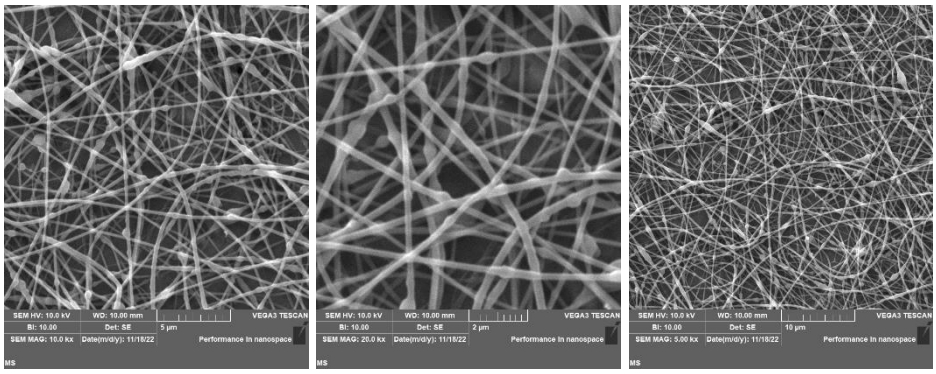

EXPERIMENT NO	SOLVENT MIXTURE	WEIGHT % OF POLYMER	VOLTAGE (kV)	DISTANCE (cm)	FLOW RATE (ml/hr)
D58	TFE:FA:TCM 55:30:15	8	24	18	0.10

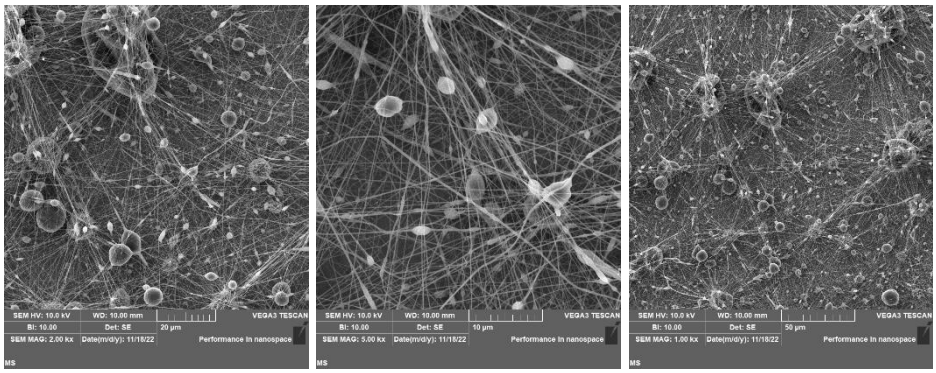

EXPERIMENT NO	SOLVENT MIXTURE	WEIGHT % OF POLYMER	VOLTAGE (kV)	DISTANCE (cm)	FLOW RATE (ml/hr)
D59	TFE:XYL 3:1	8	23	18	3.8

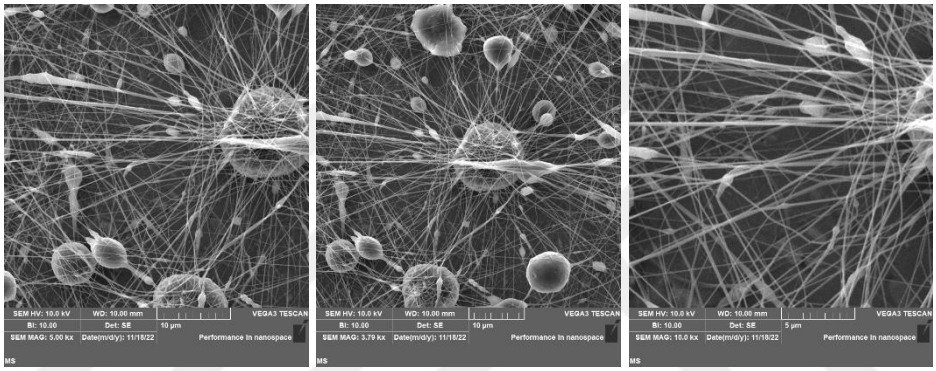

EXPERIMENT NO	SOLVENT MIXTURE	WEIGHT % OF POLYMER	VOLTAGE (kV)	DISTANCE (cm)	FLOW RATE (ml/hr)
D59	TFE:XYL 3:1	8	18	18	2.5